

CRISPR/Cas9 somatic multiplex-mutagenesis for high-throughput functional cancer genomics in mice

Julia Weber^{a,b,1}, Rupert Öllinger^{a,1}, Mathias Friedrich^c, Ursula Ehmer^a, Maxim Barenboim^{a,b}, Katja Steiger^d, Irina Heid^e, Sebastian Mueller^a, Roman Maresch^{a,b}, Thomas Engleitner^{a,b}, Nina Gross^{a,b}, Ulf Geumann^{a,b}, Beiyuan Fu^c, Angela Segler^d, Detian Yuan^f, Sebastian Lange^a, Alexander Strong^c, Jorge de la Rosa^c, Irene Esposito^g, Pentao Liu^c, Juan Cadiñanos^h, George S. Vassiliou^c, Roland M. Schmid^{a,b}, Günter Schneider^a, Kristian Ungerⁱ, Fengtang Yang^c, Rickmer Braren^e, Mathias Heikenwälder^{f,j}, Ignacio Varela^k, Dieter Saur^{a,b}, Allan Bradley^c, and Roland Rad^{a,b,2}

^aDepartment of Medicine II, Klinikum Rechts der Isar, Technische Universität München, 81675 Munich, Germany; ^bGerman Cancer Consortium (DKTK), German Cancer Research Center (DKFZ), 69120 Heidelberg, Germany; ^cThe Wellcome Trust Sanger Institute, CB10 1SA Hinxton/Cambridge, United Kingdom; ^dDepartment of Pathology, Klinikum Rechts der Isar, Technische Universität München, 81675 Munich, Germany; ^eInstitute of Radiology, Klinikum Rechts der Isar, Technische Universität München, 81675 Munich, Germany; ^fInstitute of Virology, Technische Universität München and Helmholtz Zentrum München, 81675 Munich, Germany; ^gInstitute of Pathology, Heinrich-Heine-University Düsseldorf, 40225 Düsseldorf, Germany; ^hInstitute de Medicina Oncológica y Molecular de Asturias, 33193 Oviedo, Spain; [†]Research Unit Radiation Cytogenetics, Helmholtz Zentrum München, 85764 Neuherberg, Germany; ^jDivision of Chronic Inflammation and Cancer, German Cancer Research Center (DKFZ), 69120 Heidelberg, Germany; and ^kInstituto de Biomedicina y Biotecnología de Cantabria, 39011 Santander, Spain

Edited by Neal G. Copeland, Houston Methodist Research Institute, Houston, TX, and approved September 23, 2015 (received for review June 26, 2015)

Here, we show CRISPR/Cas9-based targeted somatic multiplexmutagenesis and its application for high-throughput analysis of gene function in mice. Using hepatic single guide RNA (sgRNA) delivery, we targeted large gene sets to induce hepatocellular carcinoma (HCC) and intrahepatic cholangiocarcinoma (ICC). We observed Darwinian selection of target genes, which suppress tumorigenesis in the respective cellular/tissue context, such as Pten or Cdkn2a, and conversely found low frequency of Brca1/2 alterations, explaining mutational spectra in human ICC/HCC. Our studies show that multiplexed CRISPR/Cas9 can be used for recessive genetic screening or high-throughput cancer gene validation in mice. The analysis of CRISPR/Cas9-induced tumors provided support for a major role of chromatin modifiers in hepatobiliary tumorigenesis, including that of ARID family proteins, which have recently been reported to be mutated in ICC/HCC. We have also comprehensively characterized the frequency and size of chromosomal alterations induced by combinatorial sgRNA delivery and describe related limitations of CRISPR/Cas9 multiplexing, as well as opportunities for chromosome engineering in the context of hepatobiliary tumorigenesis. Our study describes novel approaches to model and study cancer in a high-throughput multiplexed format that will facilitate the functional annotation of cancer genomes.

in vivo CRISPR/Cas9 | somatic multiplex-mutagenesis | hepatocellular carcinoma | intrahepatic cholangiocarcinoma | chromosome engineering

or decades, a major bottleneck in cancer research has been our limited ability to identify genetic alterations in cancer. The revolution in array-based and sequencing technologies and the recent development of insertional mutagenesis tools in animal models enable the discovery of cancer-associated genetic alterations on a genome-wide scale in a high-throughput manner. Nextgeneration sequencing (NGS) of cancer genomes and transposonbased genetic screening in mice, for example, are currently creating large catalogs of putative cancer genes for principally all cancer types (1–3). A challenge for the next decades will be to validate the causative cancer relevance of these large gene sets (to distinguish drivers from passengers) and to understand their biological function. Moreover, pinpointing downstream targets of mutated cancer genes or drivers among the thousands of transcriptionally or epigenetically dysregulated genes within individual cancers is complex and limited by the lack of tools for high-throughput functional cancer genomic analyses.

The development of technologies for targeted manipulation of the mouse germ line has opened tremendous opportunities to study gene function (4, 5). Mouse models recapitulate the extensive biological complexity of human cancer and have given insights into many fundamental aspects of the disease that can be studied only at

an organismal level (6). However, the speed and efficiency of such studies is limited by the long time frames needed to genetically engineer, intercross, and breed mouse cancer models.

The prokaryotic clustered regularly interspaced short palindromic repeats (CRISPR)/CRISPR associated protein 9 (Cas9) system has been recently adapted for genetic engineering in mammalian cells (7–13). Using 20-bp single guide RNA sequences (sgRNAs), the endonuclease Cas9 can be directed to desired genomic positions to cause a double strand break. This break is repaired by nonhomologous end joining, which commonly leaves a short insertion or deletion (indel), allowing homozygous disruption of the targeted gene. Recent studies showed that CRISPR/Cas9 is functional in germ cells and somatic cells of mice and can be used for gene editing and cancer induction in the lung and the biliary compartment (14–20). Targeting of *Pten* and *p53* in the liver was reported to induce

Significance

Assigning biological relevance and molecular function to large catalogues of mutated genes in cancer is a major challenge. Likewise, pinpointing drivers among thousands of transcriptionally or epigenetically dysregulated genes within a cancer is complex and limited by the lack of tools for high-throughput functional cancer genomic analyses. We show here for the first time, to our knowledge, application of the CRISPR/Cas9 genome engineering system for simultaneous (multiplexed) mutagenesis of large gene sets in adult mice, allowing high-throughput discovery and validation of cancer genes. We characterized applications of CRISPR/Cas9 multiplexing, resulting tumor phenotypes, and limitations of the methodology. By using defined genetic or environmental predisposing conditions, we also developed, to our knowledge, the first mouse models of CRISPR/Cas9-induced hepatocellular carcinoma and show how multiplexed CRISPR/Cas9 can facilitate functional genomic analyses of hepatobiliary cancers.

Author contributions: J.W., R.Ö., and R.R. designed research; J.W., R.Ö., M.F., U.E., I.H., S.M., R.M., N.G., U.G., B.F., A. Segler, D.Y., S.L., A. Strong, J.d.I.R., K.U., and F.Y. performed research; P.L., J.C., G.S.V., R.M.S., G.S., K.U., F.Y., R.B., M.H., I.V., D.S., and A.B. contributed new reagents/analytic tools; J.W., R.Ö., M.B., K.S., T.E., I.E., K.U., F.Y., R.B., M.H., I.V., D.S., and R.R. analyzed data; and J.W., R.Ö., and R.R. wrote the paper.

The authors declare no conflict of interest.

This article is a PNAS Direct Submission.

¹J.W. and R.Ö. contributed equally to this work.

²To whom correspondence should be addressed. Email: roland.rad@tum.de.

This article contains supporting information online at www.pnas.org/lookup/suppl/doi:10. 1073/pnas.1512392112/-/DCSupplemental.

intrahepatic cholangiocarcinoma (ICC) (16), but CRISPR/Cas9-based modeling of hepatocellular carcinoma (HCC) (which accounts for 90% of liver cancers) has not been achieved so far, nor has complex combinatorial gene targeting. We therefore developed CRISPR/Cas9 hepatic mutagenesis approaches in multiplexed formats for high-throughput in vivo applications.

Results and Discussion

Inducing HCC and ICC by Hepatic Delivery of Multiplexed CRISPR/Cas9 in Adult Mice. To deliver CRISPR/Cas9 to hepatocytes, we used hydrodynamic tail vain injection (HTVI) (21). We generated a vector (*CRISPR-SB*) carrying sgRNA and Cas9 expression cassettes (11) flanked by *Sleeping Beauty* (SB) inverted repeats (*SI Appendix*, Fig. S1). HTVI of *CRISPR-SB* and an SB-transposase vector (*hSB5*) enables, in principle, both transient CRISPR/Cas9 expression from episomal plasmids and long-term expression from SB-mobilized/genome-integrated vectors. Using HTVI of two different vectors followed by fluorescence-based detection of their cellular delivery, we found that multiple plasmids can enter a cell (*SI Appendix*, Fig. S2 and *Supplementary Methods*), providing a rationale for combinatorial CRISPR/Cas9-based tumor suppressor gene (TSG) targeting.

NGS recently discovered many putative novel ICC/HCC cancer genes (22–29), but their functional validation is largely lacking. Based on a literature search (*SI Appendix*, Table S1), we have chosen to target (*i*) bona fide TSGs that are often mutated, deleted, or epigenetically silenced in ICC/HCC (e.g., *Trp53*, *Smad4*, *Pten*, *Cdkn2a*, and *Apc*), (*ii*) TSG *Arid1a*, a novel commonly mutated chromatin modifier in ICC (and less frequently in HCC), and (*iii*) TSG *Tet2*, a putative (negatively regulated) downstream target of the ICC oncogenes *Idh1/Idh2*. We also targeted the TSGs *Brca1/2*, which are not or only rarely altered in ICC/HCC. Targeting efficiencies of multiple sgRNAs per gene were validated in vitro using T7E1 assays before choosing best performing sgRNAs for HTVI (*SI Appendix*, Fig. S3). A dominant pathway activated in ICC/HCC is Ras/MAPK signaling (30, 31). We have therefore used oncogenic Kras^{G12D} to accelerate tumorigenesis.

We coinjected hSB5 transposase plasmid and 10 CRISPR-SB vectors and confirmed their successful delivery 2 wk later: real time quantitative PCR (qPCR) showed a random distribution pattern of the 10 sgRNAs in most animals (Fig. 1 A and B). We euthanized eight mice 20-30 wk post-HTVI and collected 21 macroscopic liver tumors (Fig. 1C). At this stage, mice typically had one to three small tumors (1–3 mm), occasionally more. We found both ICCs and HCCs (Fig. 1C and SI Appendix, Figs. S4 and S5). Conventional type ICCs showed CK19 positivity, reflecting biliary differentiation, and featured a Collagen-4-positive stromal reaction like the human disease (Fig. 1C and SI Appendix, Fig. S5). These early onset cancers were triggered by CRISPR/Cas9 because Kras^{G12D} alone induces only low-penetrance late-onset tumors: We observed no ICCs/HCCs in a control cohort of 53 Alb-Cre;Kras^{LSL-G12D/+} mice aged up to 38 wk. Furthermore, we didn't observe ICCs/HCCs in Alb-Cre;Kras^{LSL-G12D/+} control cohorts injected with hSB5 and Cas9-only expressing CRISPR-SB (n = 8).

Quantitative Analysis of Target Site Mutations in Healthy Livers And Cancers. We performed NGS of PCR-amplified target sites in tumors and related healthy livers (Fig. 2). Because sequence reads with large deletions are often filtered out during mapping using standard bioinformatics tools, we used manually inspected/mapped capillary sequencing data of cloned PCR products (*SI Appendix*, Fig. S6) to optimize the algorithms for NGS-based high-throughput indel detection. Whereas Cas9-only injected control mice had no mutations at the CRISPR/Cas9 target sites, we found a total of 167 indels in the 21 tumors (Fig. 2 *A* and *B*). The majority were small and located at the position of the Cas9 double strand break insertion [3 bp upstream of the protospacer adjacent motif (PAM)]. Large deletions (>50 bp) were rare (Fig. 2 and *SI Appendix*, Figs. S7 and S8).

We next compared the frequency of CRISPR/Cas9-induced frame shifts causing indels at target sites in tumors and healthy livers from the same mice (Fig. 2C and detailed view in SI Appendix, Fig. S9). In-frame deletions <10 bp are less likely to have functional consequences and are therefore shown only in SI Appendix, Fig. S7 and Table S2. Normal liver samples from

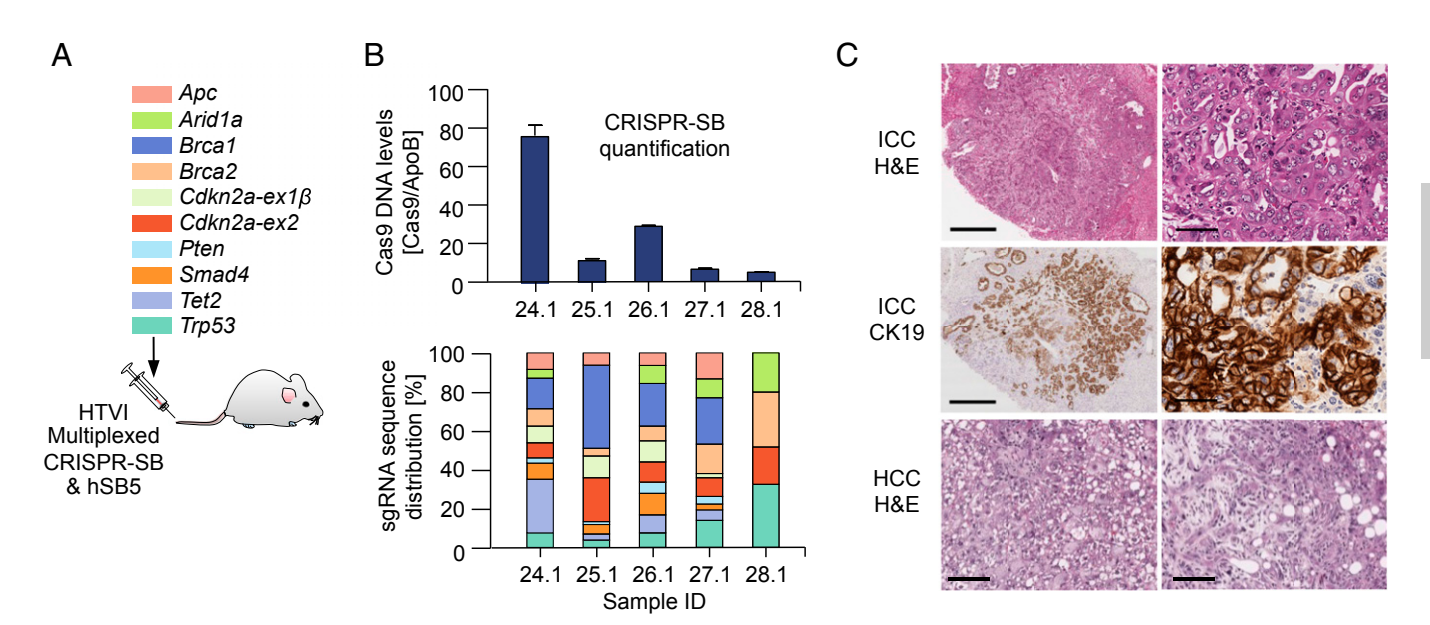


Fig. 1. Hepatic delivery of multiplexed CRISPR/Cas9 for somatic mutagenesis in mice. (A) Genes targeted simultaneously upon hydrodynamic tail vein injection (HTVI). For details of the two-vector system, see *SI Appendix*, Fig. S1. (B) Analysis of healthy livers 2 wk post-HTVI. (*Upper*) Quantification of *hSpCas9* DNA copies using qPCR; Error bars, SEM from triplicate determinations. (*Lower*) Quantitative analysis of sgRNA distribution using qPCR with guide-specific forward primers and a generic reverse primer (color code from A). (C) Microscopic images of CRISPR/Cas9-induced tumors in *Alb-Cre;Kras^{LSL-G12D/+}* mice. ICC, intrahepatic cholangiocarcinoma. (*Top*) H&E staining. (*Middle*) Cytokeratin 19 (CK19) IHC staining. HCC, hepatocellular carcinoma. (*Bottom*) Two H&E-stained HCCs. (Scale bars: *Left* panel in *Top* and *Middle* row, 50 μm; *Right* panel in *Top* and *Middle* row, 400 μm; both images in *Bottom* row, 100 μm.)

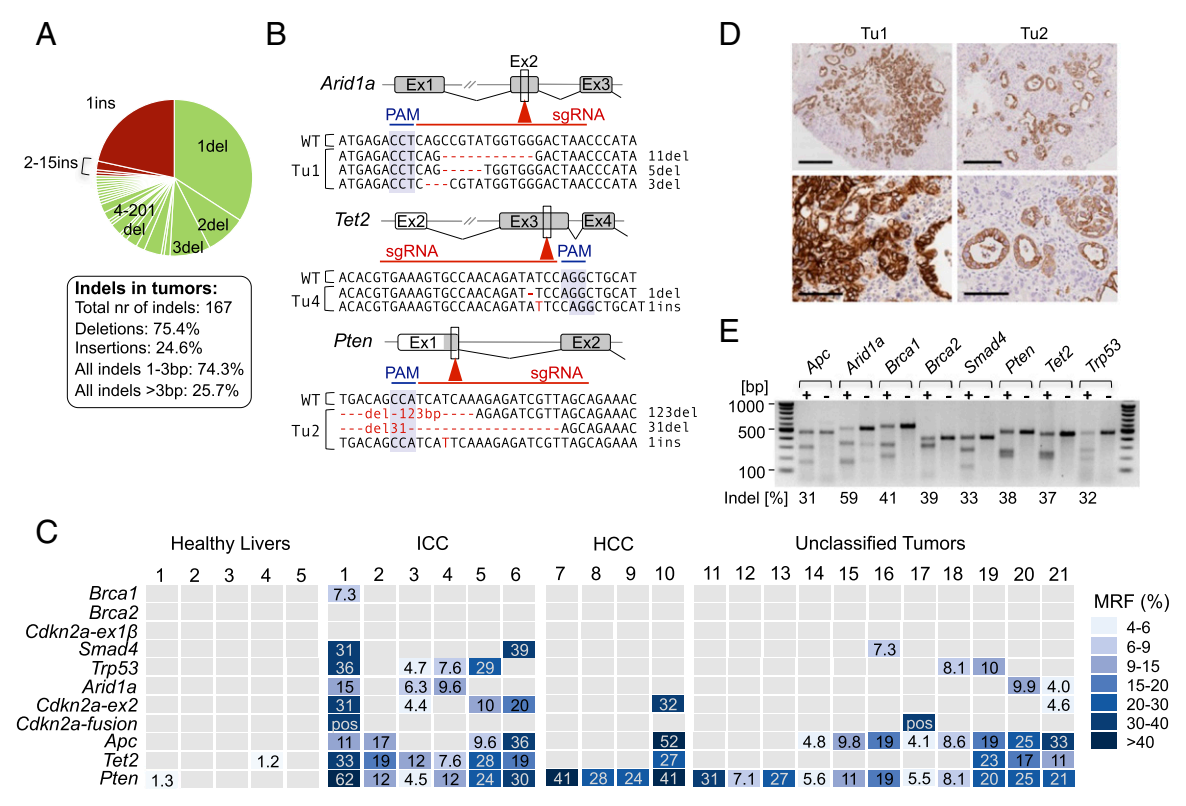


Fig. 2. Analysis of CRISPR/Cas9 target site mutations in healthy liver and liver tumors. (A) Pie chart showing the type (deletion or insertion) and size of all indels derived from liver tumors (n = 21) of Alb-Cre; Kras^{LSL-G12D/+} mice (n = 8) 20–30 wk after HTVI of hSpCas9 and ten sgRNAs. (B) Examples of indel sequence context in selected tumors for Arid1a/Tet2/Pten. PAM, protospacer adjacent motif. WT, WT sequence. (C) Mutant read frequencies (MRFs) at individual target sites as determined by amplicon-based next-generation sequencing. Multiple indels at individual target sites (shown in detail in SI Appendix, Fig. 59) are presented here as combined MRFs. Frame-shift causing indels with MRFs > 1% and 4% are shown for healthy livers and tumors, respectively. Pos, tumors with Cdkn2a-ex1\(\theta\) (Cdkn2a-ex2) fusions. Small macroscopic tumors (<1 mm) were used entirely for genomic analyses (unclassified; no histology available). (D) Comparison of cancer cell to nonneoplastic cell contents in Tu1 and Tu2. CK19 staining marks ICC. (Scale bars: Upper, 400 μm; Lower, 100 μm.) (E) Surveyor assays to assess CRISPR/Cas9 efficiency upon transient transfection of the mouse pancreatic cancer cell line PPT-53631. Indel frequencies are indicated. Cell lines were transfected with the target sqRNA (+) or a control sgRNA (-). Because PPT-53631 has homozygous Cdkn2a deletions, Cdkn2a sgRNAs were tested in a different cell line (PPT-4072) (SI Appendix, Fig. S10).

tumor-bearing mice exhibited no or only few mutations with low mutant read frequencies (MRFs) (fraction of mutant-reads/ all-reads at individual target sites) (Fig. 2C). In contrast, all tumors had several mutations above the 4% MRF threshold, which was used to exclude their origin in healthy tissue (Fig. 2C). In Tu1, for example, MRFs reached up to 62% for individual target loci, reflecting clonal expansion of mutations. Further details about the type and frequency of mutations at individual positions are shown in SI Appendix, Fig. S9 and Table S2.

Differences of MRFs between tumors can at least partly be explained by the varying content of nonneoplastic cells. Tu2, for example, which generally had lower MRFs at mutated target sites than Tu1, also had a significantly smaller tumor/normal cell ratio (Fig. 2D and SI Appendix, Fig. S5). In contrast, extensive differences between MRFs at different target sites within one tumor could reflect intratumor heterogeneity, as shown later.

Cancer-Relevant Mutations Undergo Positive Selection. A global comparison of the incidence of CRISPR/Cas9-induced target site mutations across tumors showed a nonrandom distribution ($P = 2.2 \times$ 10^{-15} ; χ^2 test). *Pten*, for example, was mutated in all 21 tumors whereas Brca1 or Brca2 mutations were largely absent (only one low-frequency Brca1 mutation in Tu1). This distribution suggests that biologically relevant mutations are selected for in vivo. The high incidence of *Pten* mutations can indeed be explained by the key importance of PI3K signaling in hepatobiliary tumorigenesis in humans and mice (32–34). Likewise, the lack of *Brca1/2* mutations reflects their extremely rare alteration in human ICC/HCC (SI Appendix, Table S1). Overall, several genes were targeted significantly more frequently than *Brca1/2*, including *Pten* ($P = 6.4 \times 10^{-15}$), Apc $(P = 9.3 \times 10^{-7})$, Tet2 $(P = 6.6 \times 10^{5})$, Cdkn2a-ex2 (P =0.0007), p53 (P = 0.007), and Arid1a (P = 0.02; Fisher's exact test).

The possibility of technical problems underlying the low incidence of Brca1/2 mutations in tumors can be excluded because (i) surveyor assays in vitro confirmed similar efficiencies of *Brca1/2* targeting to other loci (Fig. 2E), and (ii) the "background" Brca1/2 mutation rate in healthy livers was similar to other target genes (SI Appendix, Table S2). We therefore conclude that Darwinian selection of indels with pathogenetic relevance in the specific tissue context drives tumorigenesis in our model.

Another level of evidence for in vivo selection comes from the comparison of the two Cdkn2a sgRNAs that we used: one targeting exon-1 β to inactivate $p19^{4rf}$ and the second directed against exon-2 to disrupt both $p19^{4rf}$ and $p16^{Ink4a}$. Whereas Cdkn2a-ex2was mutated in 33% (7/21) of tumors, no mutations above the "background" mutation rate in healthy liver were found in $Cdkn2a-ex1\beta$ (P = 0.009; Fisher's Exact test) (Fig. 2C). This observation suggests selective pressure for the double-mutant and also reflects the predominant CDKN2A inactivation pattern in human hepatobiliary cancers. To confirm that sgRNAs against both exons are in fact functional, we performed surveyor assays, which showed similar efficiencies of Cdkn2a-ex2 and Cdkn2a $ex1\beta$ targeting (SI Appendix, Fig. S10).

The pathogenic relevance of TSGs like Pten or Trp53 in ICC/HCC has been shown in vivo (35, 36). For Arid1a, which was recently discovered to be recurrently mutated in ICC/HCC (23, 24, 26, 27),

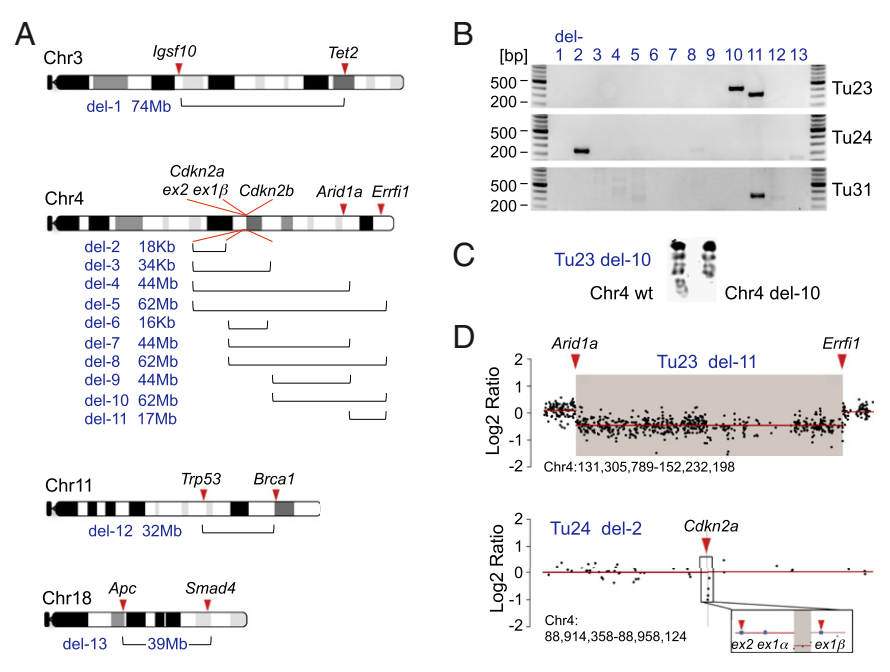


Fig. 3. Intrachromosomal fusions induced by combinatorial CRISPR/Cas9 targeting. (A) Scheme of chromosomes with two or more CRISPR/Cas9 target sites in the 18 sgRNA multiplexing experiments. Brackets indicate the predicted sizes of possible deletions (del-1 to del-13), ranging from 16 kb to 74 Mb. (B) PCR screening for all 533 possible intrachromosomal fusions in 41 liver tumors revealed four large deletions in three tumors: an 18-kb deletion (del-2, Tu24; Cdkn2a-ex1β/Cdkn2a-ex2 fusion), two large deletions in Tu23 (del-10, Cdkn2b/Errfi1, 62Mb; del-11, Arid1a/Errfi1, 17 Mb), and another Arid1a/Errfi1 fusion in Tu31. (C) DAPI staining of metaphase spreads of Tu23 cell line confirms the large deletion (del-10) in chromosome 4. (D) Del-2 in Tu24 and del-11 in Tu23 are detected as copy number losses by array CGH.

such biological information is lacking. We found *Arid1a* alterations in 24% of tumors (Fig. 2C). In addition, 80% (11/14) of hepatobiliary cancers (3/3 ICCs and 8/11 HCCs) induced in a second HTVI approach targeting a larger set of genes (described below) had CRISPR/Cas9-induced mutations of *Arid1a* and/or *Arid1b*, another chromatin modifier that was recently discovered to be frequently mutated in ICC/HCC. These observations strongly support a role of chromatin modifying enzymes in hepatobiliary tumorigenesis.

CRISPR/Cas9 has been recently adapted for genetic screening in vitro (37–39) and also in a transplantation model (40). We show that somatic mutagenesis and cancer gene discovery are also feasible directly in vivo. A surprising finding was the high frequency of CRISPR/Cas9-induced mutations in *Tet2* (particularly in ICCs) (Fig. 2C). Its tumor suppressive function might be linked to IDH1/IDH2, which carry oncogenic mutations in >10% of ICCs (23, 24, 41), leading to dioxigenase inhibition by 2-hydroxyglutarate production (42, 43). Among the 70 2OG-dependent dioxigenases, TET2 is considered a promising cancer-relevant target: TET2 and IDH1/2 mutations induce similar hypermethylation phenotypes (41, 44) and are mutually exclusive in AML, suggesting similar effects on cellular transformation (45). TET2 is not mutated in human ICC, but IDH1/2 alterations are associated with impaired TET2 function (41). Our data support TET2's pathogenetic relevance in ICC and exemplify how genetic screening can pinpoint cancer genes that are not mutated, but dysregulated by other means.

Intratumor Heterogeneity in a Small Subset of CRISPR/Cas9-Induced Cancers. In some cancers (e.g., Tu1, -4, -5, and -21), MRFs differed extensively between individual target sites, and often more than two mutations at individual sites existed within a tumor (Fig. 2 and *SI Appendix*, Fig. S9). One explanation for this observation could be that some mutations occur in the transfected founder cell whereas others happen only after the first cell division in subsequent daughter cells. To explore this possibility, we compared three different regions in Tu1 (*SI Appendix*, Fig. S11): the large area R1 and the small microdissected areas R2 (with a well-differentiated tubular growth pattern) and R3 (showing poor differentiation and more solid

growth). Target sites sequencing revealed that, even within R2/R3, many MRFs were low, suggesting additional intraregional minority clones and a complex subclonal structure, which is only partly resolved. The only mutation with consistently high MRFs in all three regions was *Cdkn2a-ex2*, suggesting its position at the trunk of a phylogenetic tree. R2/R3 comparison revealed substantial differences regarding driver mutations in dominant clones (*SI Appendix*, Fig. S11C), with *Smad4-1del* defining the dominant clone in R2 and *Pten-1del-b* in R3, suggesting that genetic heterogeneity underlies phenotypic intratumor diversity. The possibility of R1/R2/R3 being independent tumors is highly unlikely because of (*i*) the presence of specific high-frequency founder *Cdkn2a* mutations in all three regions (including a single base deletion and an 18-kb CRISPR/Cas9-induced deletion) (*SI Appendix*, Fig. S9 and Table S2), and (*ii*) the small size (3 mm) of this solitary tumor in an otherwise healthy liver.

Chromosomal Rearrangements Induced by Combinatorial CRISPR/Cas9 Targeting. One potential limitation of multiplexed CRISPR/Cas9 mutagenesis is that, in principle, combinatorial sgRNA targeting could lead to undesired large chromosomal rearrangements (18, 20). To examine this possibility, we performed PCR-based screening for all possible deletions at chromosomes that were targeted by multiple sgRNAs (SI Appendix, Fig. S12). Out of the 105 possible deletions in 21 tumors, we found evidence for fusion products between the Cdkn2a-ex1β and Cdkn2a-ex2 sgRNA target sites in two cancers (Fig. 2C). In both cases the resulting deletion of \sim 18 kb led to inactivation of both $p16^{lnk4a}$ and $p19^{Arf}$ (SI Appendix, Fig. S12). Because small indels in exon-2 mediated by a single Cdkn2a-ex2 sgRNA also inactivates both p16^{Ink4a} and p19^{Arf}, there is no selective pressure beyond exon-2 mutations for the 17.7-kb deletion to occur. It therefore seems that this relatively small deletion of 17.7 kb is a fairly efficient process.

We therefore next studied such potentially undesired effects of CRISPR/Cas9 multiplexing in a scenario of higher level multiplexing (18 sgRNAs targeting known or putative hepatobiliary cancer genes). Furthermore, to examine whether ICCs/HCCs can be induced by CRISPR/Cas9 multiplexing in environmental

cancer-predisposing contexts, we have used not only the Kras-mutant background but also a CCl₄-induced liver injury model. We have analyzed a total of 41 tumors collected in these experiments. All cancers induced in the CCl_4 context (n = 35) were HCCs whereas in Alb-Cre;Kras^{LSL-G12D} mice, we found both ICCs and HCCs. Detailed information about tumor incidences is provided in SI Appendix, Table S3. The general conclusions drawn from target site mutation sequencing were in concordance with our observations made in the 10 sgRNA studies: For example, the incidence of Brca1, Brca2, or isolated Cdkn2a-ex1β mutations was very low (20%, 10%, or 7%) whereas Pten or epigenetic regulators (Arid1a and/or Arid1b) were hit in 93% and 78% of cancers, respectively, further confirming that pathogenetically relevant mutations are selected for in vivo.

With respect to CRISPR/Cas9-induced rearrangements, we screened for all 533 possible large intrachromosomal deletion/ fusion events in the 41 tumors using PCR and in a subset of tumors also by comparative genomic hybridization (CGH) and multicolor fluorescence in situ hybridization (M-FISH) (Fig. 3 and SI Appendix, Figs. S13 and S14). We identified four deletions in three cancers: an 18-kb deletion at the Cdkn2a locus (Tu24), a 62-Mb deletion between TSGs Cdkn2b and Errfi1 (Tu23), and 17-Mb deletions between Arid1a and Errfi1 (Tu23 and Tu31). The 62-Mb deletion identified in Tu23 by fusion-PCR was "silent" in CGH because of its subclonal occurrence. It was, however, detectable by FISH (1/7 metaphases positive for the deletion) (Fig. 3C). There were no interchromosomal translocations in the cell lines analyzed by M-FISH (n = 2) (SI Appendix, Fig. S14). Because stable integration of CRISPR/Cas9 vectors was very rare in our cancers (integrations identified by PCR-based detection of CRISPR-SB vectors in only 3 out of 62 tumors), we conclude that transient expression of multiplexed CRISPR/Cas9 can be sufficient to induce one or more intrachromosomal rearrangements within a cell in vivo.

One implication of these results is that the extent of multiplexing will have limitations. Either it will require careful selection/ combination of target sites or the possibility of undesired chromosomal damage occurring will need to be tested for. These findings are also relevant for genome-wide in vitro CRISPR/Cas9 screening, particularly in experimental settings where multiple sgRNAs are delivered to a cell. On the other hand, the observation that chromosome engineering is feasible somatically in the context of liver cancer offers great opportunities. GWAS and whole genome sequencing studies are currently identifying hundreds of ICC/HCC variant hot spot regions, many of which are located in genomic deserts, coinciding with putative regulatory regions, such as enhancers (www.genome.gov/encode). Our results suggest that these regions can be systematically targeted using multiplexed CRISPR/Cas9 to study their biological role in cancer.

No Off-Target Effects in CRISPR/Cas9-Induced Liver Tumors. We have screened eight tumors for undesired off-target effects by ampliconbased NGS of each sgRNA's top five off-targets (at least three exonic off-targets). We found no indels at off-target sites with a mutant read frequency of 0.2% or higher (a cutoff used to exclude sequencing errors for both on- and off-target site analyses). We also screened CGH data from six tumors for 266,778 potential intrachromosomal deletions resulting from combinations of potential off-target cleavage events (1,010 and 1,550 off-target sites for 10 sgRNAs and 18 sgRNAs, respectively) (SI Appendix, Fig. S13). Off-target sites were defined to be potentially causative if they were within a distance of 500,000 bp (and 20 probes or fewer) to an aberration detected by CGH. These analyses did not identify chromosomal deletions attributable to off-target effects.

CRISPR/Cas9-Induced Mutations Are Predominantly Biallelic. To assess the incidence of biallelic vs. monoallelic target gene mutations, we next analyzed cancer cell lines isolated from an aggressive ICC induced by 18-sgRNA multiplexing (Fig. 4 and SI Appendix, Fig. \$15 show that these cell lines are transplantable). In contrast to all

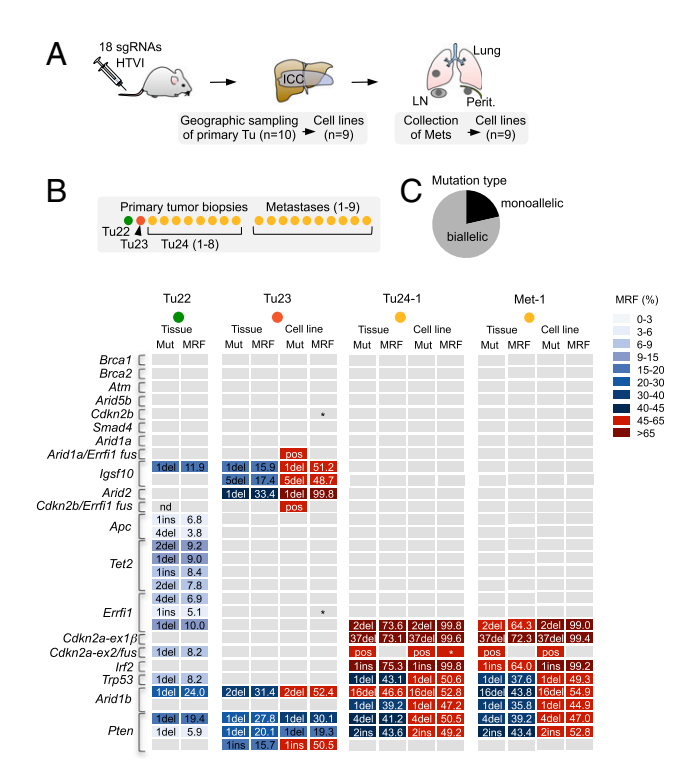


Fig. 4. Allelic frequencies of target site mutations and phylogenetic tracking of CRISPR/Cas9-induced metastatic ICC. (A) A 2-cm tumor mass (ICC) and numerous metastases (Mets) in lungs, lymph nodes (LN), and peritoneum in a mouse 20 wk after HTVI of 18 sgRNAs. (B) CRISPR/Cas9 target sites underwent NGS in a total of 35 tumor/metastasis tissues and cell lines. Indel patterns revealed three independent primary tumors. All metastases originate from Tu24. Frame-shift causing indels with a cumulative mutant read frequency (MRF) >4% per target site are shown for representative samples. Note that MRFs are underestimated in cancer tissue (because of healthy stromal components) but are accurately reflected in cell lines. Tumors with indicated fusion products are marked as positive (pos). Asterisks indicate a lack of WT sequence. (C) Allelic frequency of mutations in cell lines of Tu23 and Tu24 as determined by a combined quantitative analysis of indel frequencies, presence/absence of large fusions, and the presence/absence of WT reads.

other tumors analyzed in this study (which were identified early by regular MRI screening and were therefore small), one animal had an early onset large (>2 cm) tumor mass and numerous metastases to lymph nodes, peritoneum, and lungs (SI Appendix, Fig. S16). Extensive geographical sampling of the tumor mass (n = 10) and subsequent target site sequencing revealed three independent primary cancers (Tu22, Tu23, and Tu24), with Tu24 being predominant (8/10 samples). The analysis of CRISPR/Cas9-induced indel patterns also allowed phylogenetic tracking of metastatic clones: All metastases (n = 9) originated from Tu24 (Fig. 4B and SI Appendix, Table S4).

Comparative indel analysis of primary tumor tissue and corresponding cell lines showed that accurate estimation of MRFs is difficult in primary cancer tissue due to stromal components (Fig. 4B and SI Appendix, Table S4). A combined quantitative analysis of (i) indel frequencies, (ii) the presence or absence of large deletions (fusions), and (iii) the frequency of WT reads at target sites in these cell lines revealed that 79% of mutated target loci have biallelic inactivation (Fig. 4C and SI Appendix, Table S5), despite the fact that none of these tumors had stably integrated CRISPR/ Cas9. The predominant homozygous inactivation underlines the potential of CRISPR/Cas9 for recessive genetic screening and gene function analysis.

Hepatic loss-of-function screening has been performed using RNAi-based gene knock-down in transplantation models (e.g., intrasplenic implantation of bipotent liver progenitor cells) (46)

or by HTVI-based/transposon-mediated genome integration of shRNAs (47). Our results show that RNAi and CRISPR/Cas9 are complementary tools with unique beneficial characteristics, depending on the experimental context. CRISPR/Cas9-induced homozygous gene knockout is a major advance for recessive genetic screening whereas RNAi-based knockdown (which is typically only partial) has advantages for the study of dosage effects or reversible phenotypes. Likewise, the ability to perform chromosome engineering by CRISPR/Cas9 is an important novel technological innovation but can be disadvantageous if such effects are not desired.

Concluding Remarks

Our work describes novel approaches to model and study cancer in mice. We provide, to our knowledge, the first demonstration and characterization of highly multiplexed direct in vivo CRISPR/Cas9 mutagenesis, including (i) the description of proof-of-principle applications (genetic screening for cancer gene validation/discovery), (ii) a characterization of tumor phenotypes at the genetic level (tumor heterogeneity, allelic mutation frequency, phylogenetic metastasis tracking, single cell cloning), and (iii) a thorough analysis/discovery of possible caveats (frequency/size/extent of chromosomal rearrangements). This multilayered characterization gives comprehensive insights into the potential and limitations of in vivo CRISPR/Cas9 multiplexing and thus guidance for its appropriate use. In defined genetic (Kras^{G12D}) and liver damage models (CCl₄),

- Stratton MR (2011) Exploring the genomes of cancer cells: Progress and promise. Science 331(6024):1553–1558.
- Copeland NG, Jenkins NA (2010) Harnessing transposons for cancer gene discovery. Nat Rev Cancer 10(10):696–706.
- Rad R, et al. (2010) PiggyBac transposon mutagenesis: A tool for cancer gene discovery in mice. Science 330(6007):1104–1107.
- Bradley A, Evans M, Kaufman MH, Robertson E (1984) Formation of germ-line chimaeras from embryo-derived teratocarcinoma cell lines. *Nature* 309(5965):255–256.
- Doetschman T, et al. (1987) Targetted correction of a mutant HPRT gene in mouse embryonic stem cells. Nature 330(6148):576–578.
- van Miltenburg MH, Jonkers J (2012) Using genetically engineered mouse models to validate candidate cancer genes and test new therapeutic approaches. Curr Opin Genet Dev 22(1):21–27.
- 7. Horvath P, Barrangou R (2010) CRISPR/Cas, the immune system of bacteria and archaea. Science 327(5962):167–170.
- Garneau JE, et al. (2010) The CRISPR/Cas bacterial immune system cleaves bacteriophage and plasmid DNA. Nature 468(7320):67–71.
- Jinek M, et al. (2012) A programmable dual-RNA-guided DNA endonuclease in adaptive bacterial immunity. Science 337(6096):816–821.
- Wiedenheft B, Sternberg SH, Doudna JA (2012) RNA-guided genetic silencing systems in bacteria and archaea. Nature 482(7385):331–338.
- Cong L, et al. (2013) Multiplex genome engineering using CRISPR/Cas systems. Science 339(6121):819–823.
- Mali P, et al. (2013) RNA-guided human genome engineering via Cas9. Science 339(6121):823–826.
- Sander JD, Joung JK (2014) CRISPR-Cas systems for editing, regulating and targeting genomes. Nat Biotechnol 32(4):347–355.
- Wang H, et al. (2013) One-step generation of mice carrying mutations in multiple genes by CRISPR/Cas-mediated genome engineering. Cell 153(4):910–918.
- Yin H, et al. (2014) Genome editing with Cas9 in adult mice corrects a disease mutation and phenotype. Nat Biotechnol 32(6):551–553.
- Xue W, et al. (2014) CRISPR-mediated direct mutation of cancer genes in the mouse liver. Nature 514(7522):380–384.
- Platt RJ, et al. (2014) CRISPR-Cas9 knockin mice for genome editing and cancer modeling. Cell 159(2):440–455.
- Maddalo D, et al. (2014) In vivo engineering of oncogenic chromosomal rearrangements with the CRISPR/Cas9 system. *Nature* 516(7531):423–427.
- Sánchez-Rivera FJ, et al. (2014) Rapid modelling of cooperating genetic events in cancer through somatic genome editing. Nature 516(7531):428–431.
- Blasco RB, et al. (2014) Simple and rapid in vivo generation of chromosomal rearrangements using CRISPR/Cas9 technology. Cell Reports 9(4):1219–1227.
- Yant SR, et al. (2000) Somatic integration and long-term transgene expression in normal and haemophilic mice using a DNA transposon system. Nat Genet 25(1):35–41.
- normal and haemophilic mice using a DNA transposon system. *Nat Genet* 25(1):35–41.

 22. Ong CK, et al. (2012) Exome sequencing of liver fluke-associated cholangiocarcinoma.
- Nat Genet 44(6):690–693.

 23. Jiao Y, et al. (2013) Exome sequencing identifies frequent inactivating mutations in BAP1,
- ARID1A and PBRM1 in intrahepatic cholangiocarcinomas. *Nat Genet* 45(12):1470–1473.

 24. Chan-On W, et al. (2013) Exome sequencing identifies distinct mutational patterns in liver fluke-related and non-infection-related bile duct cancers. *Nat Genet* 45(12):1474–1478.
- Ross JS, et al. (2014) New routes to targeted therapy of intrahepatic cholangiocarcinomas revealed by next-generation sequencing. Oncologist 19(3):235–242.

we also show for the first time, to our knowledge, that CRISPR/Cas9 somatic gene targeting can be used to induce HCC, one of the leading causes of cancer-related death worldwide, and we provide support for the emerging role of chromatin modifiers in hepatobiliary tumorigenesis. Multiplexing CRISPR/Cas9 will enhance the speed and efficiency of assigning biological function to DNA sequence, one of the big scientific challenges in the postgenomic era.

Methods

A detailed description of experimental procedures is available in *SI Appendix*. Briefly, CRISPR/Cas9 cleavage efficiencies were tested in vitro using T7E1 or Surveyor assays. Hepatic delivery of CRISPR/Cas9 vectors was performed by HTVI, as described earlier (21). All animal studies were conducted in compliance with European guidelines for the care and use of laboratory animals and were approved by the Institutional Animal Care and Use Committees (IACUC) of Technische Universität München, Regierung von Oberbayern, and the UK Home Office. CRISPR/Cas9 target site mutations were identified using amplicon-based NGS. Liver tumors were characterized by immunohistochemistry (IHC), CGH, and M-FISH.

ACKNOWLEDGMENTS. We thank Olga Seelbach, Ruth Hillermann, Teresa Stauber, and Daniel Kull for excellent technical assistance. J.d.l.R. is recipient of a Federation of European Biochemical Societies (FEBS) fellowship. The work was supported by the German Cancer Consortium Joint Funding Program and the Helmholtz Gemeinschaft (Preclinical Comprehensive Cancer Center).

- Fujimoto A, et al. (2012) Whole-genome sequencing of liver cancers identifies etiological influences on mutation patterns and recurrent mutations in chromatin regulators. Nat Genet 44(7):760–764.
- Guichard C, et al. (2012) Integrated analysis of somatic mutations and focal copynumber changes identifies key genes and pathways in hepatocellular carcinoma. Nat Genet 44(6):694–698.
- 28. Huang J, et al. (2012) Exome sequencing of hepatitis B virus-associated hepatocellular carcinoma. *Nat Genet* 44(10):1117–1121.
- Schulze K, et al. (2015) Exome sequencing of hepatocellular carcinomas identifies new mutational signatures and potential therapeutic targets. Nat Genet 47(5):505–511.
- Delire B, Stärkel P (2015) The Ras/MAPK pathway and hepatocarcinoma: Pathogenesis and therapeutic implications. Eur J Clin Invest 45(6):609–623.
- Sia D, et al. (2013) Integrative molecular analysis of intrahepatic cholangiocarcinoma reveals 2 classes that have different outcomes. Gastroenterology 144(4):829–840.
- 32. Horie Y, et al. (2004) Hepatocyte-specific Pten deficiency results in steatohepatitis and hepatocellular carcinomas. *J Clin Invest* 113(12):1774–1783.
- 33. Simbolo M, et al. (2014) Multigene mutational profiling of cholangiocarcinomas identifies actionable molecular subgroups. *Oncotarget* 5(9):2839–2852.
- 34. Boyault S, et al. (2007) Transcriptome classification of HCC is related to gene alterations and to new therapeutic targets. *Hepatology* 45(1):42–52.
- 35. Xu X, et al. (2006) Induction of intrahepatic cholangiocellular carcinoma by liverspecific disruption of Smad4 and Pten in mice. *J Clin Invest* 116(7):1843–1852.
- O'Dell MR, et al. (2012) Kras(G12D) and p53 mutation cause primary intrahepatic cholangiocarcinoma. Cancer Res 72(6):1557–1567.
- Wang T, Wei JJ, Sabatini DM, Lander ES (2014) Genetic screens in human cells using the CRISPR-Cas9 system. Science 343(6166):80–84.
- Shalem O, et al. (2014) Genome-scale CRISPR-Cas9 knockout screening in human cells. Science 343(6166):84–87.
- Koike-Yusa H, Li Y, Tan EP, Velasco-Herrera MdelC, Yusa K (2014) Genome-wide recessive genetic screening in mammalian cells with a lentiviral CRISPR-guide RNA library. Nat Biotechnol 32(3):267–273.
- Chen S, et al. (2015) Genome-wide CRISPR screen in a mouse model of tumor growth and metastasis. Cell 160(6):1246–1260.
- Wang P, et al. (2013) Mutations in isocitrate dehydrogenase 1 and 2 occur frequently in intrahepatic cholangiocarcinomas and share hypermethylation targets with glioblastomas. Oncogene 32(25):3091–3100.
- Dang L, et al. (2010) Cancer-associated IDH1 mutations produce 2-hydroxyglutarate. Nature 465(7300):966.
- Ward PS, et al. (2010) The common feature of leukemia-associated IDH1 and IDH2 mutations is a neomorphic enzyme activity converting alpha-ketoglutarate to 2-hydroxyglutarate. Cancer Cell 17(3):225–234.
- Guilhamon P, et al. (2013) Meta-analysis of IDH-mutant cancers identifies EBF1 as an interaction partner for TET2. Nat Commun 4:2166.
- Figueroa ME, et al. (2010) Leukemic IDH1 and IDH2 mutations result in a hypermethylation phenotype, disrupt TET2 function, and impair hematopoietic differentiation. Cancer Cell 18(6):553–567.
- Zender L, et al. (2008) An oncogenomics-based in vivo RNAi screen identifies tumor suppressors in liver cancer. Cell 135(5):852–864.
- 47. Xue W, et al. (2012) A cluster of cooperating tumor-suppressor gene candidates in chromosomal deletions. *Proc Natl Acad Sci USA* 109(21):8212–8217.

Weber et al., CRISPR/Cas9 somatic multiplex-mutagenesis for highthroughput functional cancer genomics in mice

Supplementary Methods

Cloning of *CRISPR-SB***.** To generate the *CRISPR-SB* vector, pX330 (Addgene #42230 (1)) was sequentially opened with *AfIIII* and *NotI* single cutters. *Sleeping Beauty (SB)* terminal repeats were amplified from pTnori (2) with *AfIIII* and *NotI* overhangs, respectively and cloned into pX330.

Design and cloning of single guide RNA (sgRNA) sequences. The 20-bp sgRNA sequences were designed using the CRISPR design tool (http://crispr.mit.edu) (3) and are depicted in Table S6. For *Tet2* we used the sgRNA sequence as described in (4). Cloning of sgRNA sequences into *CRISPR-SB* was performed following protocols provided by the depositor of *pX330*.

T7 Endonuclease 1 (T7E1) assay for identification of suitable sgRNAs for somatic mutagenesis. The mouse pancreatic cancer cell line *PPT-53631* was cultured in DMEM (Sigma-Aldrich) containing 10% fetal bovine serum (Biochrom). Eighty thousand cells per well were sown in a 24-well-plate and transfected the next day with 450ng *CRISPR-SB* plasmid and 50ng *pcDNA*[™]6.2/EmGFP-Bsd/V5-DEST (Life Technologies) using Lipofectamine® 2000 (Life Technologies). Twenty four hours after transfection, cells were selected with 5µg/mL Blasticidin (Life Technologies). After two days of selection, cells were lysed with DirectPCR lysis reagent (Viagen). PCR amplification of the target region was performed with Q5® High-Fidelity DNA Polymerase (New England Biolabs) using primers listed in Table S8. We purified PCR products by gel extraction (QIAquick Gel Extraction Kit, Qiagen) and denatured and reannealed 200ng of the purified PCR product in NEBuffer 2 (New England Biolabs) using a thermocycler. Hybridized PCR products were treated with 10U of T7E1 (New England Biolabs) at 37°C for 15min in a reaction volume of 20μL. Reactions were stopped by the addition of 2μL 0.5M EDTA and analyzed by electrophoresis using a 10% polyacrylamide gel. Indel frequency was calculated according to (5).

Surveyor nuclease assay for determining indel frequency in targeted genes. For Surveyor assays we used the mouse pancreatic cancer cell lines *PPT-53631* and *PPT-4072*, which were cultured in DMEM (Sigma-Aldrich) containing 10% fetal bovine serum (Biochrom). Eighty thousand cells per well were sown in a 24-well plate and transfected the next day with 450ng *CRISPR-SB* plasmid and 50ng *pcDNA™6.2/EmGFP-Bsd/V5-DEST* (Life Technologies) using Lipofectamine® 2000 (Life Technologies). Twenty four hours after transfection, cells were selected with 5µg/mL Blasticidin (Life Technologies). After two days of selection, cells were lysed with DirectPCR lysis reagent (Viagen). Amplifications of the target regions were performed with TaKaRa Ex Taq DNA Polymerase (Clontech) using primers listed in Table S8. PCR products were denatured and reannealed in NEBuffer 2 (New England Biolabs) using a thermocycler. Surveyor nuclease reaction was performed according to manufacturer's instructions (Transgenomic) and indel frequency was calculated according to (5).

Animal Experiments. For hydrodynamic tail vein injections (HTVI), 10µg/mL *hSB5 transposase* (2) and ten (eighteen) *CRISPR-SB* sgRNA vectors (10µg/mL in total) were dissolved in 2mL 0.9% saline and injected into the tail vein of eight weeks old mice over six to ten seconds (2). In order to accelerate liver tumorigenesis, we used *Alb-Cre;Kras^{LSL-G12D/+}* mice (6, 7). For chemical acceleration of tumorigenesis, wild type mice were treated nine times with a weekly intraperitoneal injection of 1µL/g body weight 10% carbon tetrachloride (CCI₄, Sigma-Aldrich) in Corn Oil (Sigma-Aldrich) beginning two weeks after HTVI. Mice were monitored for tumor development by regular magnetic resonance imaging (MRI) screening, starting at 20 weeks post HTVI. Animals were sacrificed as soon as hepatic tumors were diagnosed or when signs of sickness were apparent (in one case of early onset metastasized cancer at 20 weeks prior to MRI screening; see data in Figure 4).

For subcutaneous implantation of cell lines derived from mouse primary hepatic tumors, trypsinized cells were washed twice with DBPS (Life Technologies) and counted using a hemocytometer. Concentration was adjusted to 3.3×10^6 cells per mL DPBS and $150 \mu L$ cell suspension (5×10^5 cells) was subcutaneously injected into the right and left flank of NOD scid gamma (NOD.Cg- $Prkdc^{scid}$ $II2rg^{tm1Wjl}$ /SzJ) mice using a 1mL syringe with a 27 gauge needle. Mice were monitored regularly for general health and tumor growth and were sacrificed once tumors reached a size of 1cm in diameter (about two weeks post implantation).

All animal studies were conducted in compliance with European guidelines for the care and use of laboratory animals and were approved by the Institutional Animal Care and Use Committees

(IACUC) of Technische Universität München, Regierung von Oberbayern and the UK Home Office.

Immunofluorescence test for HTVI-based co-delivery of multiple plasmids to hepatocytes.

To test whether hepatocytes can be transfected simultaneously with multiple plasmids by HTVI, $Rosa26^{mTmG}$ reporter mice (8) were co-injected with two transposon constructs containing expression cassettes of Flag-YAP and Cre^{ERT2} and with hSB5 transposase vector (9). Cre^{ERT2} activation by Tamoxifen ten days post HTVI leads to conversion of the $Rosa26^{mTmG}$ allele and subsequent expression of cell-membrane localized GFP. Six month after injection, livers were embedded and sections were immunostained for Flag-YAP (M2-Flag antibody, Sigma-Aldrich; green) and GFP (GFP Tag antibody, Life Technologies; red).

Magnetic resonance imaging (MRI) screening. MRI was performed using a 3 Tesla clinical MRI system (Ingenia 3T, Philips Healthcare) with a human 8-channel wrist coil (SENSE Wrist coil 8 elements) following a previously described protocol that was adapted to the 3 Tesla scanner (10). Starting at 20 weeks after HTVI, mice were screened on a regularly basis. To this end, longitudinal T2-weighted (T2w) turbo spin-echo imaging (slice thickness=0.7mm, in-plane resolution=0.3x0.38mm², TR/TE=TR/TE=4352ms/101ms, TF=21, NSA=9, total scan duration 5.22min) was performed for tumor detection and volumetric analysis. Mice were sacrificed once tumors reached a size greater or equal 3mm in diameter.

Histology and immunohistochemistry. Histological analysis was performed for all tumors >1mm. Mouse tissues were fixed in 4% formalin solution, embedded in paraffin and cut into 2µm sections. Hematoxylin and eosin (H&E) staining was performed according to standard protocols. Immunohistochemistry was conducted using primary antibodies listed in Table S7. As secondary antibodies we used a rabbit-anti-rat antibody (1:1000, Jackson Immuno Research) and a rabbit-anti-goat antibody (1:300, DAKO) and detection was performed with the Bond Polymer Refine Detection Kit (Leica). Detailed protocols of individual staining procedures are available upon request.

DNA isolation and microdissection. DNA was isolated from tissue samples stored in RNAlater (Sigma-Aldrich) with DNeasy Blood & Tissue Kit (Qiagen) according to manufacturer's instructions. For heterogeneity analysis, we microdissected sections of Tu1 under a microscope using 20 gauche needles. DNA was isolated from the microdissected regions in the same manner as from the freshly frozen tissues mentioned above with an extended tissue lysis time of 60h.

Sequencing of sgRNA target regions. Genomic sgRNA target regions (5ng DNA per 30µL reaction) were amplified with Q5® High-Fidelity DNA Polymerase (New England Biolabs) using primers displayed in Table S8. For Sanger capillary sequencing, PCR products were purified (QIAquick PCR Purification Kit, Qiagen) and each PCR product was sequenced individually. For amplicon-based next generation sequencing, the ten (eighteen) PCR products of each sample were pooled and purified (QIAquick PCR Purification Kit, Qiagen). Library preparation was carried out as described previously (11). Briefly, after end repair and A-tailing, an Illumina paired end adapter was ligated (NEBNext® Ultra DNA Library Prep Kit for Illumina®, New England Biolabs; sequences depicted in Table S8) and the individual sample pools were barcoded with eight cycles of PCR (2x KAPA HiFi HotStart ReadyMix, Kapa Biosystems; sequences listed in Table S8). Barcoded samples were pooled and quantified with qPCR (KAPA SYBR® Fast qPCR ABI Prism Mix, Kapa Biosystems) and the single pool was sequenced (300bp, paired end) on the Illumina MiSeq Desktop Sequencer (Illumina). To verify the next generation sequencing results, we cloned the PCR products for a subset of target regions into the pCR® 2.1-TOPO® TA vector (TOPO® TA Cloning® Kit, Life Technologies). For each sample, we picked 30 colonies and sequenced them individually using Sanger capillary sequencing.

Sequencing of sgRNA off-target sites. Coordinates of potential off-target sites for the ten sgRNAs were downloaded from the CRISPR design tool (http://crispr.mit.edu; Table S13) (3). For the top five off-targets (exonic, intronic, intergenic) and (if not already included in the top five list) top three exonic off-targets of each sgRNA flanking PCR primers (Table S14) were designed. PCRs and amplicon-based next generation sequencing were performed in the same manner as described above for the sgRNA target regions.

Bioinformatic analyses. MiSeq Illumina paired 300 nucleotide reads were mapped onto *mm10* assembly with *BBMAP short read aligner* (http://bbmap.sourceforge.net) using default settings. Among a number of other tested aligners, only this particular aligner was able to map correctly large deletions, such as 178bp in Tu2 (Figure S7). BAM files were sorted and indexed with *samtools* (*v0.1.19*) (12). After mapping, only paired reads (about 3% were unpaired) were extracted based on *bitwise flag 0x2*. This resulted in BAM files containing only correctly paired reads. In order to obtain data in pileup format with the number of reads covering sites we employed *samtools* (*v0.1.6*) *pileup command with option* (*-i*) which only displays lines containing indels. Pileup files were processed with *VarScan* (*v2.3.6*) *pileup2indel command* (13).

Establishment of cancer cell lines. To derive cell lines from primary mouse cancers and metastases, tumor tissues were first washed with sterile DPBS (Life Technologies) and cut into small pieces, followed by digestion in RPMI 1640 (Life Technologies) with 10% FBS (Biochrom) and 1x PenStrep (Life Technologies), supplemented with 200 U/mL collagenase (Collagenase Type II, Worthington) at 37°C until tissue pieces were disintegrated completely. Cells were then centrifuged, resuspended in RPMI 1640 containing 10% FBS and 1x PenStrep and sown in sixwell plates coated with 0.1% gelatin (Sigma-Aldrich).

Quantitative Cas9 analysis. To detect *hSpCas9* presence in the liver samples of mice two weeks post HTVI, 7.5ng genomic DNA was used for real time quantitative PCR (SYBR® Select Master Mix, Life Technologies). *HSpCas9* copy numbers were normalized to mouse *Apolipoprotein B (ApoB)* copy numbers. Primer sequences are listed in Table S9.

Quantitative guide distribution analysis. To analyze the distribution of sgRNAs in liver samples of mice two weeks after HTVI, 10ng DNA per 20µL sample was amplified with Taq Polymerase (New England Biolabs) using *CRISPR-SB-fwd* und *CRISPR-SB-rev* primers (Table S10). PCR products were purified (QIAquick PCR Purification Kit, Qiagen) and 10pg purified PCR product was used for guide specific real time quantitative PCR (SYBR® Select Master Mix, Life Technologies). The universal forward primer (*CRISPR-SB-quant-fwd*) and the guide specific reverse primers are displayed in Table S10.

CRISPR-SB integration analysis. To test for integration of the CRISPR-SB vector into the genome of mouse liver tumors, 10ng genomic DNA per 50μL reaction was amplified (Q5® High-Fidelity DNA Polymerase, New England Biolabs) using CRISPR-SB specific primers as depicted in Table S12. Liver samples of mice two weeks post HTVI (containing episomal CRISPR-SB vectors) functioned as positive controls. 25μL of each PCR was loaded on a 1.5% agarose gel.

Fusion analysis for detection of large chromosomal deletions. To test for possible intrachromosomal fusion products caused by combinatorial sgRNA targeting, we performed PCRs spanning the potential location of the fusions as predicted by the sgRNA target sites. To this end, we used 10ng genomic DNA in 30μL PCR reactions (TaKaRa Ex Taq DNA Polymerase, Clontech) using the respective forward and reverse primers of the target sites (Table S8). Resulting PCR products were purified for Sanger capillary sequencing (QIAquick PCR Purification Kit, Qiagen). To quantify the *Cdkn2a* fusion product in regions 1, 2 and 3 of Tu1, we used 10ng DNA of the respective samples for real time quantitative PCR (SYBR® Select Master Mix, Life Technologies) with primers displayed in Table S11. Primer *Cdkn2a-ex1β-quant-fwd* with *Cdkn2a-ex2-quant-rev* was used for quantification of the fusion product and *Cdkn2a-ex2-quant-fwd* and *Cdkn2a-ex2-quant-rev* were used for quantification of other alleles at that position (wild type and with small indels).

Multicolor fluorescence in situ hybridization (M-FISH). To analyze interchromosomal fusions/rearrangements in liver tumor cell lines derived from mice injected with *hSpcas9* and sgRNAs, M-FISH was carried as described before (14).

Array comparative genomic hybridization (aCGH). aCGH was carried out using Agilent 60k mouse CGH arrays with custom design (AMADID 041078) as described previously (15). CGH data was preprocessed with the Agilent Genomic Workbench software. Raw log ratios were recentered by adding or subtracting a constant value to insure that the zero point reflects the most common ploidy state (legacy centralization option). Segmentation and aberration calling were done with the implemented ADM-2 algorithm. Normalized data was imported in R version 3.1.3 (http://www.r-project.org). For each detected aberration the closest off-targets surrounding the aberration borders down- and upstream were investigated. The distance and the number of probes between the aberration border and the predicted off-target were calculated. An

aberration was called potentially induced by an off-target if 20 probes or less are located between the aberration and the off target and the distance between them is lower than 500,000 nucleotides.

Statistics. To test if CRISPR/Cas9-induced target site mutations across tumors show a random or non-random distribution, we performed a χ^2 test. To examine if some of the targeted tumor suppressor genes undergo positive selection (in comparison to Brca1/Brca2 which serve as negative controls) we performed Fisher's Exact tests and corrected p values for multiple testing with the Benjamini Hochberg procedure. Results were considered as significant for p values <0.05.

References

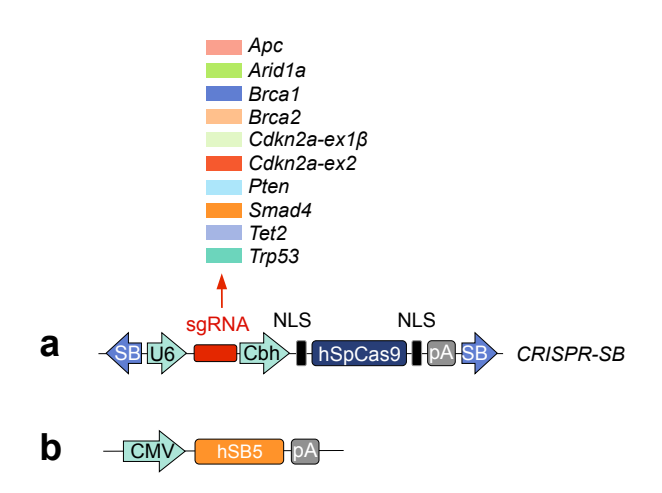
- 1. Cong L, et al. (2013) Multiplex genome engineering using CRISPR/Cas systems. *Science* 339(6121):819-823.
- 2. Yant SR, et al. (2000) Somatic integration and long-term transgene expression in normal and haemophilic mice using a DNA transposon system. *Nature genetics* 25(1):35-41.
- 3. Hsu PD, et al. (2013) DNA targeting specificity of RNA-guided Cas9 nucleases. *Nature biotechnology* 31(9):827-832.
- 4. Wang H, et al. (2013) One-step generation of mice carrying mutations in multiple genes by CRISPR/Cas-mediated genome engineering. *Cell* 153(4):910-918.
- 5. Ran FA, et al. (2013) Genome engineering using the CRISPR-Cas9 system. *Nature protocols* 8(11):2281-2308.
- 6. Postic C, et al. (1999) Dual roles for glucokinase in glucose homeostasis as determined by liver and pancreatic beta cell-specific gene knock-outs using Cre recombinase. *The Journal of biological chemistry* 274(1):305-315.
- 7. Hingorani SR, et al. (2003) Preinvasive and invasive ductal pancreatic cancer and its early detection in the mouse. *Cancer cell* 4(6):437-450.
- 8. Muzumdar MD, Tasic B, Miyamichi K, Li L, & Luo L (2007) A global double-fluorescent Cre reporter mouse. *Genesis* 45(9):593-605.
- 9. Ehmer U, et al. (2014) Organ Size Control Is Dominant over Rb Family Inactivation to Restrict Proliferation In Vivo. *Cell reports* 8(2):371-381.
- 10. Braren R, et al. (2011) Validation of preclinical multiparametric imaging for prediction of necrosis in hepatocellular carcinoma after embolization. *Journal of hepatology* 55(5):1034-1040.
- 11. Quail MA, Swerdlow H, & Turner DJ (2009) Improved protocols for the illumina genome analyzer sequencing system. *Current protocols in human genetics / editorial board, Jonathan L. Haines ... [et al.]* Chapter 18:Unit 18 12.

- 12. Li H, et al. (2009) The Sequence Alignment/Map format and SAMtools. *Bioinformatics* 25(16):2078-2079.
- 13. Koboldt DC, *et al.* (2009) VarScan: variant detection in massively parallel sequencing of individual and pooled samples. *Bioinformatics* 25(17):2283-2285.
- 14. Jentsch I, Adler ID, Carter NP, & Speicher MR (2001) Karyotyping mouse chromosomes by multiplex-FISH (M-FISH). *Chromosome research : an international journal on the molecular, supramolecular and evolutionary aspects of chromosome biology* 9(3):211-214.
- 15. Wolf MJ, et al. (2014) Metabolic activation of intrahepatic CD8+ T cells and NKT cells causes nonalcoholic steatohepatitis and liver cancer via cross-talk with hepatocytes. Cancer cell 26(4):549-564.

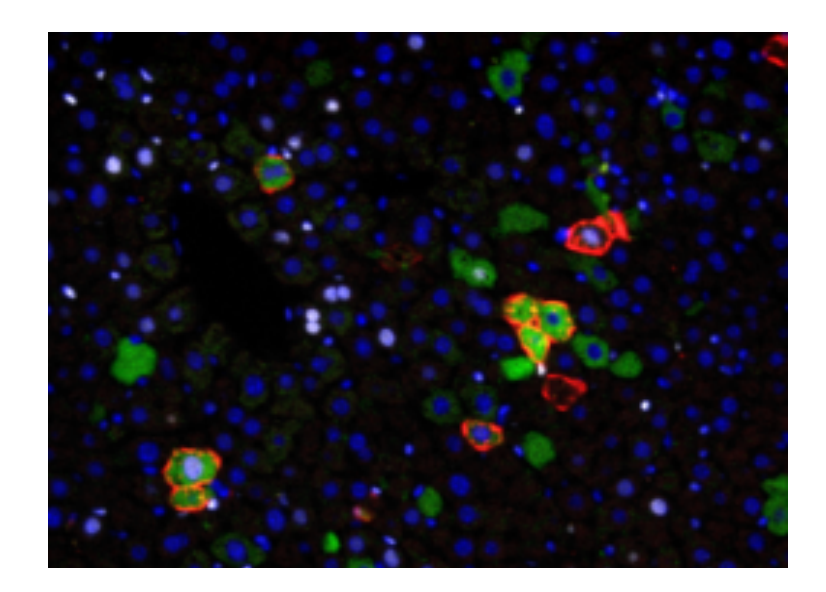
Weber et al., CRISPR/Cas9 somatic multiplex-mutagenesis for highthroughput functional cancer genomics in mice

Supplementary Figures

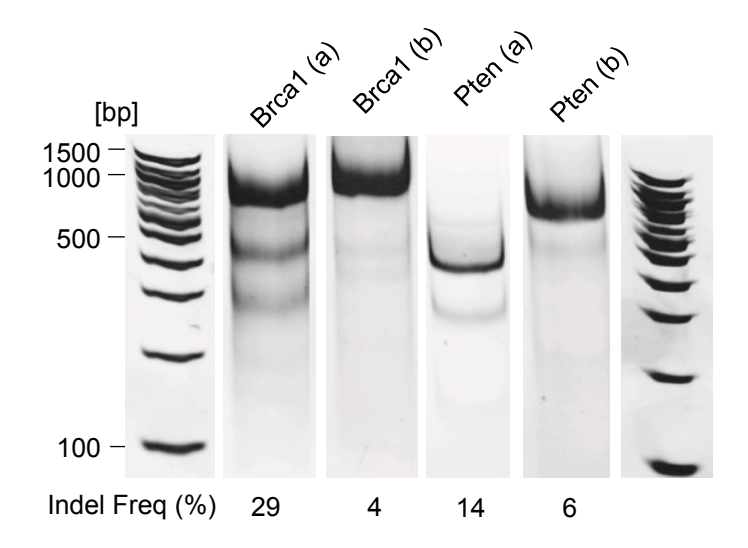
Supplementary Figure S1. Vectors used for hepatic delivery of multiplexed CRISPR/Cas9 for somatic mutagenesis in mice. (A) CRISPR-SB bicistronic expression vector consisting of a U6 promoter-driven single guide RNA (sgRNA) and a CBA (chicken β -actin) hybrid intron (CBh) promoter-driven human codon-optimized Streptococcus pyogenes Cas9 (hSpCas9) flanked by Sleeping Beauty (SB) inverted terminal repeats. (B) A cytomegalovirus (CMV) promoter-driven Sleeping Beauty transposase (hSB5) can mobilize/integrate the CRISPR-SB vector into the liver cell genome. NLS, nuclear localization signal; pA, polyadenylation signal.



Supplementary Figure S2. Simultaneous delivery of multiple vectors into hepatocytes upon hydrodynamic tail vein injection (HTVI). Rosa26^{mTmG} reporter mice were co-injected with hSB5 transposase vector and with two transposon constructs containing expression cassettes of Flag-YAP and Cre^{ERT2}. Cre^{ERT2} activation by Tamoxifen 10 days post HTVI leads to conversion of the Rosa26^{mTmG} allele and subsequent expression of cell-membrane localized GFP. Six month after injection, livers were embedded and sections were immunostained for Flag-YAP (M2-Flag antibody, Sigma-Aldrich; green) and GFP (GFP Tag antibody, Life Technologies; red).



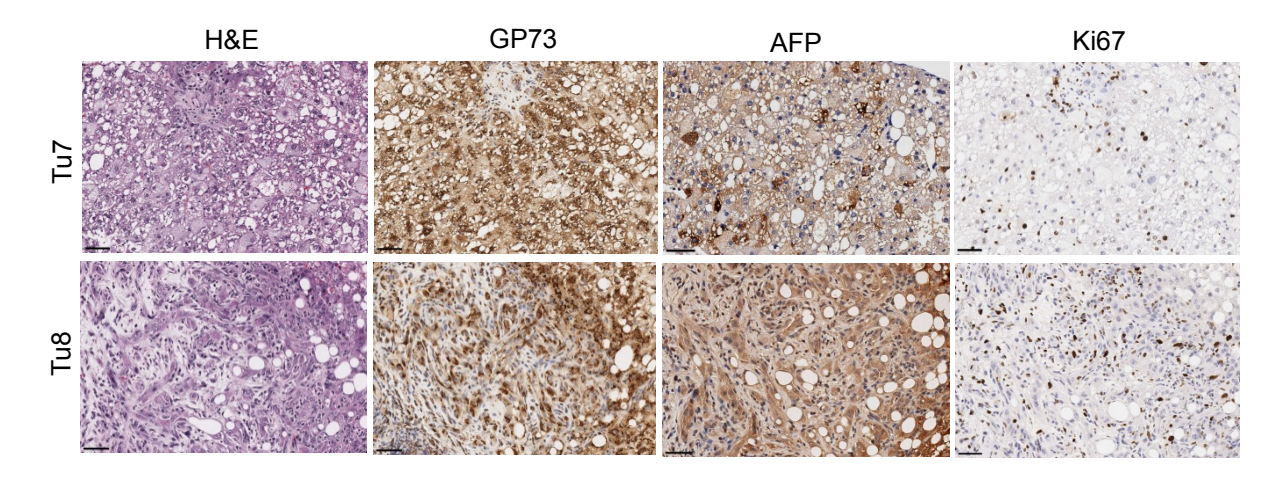
Supplementary Figure S3. Identification of suitable sgRNAs for somatic mutagenesis. Prior to *in vivo* application, multiple sgRNAs per gene were tested for their efficiency to induce frameshift-causing mutations in combination with transiently expressed Cas9. Indel frequencies were determined upon T7E1 assays in a mouse pancreatic cancer cell line. Results were used to choose the most efficient sgRNAs for *in vivo* application (in these instances: *Brca1(a)* and *Pten(a)*).



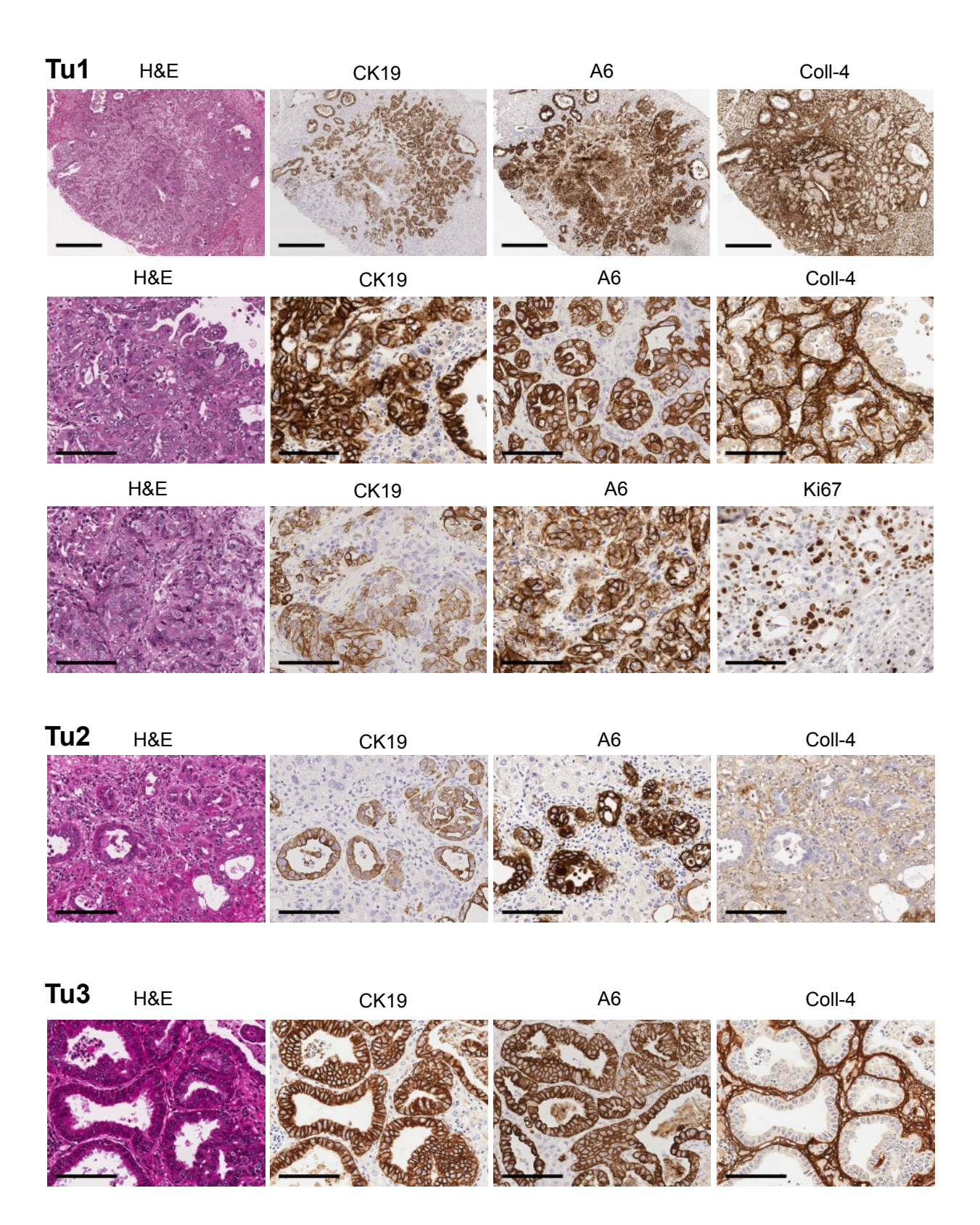
Supplementary Figure S4. Microscopic images of hepatocellular carcinomas. Representative microscopic images of hepatocellular carcinomas (HCCs) derived from mice injected with *hSpCas9* and ten sgRNAs.

Tu7 (upper panels), a moderately differentiated HCC with trabecular to solid growth pattern (H&E staining; first image), shows strong *Golgi phosphoprotein 2/Golgi membrane protein GP73* (GOLM1/GP73) expression (second image) and high proliferation activity (Ki67 staining; forth image). α -fetoprotein (AFP) is expressed slightly by the majority of tumor cells, scattered neoplastic cells show a strong expression of AFP (third image).

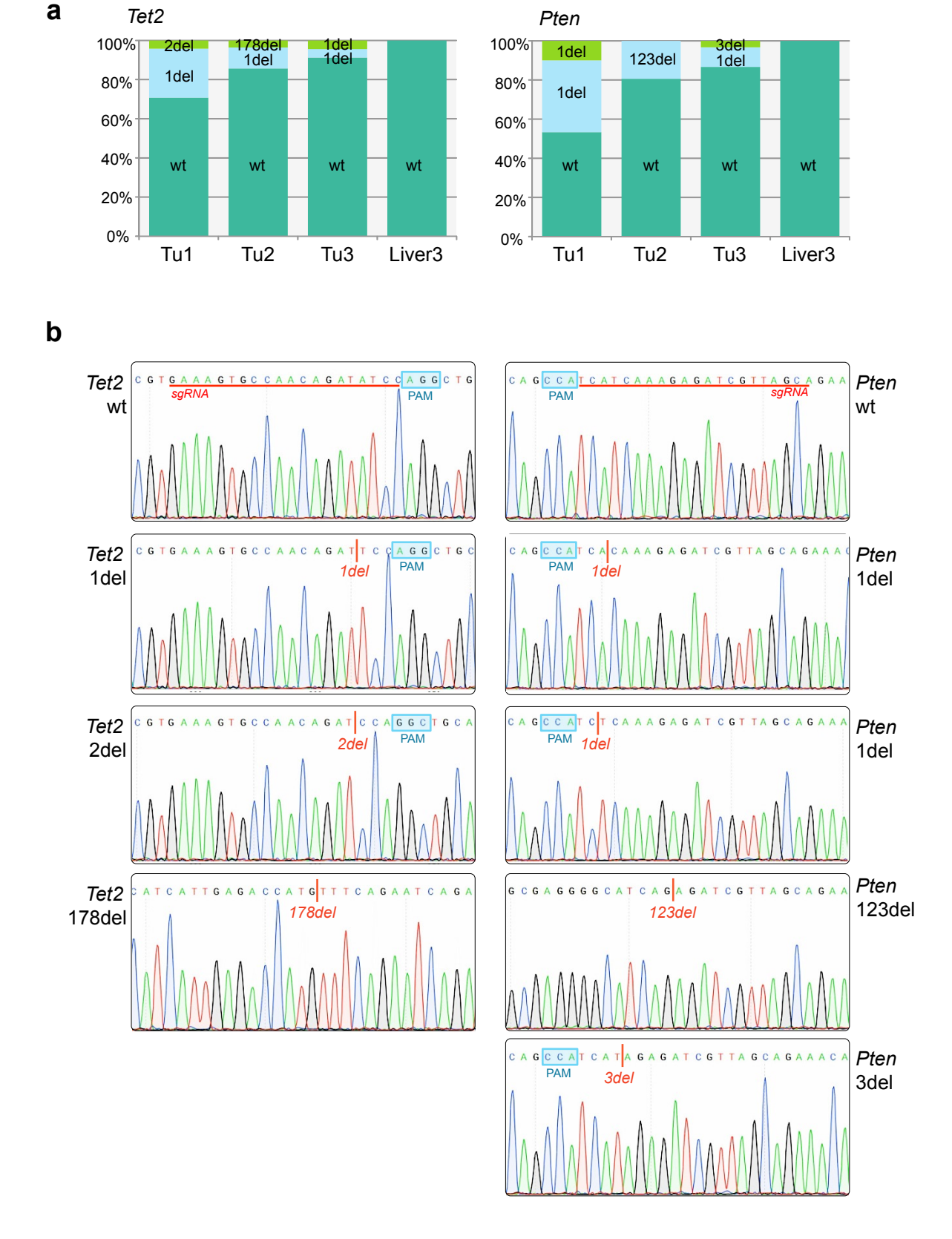
Tu8 (lower panels), a poorly differentiated HCC, shows fatty changes and a slight to moderate fibroplasia (H&E staining; first image). Tumor cells strongly express GP73 (second image) and show a very high proliferative activity (Ki67 staining; forth image). AFP is expressed with slight to moderate intensity by the majority of neoplastic cells (third image). Bars, 50µm.



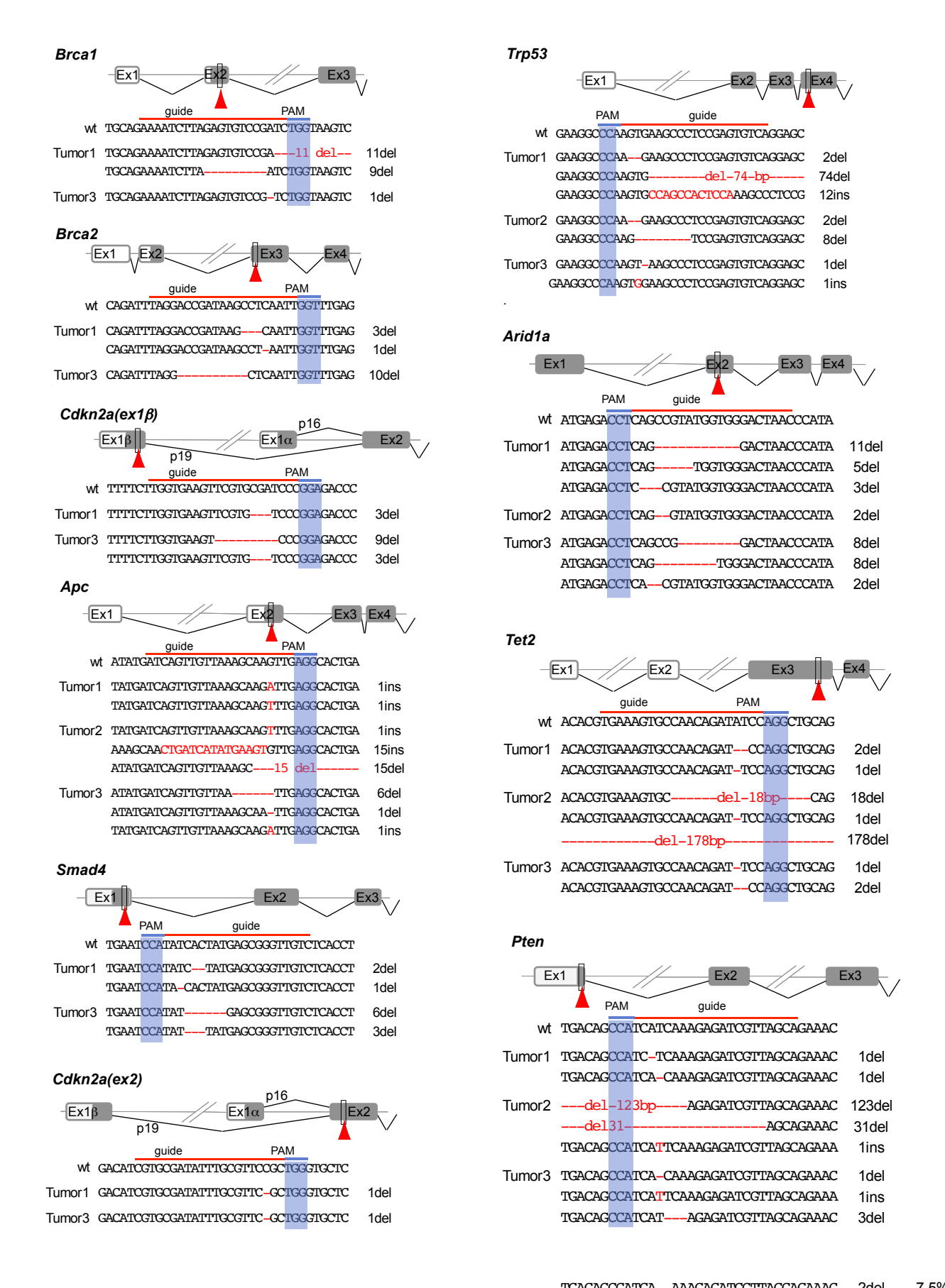
Supplementary Figure S5. Histology and IHC stainings of three intrahepatic cholangiocarcinomas (ICC). Tu1: Moderately to poorly differentiated ICC with a tubular growth pattern in the tumor periphery (middle panels) and cord-like to solid growth pattern in the central part (lower panels). Tumor cells intensely express cytokeratin 19 (CK19) and A6 (oval cell surface antigen). Collagen-4 (Coll-4) is strongly expressed in tumor-associated stroma. Tumor cells show a high proliferation rate (Ki67 in bottom right image). Bars, 400µm (upper row), 100µm (middle and lower row). Tu2: Well to moderately differentiated ICC with strong expression of CK19, A6. Coll-4 is expressed in the tumor-associated stroma. Bars, 100µm. Tu3: Well differentiated ICC. Bars, 100µm.



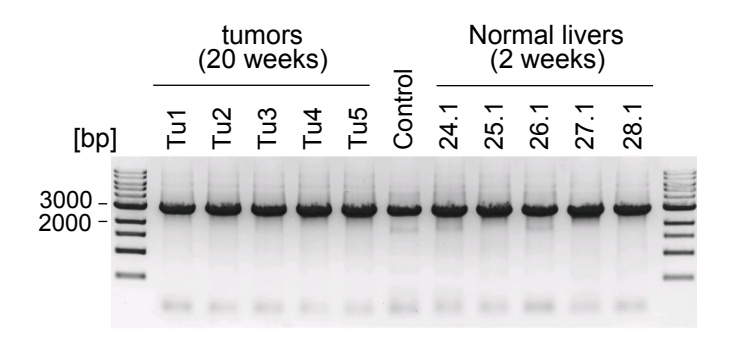
Supplementary Figure S6. Validation of NGS data by Sanger capillary sequencing of PCR-amplified sgRNA target regions. Data are shown for *Tet2* and *Pten* in Tu1, Tu2 and Tu3 as well as in healthy liver sample of a tumor-bearing mouse. PCR products of sgRNA target sites have been cloned into *E. coli* and 30 clones per target site and tumor were subjected to Sanger capillary sequencing. (A) Bar charts display percentages of wild type (wt) clones and clones with respective indels. (B) Graphical display shows alignment of the sequence traces with wt sequence using SnapGene® 2.4.3. Sanger sequencing confirmed the results from NGS, which also identified in some cases additional lower-frequency indels (see Figure S8), as expected.



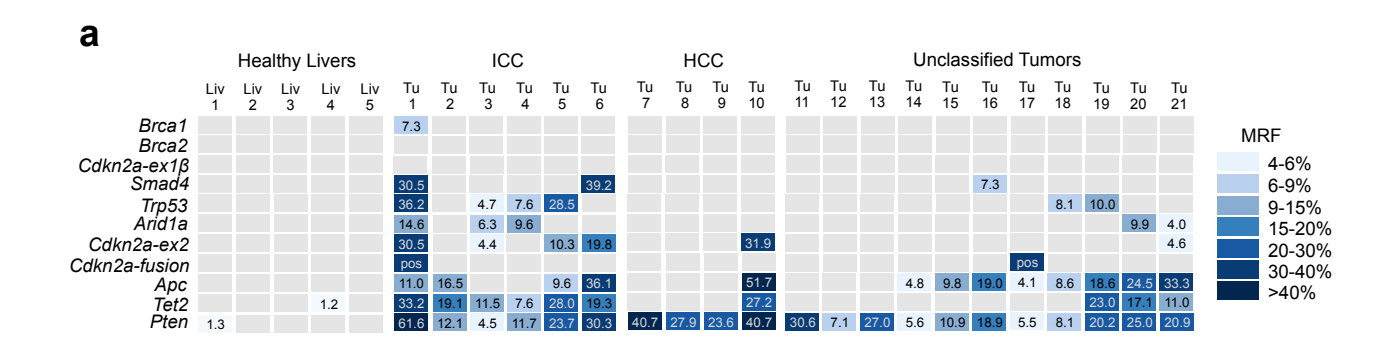
Supplementary Figure S7. Schematic view of indels induced by multiplexed CRISPR/Cas9 mutagenesis in mice. The schemes display all mutant target site sequences with frequencies above 1% in Tu1-Tu3 (the data relate to experiments described in figures 1 and 2; cancers induced by ten sgRNA multiplexing). For each mutation the altered sequence is marked in red. Note that mutations in *Brca1* and *Brca2* are either in-frame or have very low MRFs that do not exceed background mutation frequencies in healthy livers, except the 11del mutation in *Brca1* (see also Fig. S8 and Figure 2).

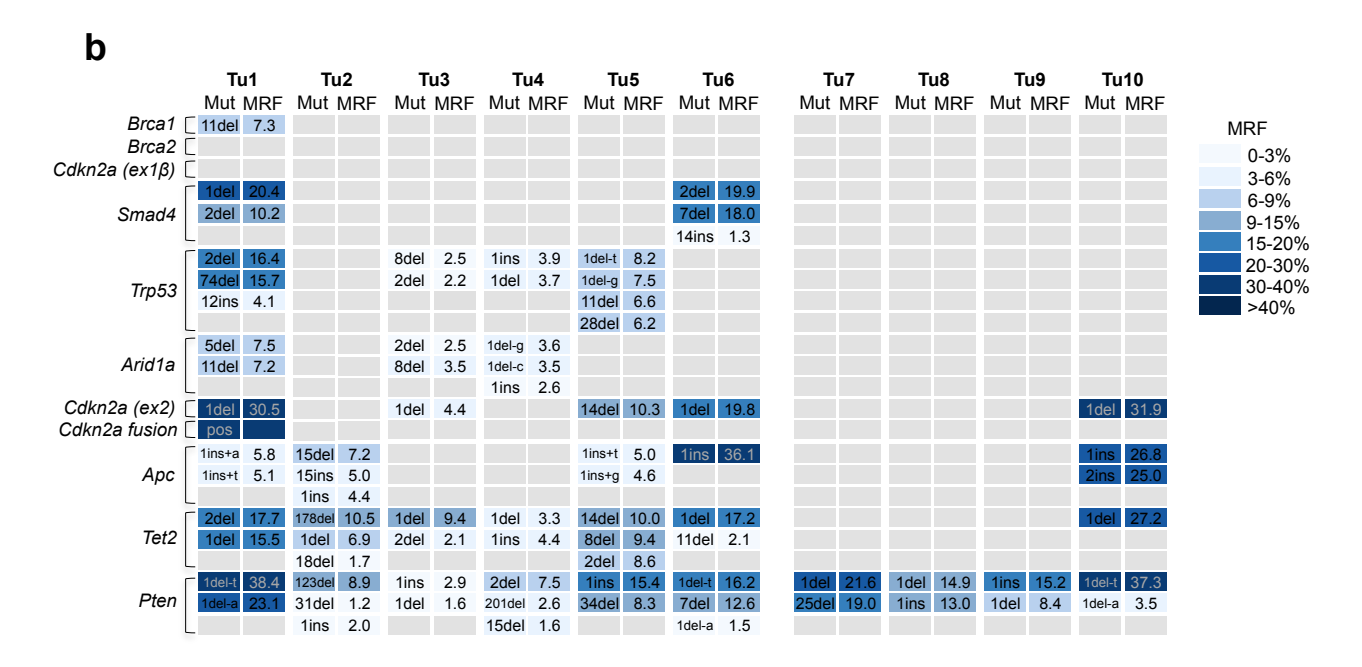


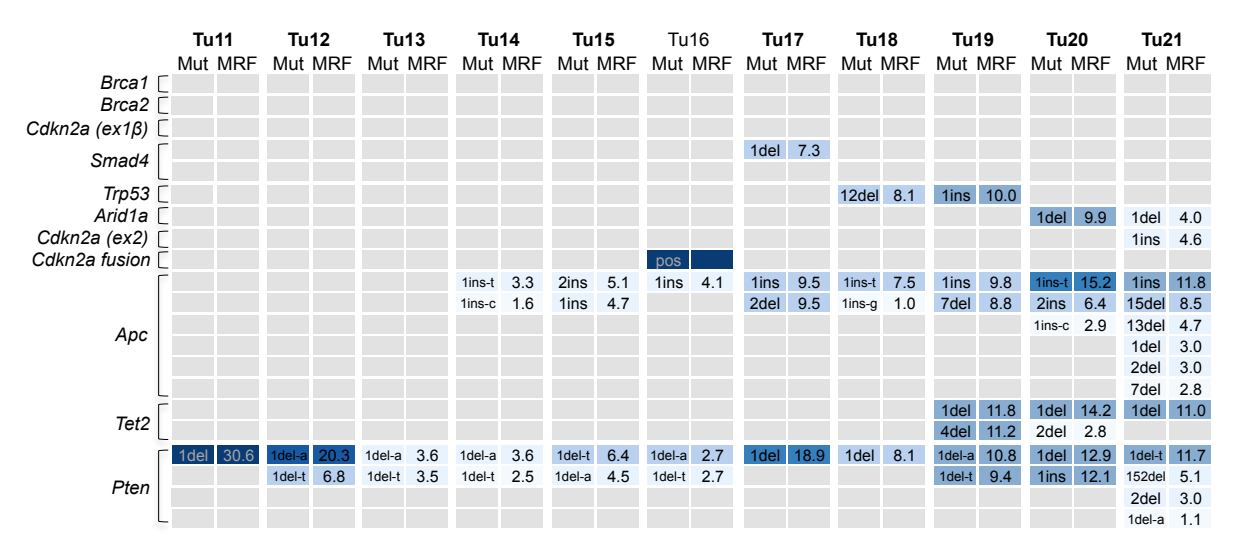
Supplementary Figure S8. Screening for large deletions at the *Cdkn2a* locus in tumors and healthy liver samples. Analysis of the *Cdkn2a-ex2* target site using long-range PCR (2900bp) was performed to screen for large deletions that could span a region beyond the standard PCR-amplified and sequenced 400-500 base pairs around target sites. No large deletion at this site could be found in any of the analysed CRISPR/Cas9-induced tumor samples or normal livers.



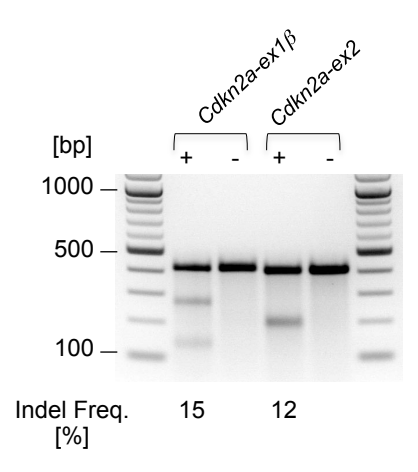
Supplementary Figure S9. Description of all frame shift causing indels in liver tumors of mice injected with *hSpCas9* and ten sgRNAs. (A) Cumulative indel frequencies above 4% are displayed for individual target sites (as also shown in figure 2). In (B) all different mutations at individual target sites are displayed separately and mutant read frequencies (MRF) are shown individually.



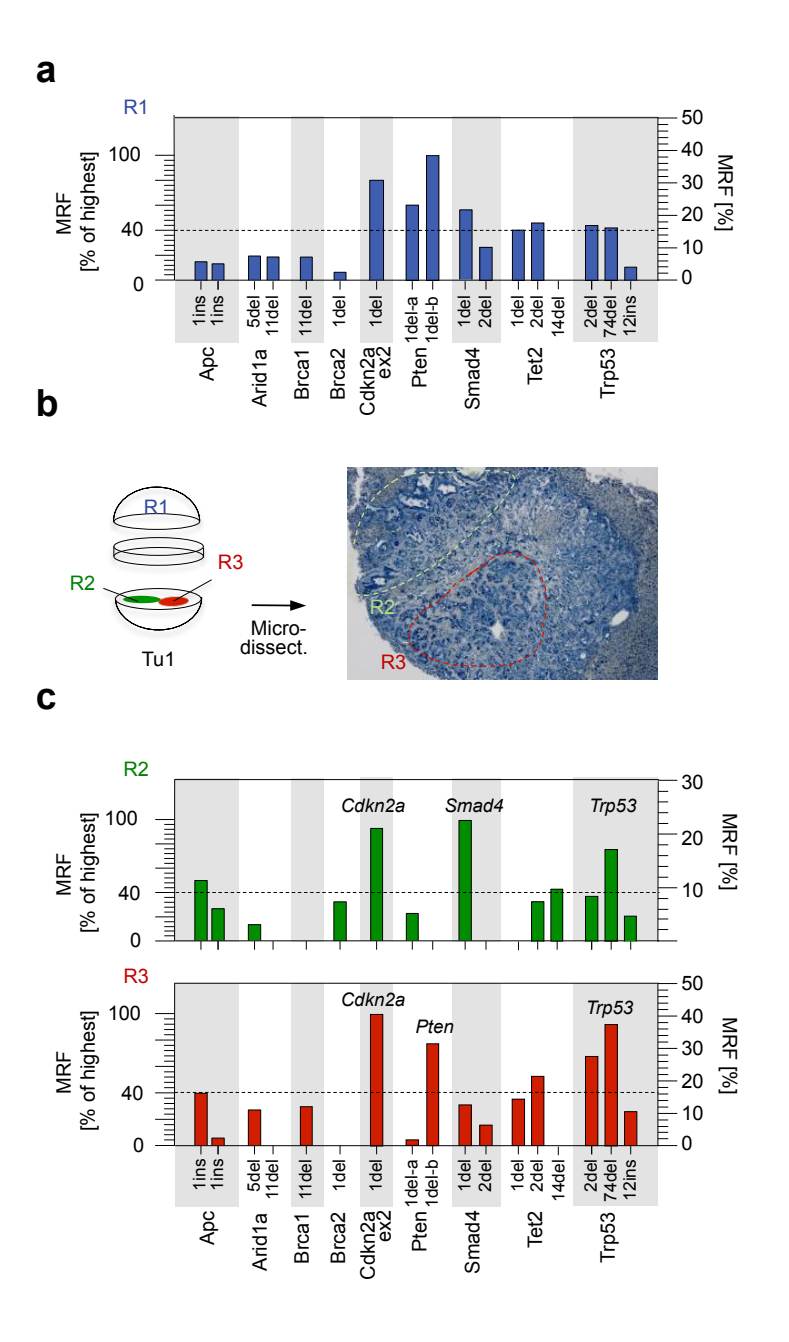




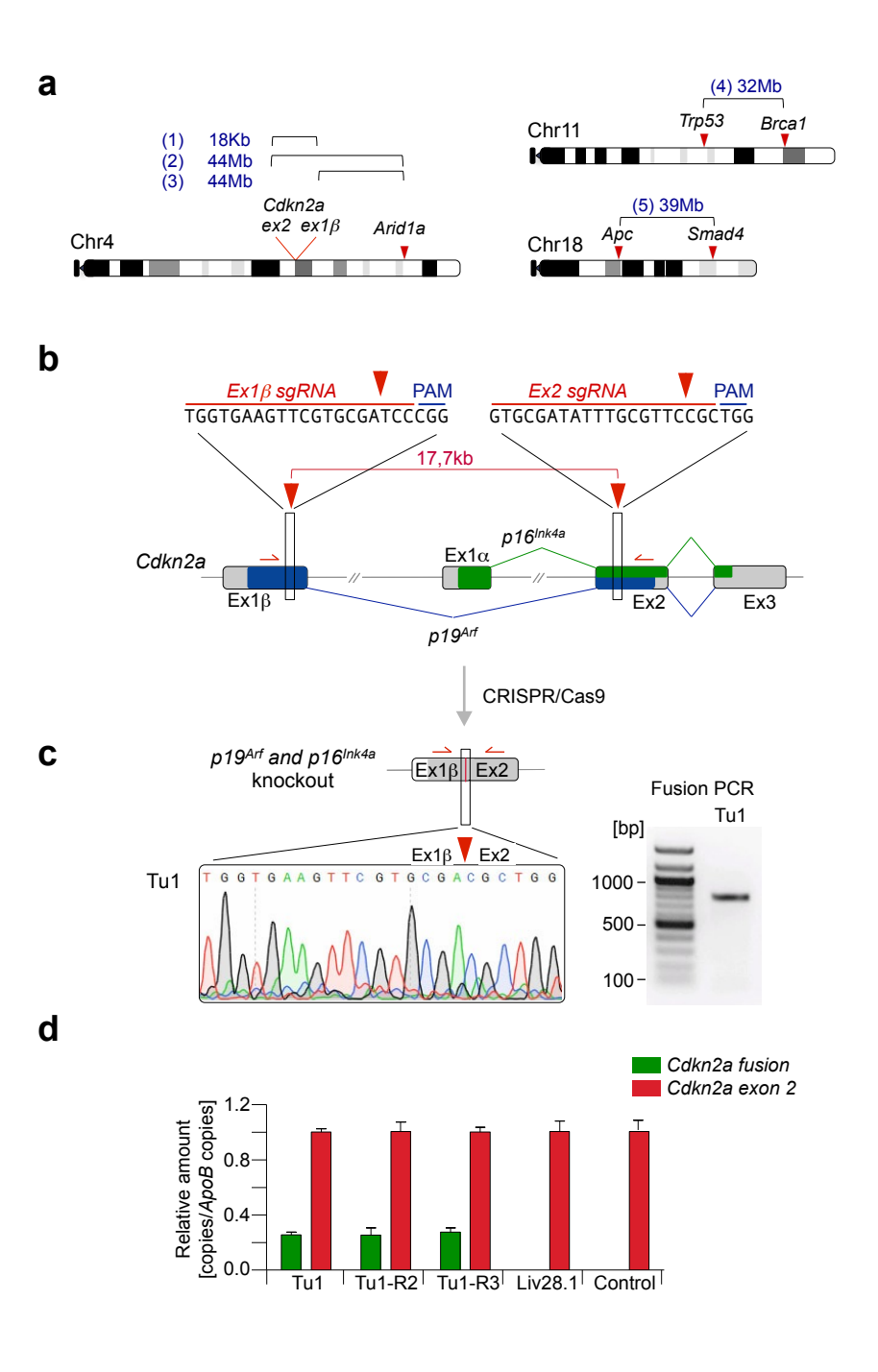
Supplementary Figure S10. Comparison of sgRNA targeting efficiencies at Cdkn2a-ex1 β and Cdkn2a-ex2. Efficiencies of the two sgRNAs targeting the Cdkn2a locus were assessed using Surveyor assays in murine pancreatic cancer cell lines upon transient transfection of CRISPR-SB plasmid as described in the Methods section. The mouse pancreatic cancer cell line 4072-PPT was chosen because it had - in contrast to most other available mouse cancer cell lines - an intact Cdkn2a locus. (+) Cell line transfected with the sgRNA as indicated above; (-) cell line transfected with the non-targeting sgRNA served as a negative control. The results show that mutation of $p19^{Arf}$ (using Cdkn2a-ex1 β sgRNA) or induction of the $p19^{Arf}/p16^{lnk4a}$ double-mutant (using Cdkn2a-ex2 sgRNA) are equally efficient.



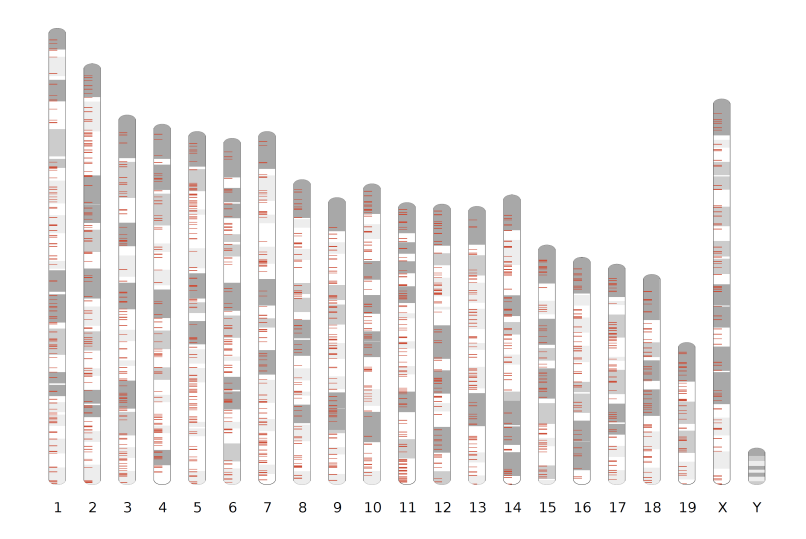
Supplementary Figure S11. Analysis of intratumor heterogeneity in a CRISPR/Cas9-induced cancer. (A) Mutant read frequencies (MRF) of frame shift causing indels detected at target sites in region-1 (R1, blue) of Tu1. (B) Regions of Tu1 used for heterogeneity analysis. R1 contains a large proportion of the tumor, R2 and R3 were microdissected. (C) MRF of frame shift causing indels for R2/R3.



Supplementary Figure S12. Intrachromosomal fusions induced by combinatorial sgRNA targeting in mice. (A) Scheme of all chromosomes with two or more CRISPR/Cas9 target sites in the ten sgRNA multiplexing approach. All targeted genes are listed in Figure 1. Out of the 105 possible deletions in 21 tumors we found evidence for fusion products between the *Cdkn2a-ex1β* and *Cdkn2a-ex2* sgRNA target sites in three cancers (see also Figure 2). In all three cases the resulting deletion of approximately 18kb led to inactivation of both *p16*^{Ink4a} and *p19*^{Arf}. (B) Scheme of *Cdkn2a* dual targeting using 2 sgRNAs. (C) Example of the PCR-amplified fusion product and its sequence trace resulting from deletion of the 17.7kb fragment in Tu1. Red arrows indicate primers. (D) Relative copy numbers of the fusion allele in comparison to other *Cdkn2a-ex2* alleles (including wild type and alleles with small indels) in Tu1, as determined by gPCR. Error bars, SEM from triplicate determinations.

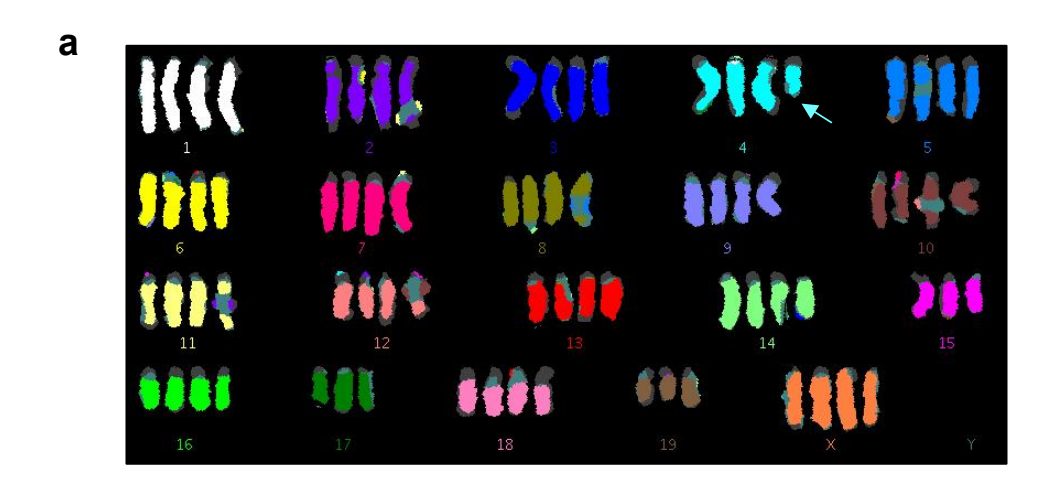


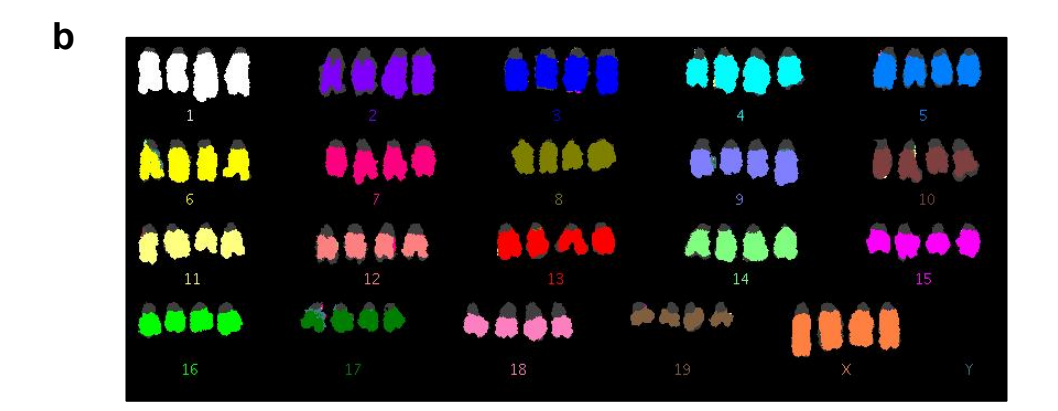
Supplementary Figure S13. Analysis of off-target effects resulting in intrachromosomal deletions. Array CGH was performed on six different tumors and analysed for aberrations (see Methods section). Intrachromosomal deletions were screened for 18 on-target and 1550 off-target sites which are distributed throughout all chromosomes.

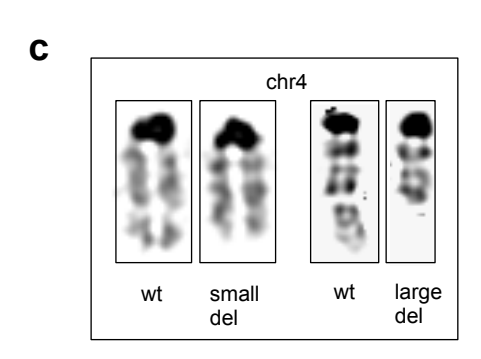


Supplementary Figure S14. M-FISH analysis of tumor cell lines. To analyze potential interchromosomal rearrangements in liver tumor cell lines derived from mice injected with *hSpCas9* and sgRNAs, multicolor in situ hybridization (M-FISH) was performed.

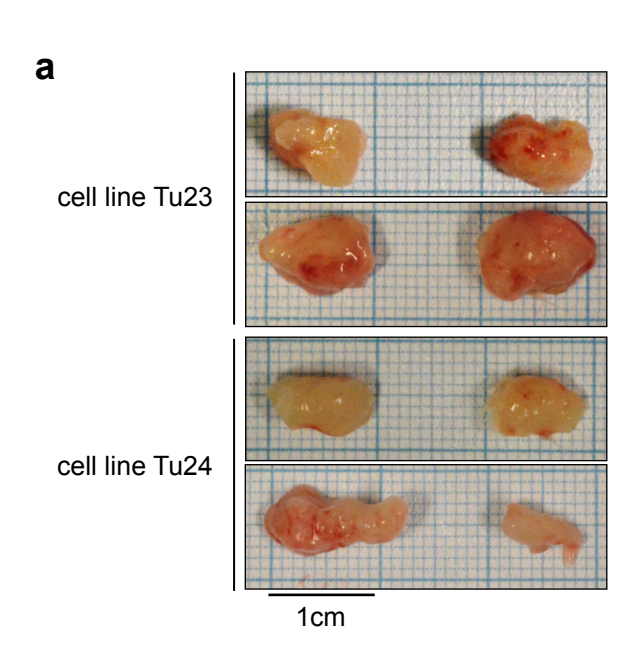
M-FISH analysis revealed a tetraploid stable chromosome set for both analyzed cell lines (a, cell line Tu23; b, cell line Tu24). The composite karyotype for cell line Tu23 is 77,XXXX,Del(4),-15,17,-19 (a) and for cell line Tu24 80,XXXX (b). For Tu23, the CRISPR/Cas9 induced large deletion on chromosome 4 is clearly visible in one out of four chromosomes (a, arrow). Further analysis of additional metaphases of cell line Tu23 confirms three different states of chromosome 4 as already identified by PCR: 1. without any visible alterations (wt), 2. with the CRISPR/Cas9 induced 17Mb deletion (small del; *Arid1a-Errfi1* fusion) and 3. with the CRISPR/Cas9 induced 62Mb deletion (large del; *Cdkn2b-Errfi1* fusion) (c).

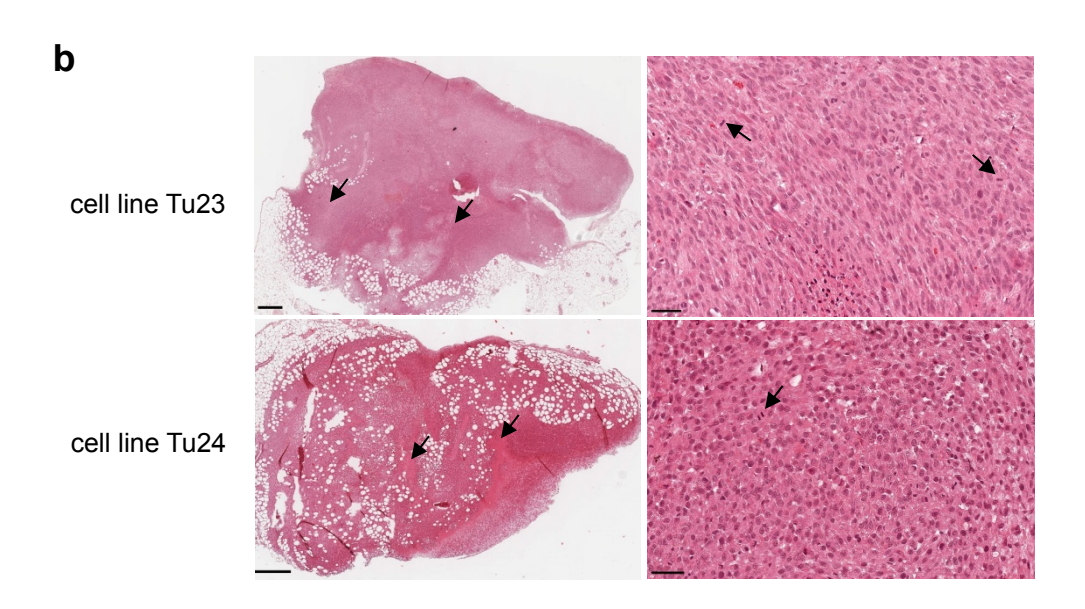




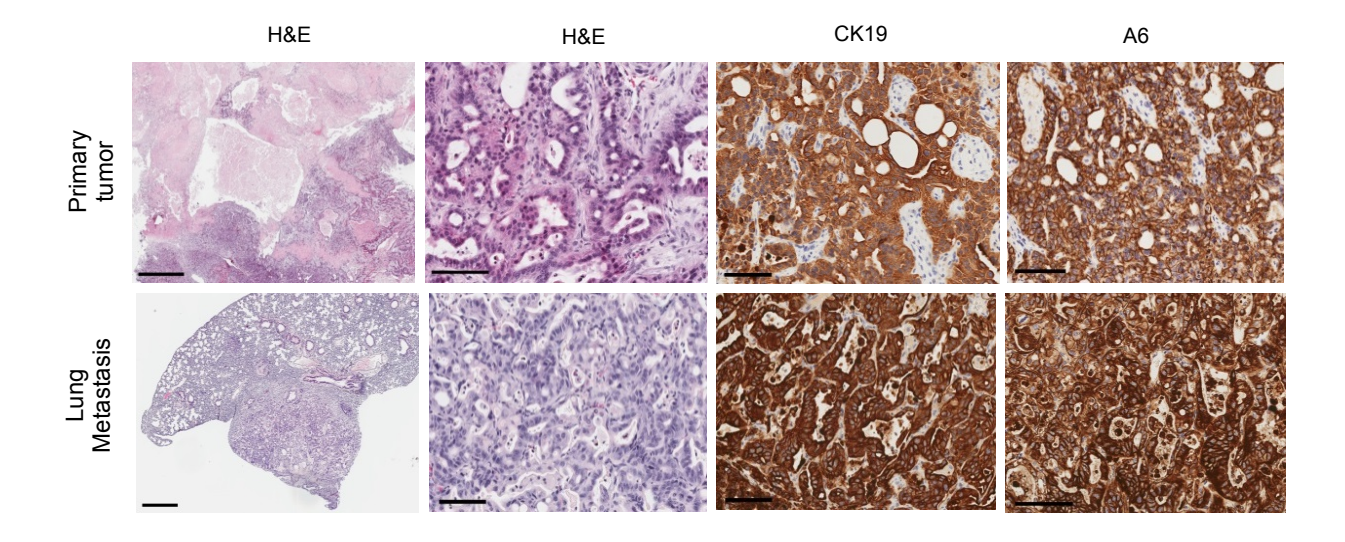


Supplementary Figure S15. Subcutaneous implantation of tumor cell lines. Cell lines derived from two primary intrahepatic cholangiocarcinomas (Tu23 and Tu24; 5x10⁵ cells/implantation) were implanted subcutaneously into the right and left flanks of NOD scid gamma (NOD.Cg-Prkdcscid Il2rgtm1Wjl/SzJ) mice. (A) All mice developed tumors (n=4 per cell line) up to 1cm in diameter within two weeks after implantation. (B) Representative microscopic H&E images of the allograft tumors. The neoplasias show a solid growth pattern with infiltration of the adjacent adipose tissue (left panel) and multifocal necroses (arrows, left panel). The tumor cells are elongated (cell line Tu23, upper left image) or polygonal (cell line 24, lower left image) with a high number of mitoses (arrows, right panel). Bars, 500µm left panels, 50µm right panels.





Supplementary Figure S16. Microscopic images of Tu24 and a corresponding lung metastasis. Moderately to poorly differentiated intrahepatic cholangiocarcinoma (ICC) with extensive central necrosis (upper panels). Tumor cells intensely express cytokeratin 19 (CK19) and A6 (oval cell surface antigen). Subpleural metastasis of the moderately to poorly differentiated cholangiocarcinoma (lower panels). The metastasis shows a tubular growth pattern with CK19 and A6 positivity, as seen in the primary tumor. Bars, 100µm except upper left: 500µm and lower left: 1mm.



Weber et al., CRISPR/Cas9 somatic multiplex-mutagenesis for highthroughput functional cancer genomics in mice

Supplementary Tables

Supplementary Table 1. Literature-based analysis of tumor suppressor gene alterations in human

liver cancers. A systematic literature-based analysis of tumor suppressor gene alterations in human intrahepatic cholangiocarcinoma (ICC) (A) and hepatocellular carcinoma (HCC) (B) was performed. The tables show alterations found in the ten tumor suppressor genes targeted with CRISPR/Cas9 in the mouse liver using hydrodynamic tail vein injection (HTVI). We used information about mutated genes (MUT) found in recent whole genome/whole exome sequencing studies and about genes being described to be located in commonly deleted regions (DEL) or to be silenced by promoter methylation (PM). In addition, studies analyzing expression of the respective proteins in ICC/HCC (LOSS; loss of expression) were taken into account. For APC, WNT pathway activation (WNT) in ICC was studied.

Α

Gene	Туре	Range [%]	References
APC	PM WNT - reduced membranous expression of β-catenin - aberrant nuclear expression of β-catenin	26.6 - 47.2 82 15	(1, 2) (3) (3)
ARID1A	MUT	9 - 35.5	(4-7)
BRCA1	мит	0 - 3.6*	(4-7)
BRCA2			
CDKN2A	MUT PM LOSS DEL	0 - 5.6 15.7 - 83.0 35.7 18.0	(4-7) (1, 2, 8, 9) (10) (11)
PTEN	MUT PM	0 - 10.7 35.3	(4-7) (8)
SMAD4	MUT LOSS	0 - 16.7 45.2	(4-7) (10)
TET2			
TP53	MUT PM	6 - 44.4 61.1	(4-7) (12)

^{*} Only 1 Brca1 mutation in 1 patient

Legend

loss of expression LOSS DEL large deletions

mutations found in exome sequencing studies MUT

PM promoter methylation WNT Wnt pathway activation

References

- B. Yang, M. G. House, M. Guo, J. G. Herman, D. P. Clark, Modern pathology 18, 412 (2005).
- S. Lee, W. H. Kim, H. Y. Jung, M. H. Yang, G. H. Kang, The American journal of pathology 161, 1015 (2002). 2.
- 3. K. Sugimachi et al., Modern pathology, 900 (2001).
- B. Goeppert et al., *Hepatology* 59, **544** (2014). 4.
- 5. Y. Jiao et al., Nature genetics 45, 1470 (2013).
- 6. W. Chan-On et al., Nature genetics 45, 1474 (2013).
- 7. C. K. Ong et al., Nature genetics 44, 690 (2012).
- 8. J. S. Ross et al., The oncologist 19, 235 (2014). 9.
- R. Sriraksa et al., British journal of cancer 104, 1313 (2011).
- 10. A. Tannapfel et al., Gut 47, 721 (2000).
- Y. K. Kang, W. H. Kim, J. J. Jang, Human pathology 33, 877 (2002). 11.
- 12. D. Sia et al., Gastroenterology 144, 829 (2013).
- L. Xiaofang, T. Kun, Y. Shaoping, W. Zaiqiu, S. Hailong, World journal of surgical oncology 10, 5 (2012). 13.

Gene	Туре	Range [%]	References
	MUT	0 – 3.0	(13-20)
APC	DEL	0 - 0.5	(13-15, 18)
	LOSS	53.0	(21)
ARID1A	MUT	2.0 – 16.0	(13-20)
AKIDTA	DEL	0 – 1.4	(13-15, 18)
BRCA1	MUT	0 – 2.0	(13-20)
BRCAT	DEL	0 - 0.3	(13-15, 18)
BRCA2	MUT	0 - 5.7	(13-20)
BROAZ	DEL	0 - 0.8	(13-15, 18)
	MUT	0 - 2.9	(13-20)
CDKN2A	DEL	4.0 - 6.4	(13-15, 18)
ODMINZA	PM	17.6	(22)
	LOSS	72.2	(22)
	MUT	0 - 4.0	(13-20)
PTEN	DEL	4.0	(13-15, 18)
7 7 2 14	PM	16.1	(23)
	LOSS	40.9 – 57.1	(24, 25)
SMAD4	MUT	0 - 0.9	(13-20)
OHIAD4	DEL	0 - 0.8	(13-15, 18)
TET2	MUT	0 - 2.0	(13-20)
	DEL	0 - 0.8	(13-15, 18)
TP53	MUT	18 - 51.8	(13-20)
11 00	DEL	0 - 3.0	(13-15, 18)

Legend

LOSS loss of expression large deletions DEL

mutations found in exome sequencing studies MUT

РМ promoter methylation

References

- 14.
- 15.
- E. Cerami et al., Cancer discovery 2, 401 (2012).
 J. Gao et al., Science signaling 6, pl1 (2013).
 C. Guichard et al., Nature genetics 44, 694 (2012).
 A. Fujimoto et al., Nature genetics 44, 760 (2012). 16.
- 17.
- J. Huang et al., Nature genetics 44, 1117 (2012). K. Schulze et al., Nature genetics 47, 505 (2015). 18.
- 19. 20.
- S. P. Cleary et al., Hepatology 58, 1693 (2013). Z. Kan et al., Genome research 23, 1422 (2013).
- 21.
- 22.
- B. Yang, M. Guo, J. G. Herman, D. P. Clark, The American journal of pathology 163, 1101 (2003). K. Fukai et al., Liver international: official journal of the International Association for the Study of the Liver 23. 25, 1209 (2005).

 L. Wang et al., Hepatology research : the official journal of the Japan Society of Hepatology 37, 389 (2007).
- 24.
- Y. Totoki et al., Nature genetics 43, 464 (2011). 25.
- T. H. Hu et al., Cancer 97, 1929 (2003). 26.

Supplementary Table 2. Indel analysis in healthy livers and liver tumors derived from mice injected with *hSpCas9* and ten sgRNAs. *CRISPR-SB* vectors expressing *hSpCas9* and ten sgRNAs (targeting ten different tumor suppressor genes) were delivered into livers of *Alb-Cre;Kras^{LSL-G12D/+}* mice using hydrodynamic tail vein injection (HTVI). 20 to 30 weeks post HTVI, mice developed liver tumors (ICCs and HCCs). DNA was isolated from healthy livers of tumor-bearing mice (n=5; Liver1-Liver5) and liver tumors (n=21; Tu1-Tu21) (see Figure 2). CRISPR/Cas9 target regions were amplified and sequenced using amplicon-based next-generation sequencing (see Methods section). The table below shows all indels derived from healthy livers of tumor-bearing mice and liver tumors detected with a mutant read frequency (MRF) of 0.2% or higher. This cut-off was set to account for technical sequencing errors.

Liver 1				
Gene	MRF	Mut	Position	Indel
Brca1	0.23%	68del	11: 101549019	-CGGATA
Apc	0.20%	27del	18: 34261044	-AGTTGA
Apc	0.21%	1del	18: 34261059	-Т
Apc	0.25%	1ins	18: 34261059	+A
Apc	0.55%	1ins	18: 34261059	+T
Trp53	0.22%	11del	11: 69587432	-GCCGAA
Trp53	0.22%	3del	11: 69587440	-GAA
Arid1a	0.36%	1del	4: 133723009	-C
Tet2	0.37%	11del	3: 133485654	-TGGTGT
Tet2	0.20%	2del	3: 133485657	-AT
Tet2	0.73%	1del	3: 133485658	-T
Pten	0.50%	14del	19: 32758455	-CATTCG
Pten	1.30%	1del	19: 32758456	-A
Pten	0.27%	1del	19: 32758457	-T
Liver 2				
Gene	MRF	Mut	Position	Indel
Cdkn2a(Ex2)	0.21%	7del	4: 89276737	-GCGGAAC
Pten	0.67%	23del	19: 32758440	-AGAAAG
Pten	0.83%	1ins	19: 32758457	+T
Liver 3				
Gene	MRF	Mut	Position	Indel
Pten	0.48%	11del	19: 32758457	-TCAATC
Pten	0.31%	2del	19: 32758458	-CA
Liver 4				
Gene	MRF	Mut	Position	Indel
Smad4	0,95%	3del	18: 73675798	-GTG
Apc	0,29%	6del	18: 34261053	-AGCAAG
Apc	0,27%	1ins	18: 34261058	+G
Apc	0,37%	1ins	18: 34261059	+T
Trp53	0,68%	1del	11: 69587439	-Т
Trp53	0,52%	28del	11: 69587440	-GAACTG
Trp53	0,66%	1del	11: 69587440	-G
Trp53	0,66%	11del	11: 69587440	-GAACCG
Arid1a	0,54%	3del	4: 133723006	-CGG
Tet2	0,94%	8del	3: 133485653	-CTGGATAT
Tet2	0,40%	2del	3: 133485657	-AT
Tet2	1,17%	14del	3: 133485658	-TATACT
Pten	0,85%	1ins	19: 32758457	+T
Liver 5				
Gene	MRF	Mut	Position	Indel

Tu1					
Gene	MRF	Mut	Position	Indel	
Brca1	7.29%	11del	11: 101549007	-GACAGA	
Brca1	7.28%	9del	11: 101549019	-CGGACACTC	
Brca2	5.31%	3del	5: 150529485	-CCT	
Brca2	2.52%	1del	5: 150529488	-C	
Cdkn2a(Ex1β)	0.51%	3del	4: 89294435	-ATC	
Cdkn2a(Ex1ß)	0.58%	15del	4: 89294436	-TCGCAC	
Cdkn2a(Ex1β)	9.88%	3del	4: 89294436	-TCG	
Apc	5.13%	1ins	18: 34261059	+T	
Apc	5.84%	1ins	18: 34261059	+A	
Smad4	10.17%	2del	18: 73675798	-GT	
Smad4	20.36%	1del	18: 73675801	-A	
Cdkn2a(Ex2)	30.53%	1del	4: 89276739	-G	
Trp53	0.46%	2del	11: 69587437	-AG	
Trp53	16.38%	2del	11: 69587438	-GT	
Trp53	0.37%	2del	11: 69587439	-TG	
Trp53	0.20%	2del	11: 69587440	-GA	
Trp53	0.34%	1del	11: 69587440	-G	
Trp53	0.21%	2ins	11: 69587441	+CC	
Trp53	0.34%	1ins	11: 69587441	+C	
Trp53	4.09%	12ins	11: 69587441	+CCACCA	
Trp53	15.75%	74del	11: 69587441	-AAGGCC	
Trp53	0.26%	1ins	11: 69587446	+A	
Arid1a	7.16%	11del	4: 133722998	-CCACGG	
Arid1a	7.48%	5del	4: 133723004	-TACGG	
Arid1a	8.35%	3del	4: 133723008	-GCT	
Tet2	17.69%	2del	3: 133485657	-AT	
Tet2	15.47%	1del	3: 133485658	-T	
Pten	23.13%	1del	19: 32758456	-A	
Pten	38.43%	1del	19: 32758457	-T	
Tu1 - Regior	12				
Gene	MRF	Mut	Position	Indel	
Brca2	12.50%	3del	5: 150529485	-CCT	
Brca2	7.57%	1del	5: 150529488	-C	
Apc	5.88%	1ins	18: 34261059	+T	
Apc	11.11%	1ins	18: 34261059	+A	
Smad4	21.56%	1del	18: 73675801	-A	
Cdkn2a(Ex2)	20.46%	1del	4: 89276739	-G	
Trp53	0.20%	2del	11: 69587437	-AG	
Trp53	8.23%	2del	11: 69587438	-GT	
Trp53	0.21%	11ins	11: 69587441	+CCATCC	
Trp53	0.24%	12ins	11: 69587441	+CCACCC	
Trp53	0.25%	2ins	11: 69587441	+CC	
Trp53	0.38%	1ins	11: 69587441	+C	
Trp53	5.10%	12ins	11: 69587441	+CCACCA	
Trp53	16.65%	74del	11: 69587441	-AAGGCC	
Trp53	0.21%	1ins	11: 69587446	+A	
Arid1a	2.97%	5del	4: 133723004	-TACGG	
Tet2	7.43%	2del	3: 133485657	-AT	
Tet2	9.48%	14del	3: 133485658	-TATACT	

Pten

4.86%

1del

19: 32758456

-A

Tu1 - Regior	13				
Gene	MRF	Mut	Pos	ition	Indel
Brca1	11.93%	11del	_	101549007	-GACAGA
Brca1	6.40%	9del	11:	101549019	-CGGACACTC
Cdkn2a(Ex1β)	1.00%	3del	4: 89	9294435	-ATC
Cdkn2a(Ex1ß)	19.48%	3del	4: 89	9294436	-TCG
Apc	2.34%	1ins	18: 3	34261059	+T
Apc	15.99%	1ins	18: 3	34261059	+A
Smad4	6.21%	2del	18:	73675798	-GT
Smad4	12.30%	1del		73675801	-A
Cdkn2a(Ex2)	40.58%	1del	4: 89	9276739	-G
Trp53	0.75%	2del	11: (39587437	-AG
Trp53	27.32%	2del	11: (59587438	-GT
Trp53	0.72%	2del	11: (39587439	-TG
Trp53	0.24%	74del	11: (39587440	-GAATGC
Trp53	0.33%	12ins	11: (39587440	+TCCTCC
Trp53	0.32%	2ins	11: (39587441	+CC
Trp53	0.34%	11ins	11: (39587441	+CCATCC
Trp53	0.37%	12ins	11: (39587441	+CCACCC
Trp53	0.66%	1ins	11: (69587441	+C
Trp53	10.09%	12ins	11: (69587441	+CCACCA
Trp53	37.12%	74del	11: (69587441	-AAGGCC
Trp53	0.45%	1ins	11: (69587446	+A
Arid1a	10.95%	5del	4: 1:	33723004	-TACGG
Arid1a	16.93%	3del	4: 1:	33723008	-GCT
Tet2	21.18%	2del	3: 1:	33485657	-AT
Tet2	14.29%	1del	3: 1:	33485658	-Ţ
Pten	1.72%	1del	19: 3	32758456	-A
Pten	30.86%	1del	19: 3	32758457	-T
Tu2					
Gene	MRF	Mut		Position	Indel
Apc	7.18%	15del		18: 34261056	-AAGTGA
Apc	4.99%	15ins		18: 34261057	+CTGAGT
Apc	4.35%	1ins		18: 34261059	+T
Cdkn2a(Ex2)	0.29%	7del		4: 89276737	-GCGGAAC
Cdkn2a(Ex2)	0.28%	1del		4: 89276739	-G
Arid1a	0.41%	1del		4: 133723007	-G
Arid1a	1.29%	2del		4: 133723007	-GG
Tet2	10.53%	178del		3: 133485574	-CATTTC
Tet2	1.74%	18del		3: 133485647	-TGCTGT
Tet2	6.87%	1del		3: 133485658	-T
Pten	8.87%	123del		19: 32758338	-AGCCAA
Pten	1.19%	31del		19: 32758440	-AGAGTT
Pten	2.00%	1ins		19: 32758457	+T

Tu3				
Gene	MRF	Mut	Position	Indel
Brca1	1.43%	1del	11: 101549018	-T
Brca2	1.64%	10del	5: 150529476	-ACCAGC
Cdkn2a(Ex1β)	2.99%	9del	4: 89294435	-ATCGCACGA
Cdkn2a(Ex1β)	1.19%	3del	4: 89294436	-TCG
Apc Apc	1.65%	6del	18: 34261051	-AAAGCA
Apc	1.52%	1del	18: 34261058	-G
Apc	0.23%	1ins	18: 34261059	+T
Apc	1.56%	1ins	18: 34261059	+A
Smad4	5.59%	6del	18: 73675795	-ATAGTG
Smad4	3.33%	3del	18: 73675798	-GTG
Cdkn2a(Ex2)	4.39%	1del	4: 89276739	-G
Trp53	2.23%	2del	11: 69587438	-GT
Trp53	2.46%	8del	11: 69587439	-TGAAGCCC
Trp53	0.85%	5ins	11: 69587440	+TAGAA
Trp53	0.64%	15ins	11: 69587443	+CTTAAT
Arid1a	1.89%	8del	4: 133722998	-CCACCATA
Arid1a	1.91%	8del	4: 133723001	-CCATACGG
Arid1a	2.51%	2del	4: 133723009	-CT
Tet2	9.35%	2del	3: 133485657	-AT
Tet2	2.15%	1del	3: 133485658	-T
Pten	0.38%	2del	19: 32758457	-TC
Pten	1.59%	1del	19: 32758457	-T
Pten	2.94%	1ins	19: 32758457	+T
Pten	3.15%	3del	19: 32758458	-CAA
Tu4				
Gene	MRF	Mut	Position	Indel
Cdkn2a(Ex1β)	3.04%	1ins	4: 89294436	+T
Λ				
Apc	1.84%	3del	18: 34261058	-GTT
	1.84% 3.73%	3del 1del	18: 34261058 11: 69587440	-GTT -G
Trp53 Trp53				
Trp53	3.73%	1del	11: 69587440	-G
Trp53 Trp53	3.73% 3.87%	1del 1ins	11: 69587440 11: 69587440	-G +G
Trp53 Trp53 Arid1a	3.73% 3.87% 3.56% 2.61% 3.45%	1del 1ins 1del	11: 69587440 11: 69587440 4: 133723007	-G +G -G
Trp53 Trp53 Arid1a Arid1a	3.73% 3.87% 3.56% 2.61%	1del 1ins 1del 1ins	11: 69587440 11: 69587440 4: 133723007 4: 133723009	-G +G -G +A
Trp53 Trp53 Arid1a Arid1a Arid1a	3.73% 3.87% 3.56% 2.61% 3.45% 4.37% 3.27%	1del 1ins 1del 1ins 1del 1ins 1del 1ins 1del	11: 69587440 11: 69587440 4: 133723007 4: 133723009 4: 133723009 3: 133485657 3: 133485658	-G +G -G +A -C +A -T
Trp53 Trp53 Arid1a Arid1a Arid1a Arid1a Tet2 Tet2 Pten	3.73% 3.87% 3.56% 2.61% 3.45% 4.37% 3.27% 2.62%	1del 1ins 1del 1ins 1del 1ins 1del 201del	11: 69587440 11: 69587440 4: 133723007 4: 133723009 4: 133723009 3: 133485657 3: 133485658 19: 32758270	-G +G -G +A -C +A -T -AGCGTT
Trp53 Trp53 Arid1a Arid1a Arid1a Tet2 Tet2	3.73% 3.87% 3.56% 2.61% 3.45% 4.37% 3.27% 2.62% 1.62%	1del 1ins 1del 1ins 1del 1ins 1del 201del 15del	11: 69587440 11: 69587440 4: 133723007 4: 133723009 4: 133723009 3: 133485657 3: 133485658 19: 32758270 19: 32758447	-G +G -G +A -C +A -T
Trp53 Trp53 Arid1a Arid1a Arid1a Tet2 Tet2 Pten Pten Pten	3.73% 3.87% 3.56% 2.61% 3.45% 4.37% 3.27% 2.62% 1.62% 0.25%	1del 1ins 1del 1ins 1del 1ins 1del 201del 15del 2del	11: 69587440 11: 69587440 4: 133723007 4: 133723009 4: 133723009 3: 133485657 3: 133485658 19: 32758270 19: 32758447 19: 32758456	-G +G -G +A -C +A -T -AGCGTT -ACAAAA -AT
Trp53 Trp53 Arid1a Arid1a Arid1a Tet2 Tet2 Pten Pten Pten Pten	3.73% 3.87% 3.56% 2.61% 3.45% 4.37% 3.27% 2.62% 1.62%	1del 1ins 1del 1ins 1del 1ins 1del 201del 15del	11: 69587440 11: 69587440 4: 133723007 4: 133723009 4: 133723009 3: 133485657 3: 133485658 19: 32758270 19: 32758447	-G +G -G +A -C +A -T -AGCGTT -ACAAAA
Trp53 Trp53 Arid1a Arid1a Arid1a Tet2 Tet2 Pten Pten Pten	3.73% 3.87% 3.56% 2.61% 3.45% 4.37% 3.27% 2.62% 1.62% 0.25%	1del 1ins 1del 1ins 1del 1ins 1del 201del 15del 2del	11: 69587440 11: 69587440 4: 133723007 4: 133723009 4: 133723009 3: 133485657 3: 133485658 19: 32758270 19: 32758447 19: 32758456	-G +G -G +A -C +A -T -AGCGTT -ACAAAA -AT
Trp53 Trp53 Arid1a Arid1a Arid1a Tet2 Tet2 Pten Pten Pten Pten	3.73% 3.87% 3.56% 2.61% 3.45% 4.37% 3.27% 2.62% 1.62% 0.25% 7.49%	1del 1ins 1del 1ins 1del 1ins 1del 201del 15del 2del	11: 69587440 11: 69587440 4: 133723007 4: 133723009 4: 133723009 3: 133485657 3: 133485658 19: 32758270 19: 32758447 19: 32758456 19: 32758457	-G +G -G +A -C +A -T -AGCGTT -ACAAAA -AT
Trp53 Trp53 Arid1a Arid1a Arid1a Tet2 Tet2 Pten Pten Pten Pten Tu5 Gene Apc	3.73% 3.87% 3.56% 2.61% 3.45% 4.37% 3.27% 2.62% 1.62% 0.25% 7.49% MRF 4.08%	1del 1ins 1del 1ins 1del 1ins 1del 201del 15del 2del 2del	11: 69587440 11: 69587440 4: 133723007 4: 133723009 4: 133723009 3: 133485657 3: 133485658 19: 32758270 19: 32758447 19: 32758456 19: 32758457 Position 18: 34261053	-G +G -G +A -C +A -T -AGCGTT -ACAAAA -AT -TC
Trp53 Trp53 Arid1a Arid1a Arid1a Tet2 Tet2 Pten Pten Pten Pten Tu5 Gene Apc Apc	3.73% 3.87% 3.56% 2.61% 3.45% 4.37% 3.27% 2.62% 1.62% 0.25% 7.49% MRF 4.08% 4.59%	1del 1ins 1del 1ins 1del 1ins 1del 201del 15del 2del 2del	11: 69587440 11: 69587440 4: 133723007 4: 133723009 4: 133723009 3: 133485657 3: 133485658 19: 32758270 19: 32758447 19: 32758456 19: 32758457 Position 18: 34261053 18: 34261058	-G +G -G +A -C +A -T -AGCGTT -ACAAAA -AT -TC
Trp53 Trp53 Arid1a Arid1a Arid1a Tet2 Tet2 Pten Pten Pten Pten Tu5 Gene Apc Apc Apc	3.73% 3.87% 3.56% 2.61% 3.45% 4.37% 3.27% 2.62% 1.62% 0.25% 7.49% MRF 4.08% 4.59% 5.01%	1del 1ins 1del 1ins 1del 1ins 1del 201del 15del 2del 2del Mut 6del 1ins 1ins	11: 69587440 11: 69587440 4: 133723007 4: 133723009 4: 133723009 3: 133485657 3: 133485658 19: 32758270 19: 32758447 19: 32758456 19: 32758457 Position 18: 34261053 18: 34261058 18: 34261059	-G +G -G +A -C +A -T -AGCGTT -ACAAAA -AT -TC Indel -AGCAAG +G +T
Trp53 Trp53 Arid1a Arid1a Arid1a Tet2 Tet2 Pten Pten Pten Pten Tu5 Gene Apc Apc Smad4	3.73% 3.87% 3.56% 2.61% 3.45% 4.37% 3.27% 2.62% 1.62% 0.25% 7.49% MRF 4.08% 4.59% 5.01% 5.67%	1del 1ins 1del 1ins 1del 1ins 1del 1ins 1del 201del 15del 2del 2del 4 Mut 6del 1ins 1ins 1ins 3del	11: 69587440 11: 69587440 4: 133723007 4: 133723009 4: 133723009 3: 133485657 3: 133485658 19: 32758270 19: 32758447 19: 32758456 19: 32758457 Position 18: 34261053 18: 34261058 18: 34261059 18: 73675798	-G +G -G +A -C +A -T -AGCGTT -ACAAAA -AT -TC Indel -AGCAAG +G +T
Trp53 Trp53 Arid1a Arid1a Arid1a Tet2 Tet2 Pten Pten Pten Pten Tu5 Gene Apc Apc Apc Smad4 Cdkn2a(Ex2)	3.73% 3.87% 3.56% 2.61% 3.45% 4.37% 3.27% 2.62% 1.62% 0.25% 7.49% MRF 4.08% 4.59% 5.01% 5.67% 10.28%	1del 1ins 1del 1ins 1del 1ins 1del 1ins 1del 201del 15del 2del 2del Mut 6del 1ins 1ins 3del 14del	11: 69587440 11: 69587440 4: 133723007 4: 133723009 4: 133723009 3: 133485657 3: 133485658 19: 32758270 19: 32758447 19: 32758456 19: 32758457 Position 18: 34261053 18: 34261058 18: 34261059 18: 73675798 4: 89276738	-G +G -G +A -C +A -T -AGCGTT -ACAAAA -AT -TC Indel -AGCAAG +G +T -GTG -CGGTAT
Trp53 Trp53 Arid1a Arid1a Arid1a Tet2 Tet2 Pten Pten Pten Pten Pten Constant Specific Specifi	3.73% 3.87% 3.56% 2.61% 3.45% 4.37% 3.27% 2.62% 1.62% 0.25% 7.49% MRF 4.08% 4.59% 5.01% 5.67% 10.28% 8.23%	1del 1ins 1del 1ins 1del 1ins 1del 1ins 1del 201del 201del 2del 2del Mut 6del 1ins 1ins 3del 14del 1del	11: 69587440 11: 69587440 4: 133723007 4: 133723009 4: 133723009 3: 133485657 3: 133485658 19: 32758270 19: 32758447 19: 32758456 19: 32758457 Position 18: 34261053 18: 34261058 18: 34261059 18: 73675798 4: 89276738 11: 69587439	-G +G -G +A -C +A -T -AGCGTT -ACAAAA -AT -TC Indel -AGCAAG +G +T -GTG -CGGTAT
Trp53 Trp53 Arid1a Arid1a Arid1a Arid1a Tet2 Tet2 Pten Pten Pten Pten Pten Constant Apc Apc Apc Apc Apc Smad4 Cdkn2a(Ex2) Trp53 Trp53	3.73% 3.87% 3.56% 2.61% 3.45% 4.37% 3.27% 2.62% 1.62% 0.25% 7.49% MRF 4.08% 4.59% 5.01% 5.67% 10.28% 8.23% 6.16%	1del 1ins 1del 1ins 1del 1ins 1del 1ins 1del 201del 15del 2del 2del Mut 6del 1ins 1ins 1del 2del 4del 1del 2del	11: 69587440 11: 69587440 4: 133723007 4: 133723009 4: 133723009 3: 133485657 3: 133485658 19: 32758270 19: 32758447 19: 32758456 19: 32758457 Position 18: 34261053 18: 34261058 18: 34261059 18: 73675798 4: 89276738 11: 69587440	-G +G -G +A -C +A -T -AGCGTT -ACAAAA -AT -TC Indel -AGCAAG +G +T -GTG -CGGTAT -T -GAACTG
Trp53 Trp53 Arid1a Arid1a Arid1a Arid1a Tet2 Tet2 Pten Pten Pten Pten Pten Apc Apc Apc Smad4 Cdkn2a(Ex2) Trp53 Trp53 Trp53	3.73% 3.87% 3.56% 2.61% 3.45% 4.37% 3.27% 2.62% 1.62% 0.25% 7.49% MRF 4.08% 4.59% 5.01% 5.67% 10.28% 8.23% 6.16% 6.62%	1del 1ins 1del 1ins 1del 1ins 1del 1ins 1del 201del 15del 2del 2del Mut 6del 1ins 1ins 1del 2del 2del 11del 11del	11: 69587440 11: 69587440 4: 133723007 4: 133723009 4: 133723009 3: 133485657 3: 133485658 19: 32758270 19: 32758447 19: 32758456 19: 32758457 Position 18: 34261053 18: 34261058 18: 34261059 18: 73675798 4: 89276738 11: 69587440 11: 69587440 11: 69587440	-G +G -G +A -C +A -T -AGCGTT -ACAAAA -AT -TC Indel -AGCAAG +G +T -GTG -CGGTAT -T -GAACTG -GAACCG
Trp53 Trp53 Arid1a Arid1a Arid1a Arid1a Tet2 Tet2 Pten Pten Pten Pten Pten Apc Apc Apc Apc Smad4 Cdkn2a(Ex2) Trp53 Trp53 Trp53 Trp53 Trp53	3.73% 3.87% 3.56% 2.61% 3.45% 4.37% 3.27% 2.62% 1.62% 0.25% 7.49% MRF 4.08% 4.59% 5.01% 5.67% 10.28% 8.23% 6.16% 6.62% 7.53%	1del 1ins 1del 1ins 1del 1ins 1del 1ins 1del 201del 15del 2del 2del Mut 6del 1ins 1del 1ins 1del 2del 2del 1del 1del 1del 1del 1del	11: 69587440 11: 69587440 4: 133723007 4: 133723009 4: 133723009 3: 133485657 3: 133485658 19: 32758270 19: 32758457 Position 18: 34261053 18: 34261058 18: 34261059 18: 73675798 4: 89276738 11: 69587440 11: 69587440 11: 69587440 11: 69587440	-G +G -G +A -C +A -T -AGCGTT -ACAAAA -AT -TC Indel -AGCAAG +G -G -CGGTAT -T -GAACTG -GAACCG -G
Trp53 Trp53 Arid1a Arid1a Arid1a Arid1a Tet2 Tet2 Pten Pten Pten Pten Pten Apc Apc Apc Smad4 Cdkn2a(Ex2) Trp53 Trp53 Trp53 Arid1a	3.73% 3.87% 3.56% 2.61% 3.45% 4.37% 3.27% 2.62% 1.62% 0.25% 7.49% MRF 4.08% 4.59% 5.01% 5.67% 10.28% 8.23% 6.16% 6.62% 7.53% 7.78%	1del 1ins 1del 1ins 1del 1ins 1del 1ins 1del 201del 15del 2del 2del Mut 6del 1ins 1ins 1del 2del 1del 1del 1del 1del 28del 1del 1del 3del	11: 69587440 11: 69587440 4: 133723007 4: 133723009 4: 133723009 3: 133485657 3: 133485658 19: 32758270 19: 32758447 19: 32758456 19: 32758457 Position 18: 34261053 18: 34261058 18: 34261058 18: 34261059 18: 73675798 4: 89276738 11: 69587440 11: 69587440 11: 69587440 4: 133723006	-G +G -G +A -C +A -C +A -T -AGCGTT -ACAAAA -AT -TC Indel -AGCAAG +G -G -GGGTAT -T -GAACTG -GAACCG -G -CGG
Trp53 Trp53 Arid1a Arid1a Arid1a Arid1a Tet2 Tet2 Pten Pten Pten Pten Pten Apc Apc Apc Apc Apc Apc Apc Trp53 Trp53 Trp53 Trp53 Arid1a Tet2	3.73% 3.87% 3.56% 2.61% 3.45% 4.37% 2.62% 1.62% 0.25% 7.49% MRF 4.08% 4.59% 5.01% 5.67% 10.28% 8.23% 6.16% 6.62% 7.53% 7.78% 9.42%	1del 1ins 1del 1ins 1del 1ins 1del 1ins 1del 201del 15del 2del 2del Mut 6del 1ins 1ins 1del 2del 1del 1del 1del 2del 3del 8del	11: 69587440 11: 69587440 4: 133723007 4: 133723009 4: 133723009 3: 133485657 3: 133485658 19: 32758270 19: 32758447 19: 32758456 19: 32758457 Position 18: 34261053 18: 34261058 18: 34261059 18: 73675798 4: 89276738 11: 69587440 11: 69587440 11: 69587440 4: 133723006 3: 133485653	-G +G -G +A -C +A -C +A -T -AGCGTT -ACAAAA -AT -TC Indel -AGCAAG +G +T -GTG -CGGTAT -T -GAACTG -GAACCG -G -CGG -CTGGATAT
Trp53 Trp53 Arid1a Arid1a Arid1a Arid1a Tet2 Tet2 Pten Pten Pten Pten Tu5 Gene Apc Apc Apc Smad4 Cdkn2a(Ex2) Trp53 Trp53 Trp53 Trp53 Arid1a Tet2 Tet2 Tet2 Tet2	3.73% 3.87% 3.56% 2.61% 3.45% 4.37% 3.27% 2.62% 1.62% 0.25% 7.49% MRF 4.08% 4.59% 5.01% 5.67% 10.28% 8.23% 6.16% 6.62% 7.53% 7.78% 9.42% 8.63%	1del 1ins 1del 1ins 1del 1ins 1del 1ins 1del 1ins 1del 201del 15del 2del 2del Mut 6del 1ins 1ins 1del 2del 1del 1del 1del 28del 11del 1del 3del 8del 2del	11: 69587440 11: 69587440 4: 133723007 4: 133723009 4: 133723009 3: 133485657 3: 133485658 19: 32758270 19: 32758447 19: 32758456 19: 32758457 Position 18: 34261053 18: 34261058 18: 34261058 18: 34261059 18: 73675798 4: 89276738 11: 69587440 11: 69587440 11: 69587440 4: 133723006 3: 133485653 3: 133485657	-G +G -G +A -C +A -C +A -T -AGCGTT -ACAAAA -AT -TC Indel -AGCAAG +G +T -GTG -CGGTAT -T -GAACTG -GAACCG -G -CGG -CTGGATAT -AT
Trp53 Trp53 Arid1a Arid1a Arid1a Arid1a Tet2 Tet2 Pten Pten Pten Pten Tu5 Gene Apc Apc Apc Smad4 Cdkn2a(Ex2) Trp53 Trp53 Trp53 Trp53 Arid1a Tet2 Tet2 Tet2 Tet2 Tet2 Tet2 Tet2 Tet2	3.73% 3.87% 3.56% 2.61% 3.45% 4.37% 2.62% 1.62% 0.25% 7.49% MRF 4.08% 4.59% 5.01% 5.67% 10.28% 8.23% 6.16% 6.62% 7.53% 7.78% 9.42% 8.63% 9.96%	1del 1ins 1del 1ins 1del 1ins 1del 1ins 1del 201del 15del 2del 2del Mut 6del 1ins 1ins 1del 2del 1del 2del 1del 1del 2del 1del 2del 1del 2del 1del 2del 1del 1del 3del 8del 2del 14del	11: 69587440 11: 69587440 4: 133723007 4: 133723009 4: 133723009 3: 133485657 3: 133485658 19: 32758270 19: 32758447 19: 32758456 19: 32758457 Position 18: 34261053 18: 34261058 18: 34261059 18: 73675798 4: 89276738 11: 69587440 11: 69587440 11: 69587440 4: 133723006 3: 133485657 3: 133485657	-G +G -G +A -C +A -T -AGCGTT -ACAAAA -AT -TC Indel -AGCAAG +G +T -GTG -CGGTAT -T -GAACTG -GAACCG -G -CGG -CTGGATAT -AT -TATACT
Trp53 Trp53 Arid1a Arid1a Arid1a Arid1a Tet2 Tet2 Pten Pten Pten Pten Tu5 Gene Apc Apc Apc Apc Smad4 Cdkn2a(Ex2) Trp53 Trp53 Trp53 Trp53 Arid1a Tet2 Tet2 Tet2 Pten	3.73% 3.87% 3.56% 2.61% 3.45% 4.37% 2.62% 1.62% 0.25% 7.49% MRF 4.08% 4.59% 5.01% 5.67% 10.28% 8.23% 6.16% 6.62% 7.78% 9.42% 8.63% 9.96% 8.28%	1del 1ins 1del 1ins 1del 1ins 1del 1ins 1del 1ins 1del 201del 15del 2del 2del Mut 6del 1ins 1ins 1del 1del 2del 1del 1del 28del 11del 1del 3del 8del 2del 14del 14del 34del	11: 69587440 11: 69587440 4: 133723007 4: 133723009 4: 133723009 3: 133485657 3: 133485658 19: 32758270 19: 32758447 19: 32758456 19: 32758457 Position 18: 34261053 18: 34261058 18: 34261059 18: 73675798 4: 89276738 11: 69587440 11: 69587440 11: 69587440 4: 133723006 3: 133485653 3: 133485657 3: 133485658 19: 32758439	-G +G -G +A -C +A -C +A -T -AGCGTT -ACAAAA -AT -TC Indel -AGCAAG +G +T -GTG -CGGTAT -T -GAACTG -GAACCG -G -CGG -CTGGATAT -AT -TATACT -CAGTAG
Trp53 Trp53 Arid1a Arid1a Arid1a Arid1a Tet2 Tet2 Pten Pten Pten Pten Tu5 Gene Apc Apc Apc Smad4 Cdkn2a(Ex2) Trp53 Trp53 Trp53 Trp53 Arid1a Tet2 Tet2 Tet2 Tet2 Tet2 Tet2 Tet2 Tet2	3.73% 3.87% 3.56% 2.61% 3.45% 4.37% 2.62% 1.62% 0.25% 7.49% MRF 4.08% 4.59% 5.01% 5.67% 10.28% 8.23% 6.16% 6.62% 7.53% 7.78% 9.42% 8.63% 9.96%	1del 1ins 1del 1ins 1del 1ins 1del 1ins 1del 201del 15del 2del 2del Mut 6del 1ins 1ins 1del 2del 1del 2del 1del 1del 2del 1del 2del 1del 2del 1del 2del 1del 1del 3del 8del 2del 14del	11: 69587440 11: 69587440 4: 133723007 4: 133723009 4: 133723009 3: 133485657 3: 133485658 19: 32758270 19: 32758447 19: 32758456 19: 32758457 Position 18: 34261053 18: 34261058 18: 34261059 18: 73675798 4: 89276738 11: 69587440 11: 69587440 11: 69587440 4: 133723006 3: 133485657 3: 133485657	-G +G -G +A -C +A -T -AGCGTT -ACAAAA -AT -TC Indel -AGCAAG +G +T -GTG -CGGTAT -T -GAACTG -GAACCG -G -CGG -CTGGATAT -AT -TATACT

Tu6				
Gene	MRF	Mut	Position	Indel
Smad4	1.33	14del	18: 73675797	-AGTTTC
Smad4 Smad4	17.96 19.93	7del 2del	18: 73675800 18: 73675798	-GATATGG -GT
Arid1a	19.89	6del	4: 133723007	-GGCTGA
Arid1a	20.98	3del	4: 133723007	-CGG
Cdkn2a(Ex2)	19.79	1del	4: 89276739	-G
Apc	36.13	1ins	18: 34261059	+T
Tet2	0.22	2del	3:133485657	-AT
Tet2	2.10	11del	3:133485654	-TGGTGT
Tet2	17.22	1del	3:133485658	-T
Pten	0.71	1ins	19: 32758457	+C
Pten	1.45	1del	19: 32758456	-A
Pten	12.61	7del	19: 32758456	-ATCAAAG
Pten	16.21	1del	19: 32758457	-T
Tu7				
Gene	MRF	Mut	Position	Indel
Pten	19.04	25del	19: 32758453	-ATCGAA
Pten	21.61	1del	19: 32758456	-A
Tu8				
Gene	MRF	Mut	Position	Indel
Brca1	0.74	59ins	11: 101549027	+TTGTAG
Pten	12.98	1ins	19: 32758457	+T
Pten	14.93	1del	19: 32758456	-A
Tu9	MDE	3.5	D 111	
Gene	MRF	Mut	Position 19: 32758457	Indel
Pten Pten	0.40	1ins 1ins	19: 32758457	+A +C
Pten	0.51 8.37	1del	19: 32758457	-T
Pten	15.19	1ins	19: 32758456	+A
Tu10	10.10	TITIO	10. 02700400	'71
Gene	MRF	Mut	Position	Indel
Cdkn2a(Ex2)	31.86	1del	4: 89276739	-G
Apc	24.96	2ins	18: 34261059	+TT
Apc	26.78	1ins	18: 34261058	+G
Tet2	27.18	1del	3:133485658	-T
Pten	3.45	1del	19: 32758456	-A
Pten	37.25	1del	19: 32758457	-T
Tu11				
Gene	MRF	Mut	Position	Indel
Apc	0.24	1ins	18: 34261059	+T
Apc	0.24	1ins	18: 34261059	+A
Pten	30.55	1del	19: 32758456	-A
Tu12				
Gene	MRF	Mut	Position	Indel
Cdkn2a(Ex1β)	1.73	1ins	4: 89294435	+A
Pten	3.47	1del	19: 32758457	-T
Pten	3.59	1del	19: 32758456	-A
Tu13				
Gene	MRF	Mut	Position	Indel
Pten	6.75	1del	19: 32758457	-T
		1		
Pten	20.25	1del	19: 32758456	-A
Pten Tu14	20.25	1del	19: 32758456	-A
Pten Tu14 Gene	20.25 MRF	1del Mut	19: 32758456 Position	-A Indel
Pten Tu14 Gene Brca1	20.25 MRF 1.52	1del Mut 3del	19: 32758456 Position 11: 101549016	-A Indel -GAT
Pten Tu14 Gene Brca1 Cdkn2a(Ex1β)	20.25 MRF 1.52 1.93	Mut 3del 6del	19: 32758456 Position 11: 101549016 4: 89294430	-A Indel -GAT -CCGGGA
Pten Tu14 Gene Brca1 Cdkn2a(Ex1β) Arid1a	20.25 MRF 1.52 1.93 2.19	Mut 3del 6del 3del	19: 32758456 Position 11: 101549016 4: 89294430 4: 133723006	-A Indel -GAT -CCGGGA -CGG
Pten Tu14 Gene Brca1 Cdkn2a(Ex1β) Arid1a Cdkn2a(Ex2)	20.25 MRF 1.52 1.93 2.19 1.59	Mut 3del 6del 3del 1del	19: 32758456 Position 11: 101549016 4: 89294430 4: 133723006 4: 89276739	-A Indel -GAT -CCGGGA -CGG
Pten Tu14 Gene Brca1 Cdkn2a(Ex1β) Arid1a Cdkn2a(Ex2) Apc	20.25 MRF 1.52 1.93 2.19 1.59 1.56	Mut 3del 6del 3del 1del 1ins	Position 11: 101549016 4: 89294430 4: 133723006 4: 89276739 18: 34261058	-A Indel -GAT -CCGGGA -CGG -G +G
Pten Tu14 Gene Brca1 Cdkn2a(Ex1β) Arid1a Cdkn2a(Ex2) Apc Apc	20.25 MRF 1.52 1.93 2.19 1.59 1.56 1.60	Mut 3del 6del 3del 1del 1ins 3del	Position 11: 101549016 4: 89294430 4: 133723006 4: 89276739 18: 34261058 18: 34261058	-A Indel -GAT -CCGGGA -CGG -G +G -GTT
Pten Tu14 Gene Brca1 Cdkn2a(Ex1β) Arid1a Cdkn2a(Ex2) Apc Apc Apc	20.25 MRF 1.52 1.93 2.19 1.59 1.56 1.60 3.25	Mut 3del 6del 3del 1del 1ins 3del 1ins	Position 11: 101549016 4: 89294430 4: 133723006 4: 89276739 18: 34261058 18: 34261058 18: 34261059	-A Indel -GAT -CCGGGA -CGG -G +G -GTT +T
Pten Tu14 Gene Brca1 Cdkn2a(Ex1β) Arid1a Cdkn2a(Ex2) Apc Apc Apc Tet2	20.25 MRF 1.52 1.93 2.19 1.59 1.56 1.60 3.25 0.21	Mut 3del 6del 3del 1del 1ins 3del 1ins 1del	Position 11: 101549016 4: 89294430 4: 133723006 4: 89276739 18: 34261058 18: 34261058 18: 34261059 3: 133485658	-A Indel -GAT -CCGGGA -CGG -G +G -GTT +T
Pten Tu14 Gene Brca1 Cdkn2a(Ex1β) Arid1a Cdkn2a(Ex2) Apc Apc Apc	20.25 MRF 1.52 1.93 2.19 1.59 1.56 1.60 3.25	Mut 3del 6del 3del 1del 1ins 3del 1ins	Position 11: 101549016 4: 89294430 4: 133723006 4: 89276739 18: 34261058 18: 34261058 18: 34261059	-A Indel -GAT -CCGGGA -CGG -G +G -GTT +T

Gene	Tu15				
Apc 4,70 4 lins 18:34261059 +T Apc 5.10 2 lins 18:34261059 +TT Pten 4.46 1del 19:32758456 -A Pten 6.44 1del 19:32758457 -T Tu16 Gene MRF Mut Position Indel Smad4 7.33 1del 18:73675801 -A Apc 9.54 2del 18:34261056 +A Apc 9.54 2del 18:34261059 -TT Pten 18.87 1del 19:32758456 -A TU17 Gene MRF Mut Position Indel Smad4 0.32 2del 18:7367598 -GT Smad4 0.32 2del 18:7367598 -GT Smad4 0.32 2del 18:7367598 -GT Cdkn2a(Ex2) 0.20 1del 4:89276739 -G Cdryal 14:1 1ins 18:34261059		MRF	Mut	Position	Indel
Apc					
Pten					
Pten					
Tu16					
Gene MRF Mut Position Indel					
Smad4		MRF	Mut	Position	Indel
Apc 9.47 1ins 18: 34261056 +A Apc 9.54 2del 18: 34261059 -TT Pten 18.87 1del 19: 32758456 -A Tu17 Gene MRF Mut Position Indel Smad4 0.36 7del 18: 7367590 -GT Smad4 0.36 7del 18: 73675800 -GATATGG Cdkn2a(Ex2) 0.20 1del 4: 89276739 -G Apc 4.14 1ins 18: 34261059 +T Tet2 2.04 1del 3:133485659 +A Pten 2.72 1del 19: 32758456 -A Pten 2.74 1del 19: 32758456 -A Pten 2.74 1del 19: 32758456 -A Pten 2.74 1del 5: 150529488 -C p53 8:13 12del 11: 69587427 -TGAAAG Apc 1.04 1ins <					
Apc 9.54 2del 18: 34261059 -TT Pten 18.87 1del 19: 32758456 -A Tu17 Gene MRF Mut Position Indel Smad4 0.32 2del 18: 73675798 -GT Smad4 0.32 2del 18: 73675798 -GT Smad4 0.32 7del 18: 73675798 -G Gdkn2a(Ex2) 0.20 1del 4: 88276739 -G Apc 4.14 1ins 18: 34261059 +T Tet2 1.77 1ins 3:133485659 +A Tet2 2.04 1del 19: 32758456 -A Pten 2.72 1del 19: 32758456 -A Pten 2.74 1del 19: 32758457 -T Tu18 Gene MRF Mut Position Indel Brca2 0.27 1del 5: 150529488 -C Apc 1.04 1ins 18: 34261059					
Pten					
Tu17					
Gene MRF Mut Position Indel Smad4 0.32 2del 18: 73675798 -GT Smad4 0.36 7del 18: 73675800 -GATATGG Cdkn2a(Ex2) 0.20 1del 4: 89276739 -G Apc 4.14 1ins 18: 34261059 +T Tet2 1.77 1ins 3:133485659 +A Tet2 2.04 1del 19: 32758456 -A Pten 2.72 1del 19: 32758456 -A Pten 2.74 1del 19: 32758457 -T TU18 Gene MRF Mut Position Indel Brca2 0.27 1del 5: 150529488 -C p53 8.13 12del 11: 69587427 -TGAAAG Apc 1.04 1ins 18: 34261059 +T Pten 0.27 22del 19: 32758457 -T Pten 0.28 1del 19: 32758456 <t< th=""><th></th><th></th><th></th><th></th><th></th></t<>					
Smad4		MRF	Mut	Position	Indel
Smad4					
Cdkn2a(Ex2) 0.20 1del 4: 89276739 -G Apc 4.14 1ins 18: 34261059 +T Tet2 1.77 1ins 3:133485659 +A Tet2 2.04 1del 3:133485659 -A Pten 2.72 1del 19: 32758456 -A Pten 2.74 1del 19: 32758457 -T Tu18 Gene MRF Mut Position Indel Brca2 0.27 1del 5: 150529488 -C p53 8.13 12del 11: 69587427 -TGAAAG Apc 1.04 1ins 18: 34261061 +G Apc 1.04 1ins 18: 34261059 +T Pten 0.27 22del 19: 32758448 -CAGCGT Pten 0.28 1del 19: 32758456 -A Tu19 Tu19 Tu19 Tu19 Tu19 Tu19 Tu19 Tu19 Tu19					_
Apc 4.14 1ins 18: 34261059 +T Tet2 1.77 1ins 3:133485659 +A Tet2 2.04 1del 3:133485658 -T Pten 2.72 1del 19: 32758456 -A Pten 2.74 1del 19: 32758457 -T Tu18 Gene MRF Mut Position Indel Brca2 0.27 1del 5: 150529488 -C p53 8.13 12del 11: 69587427 -TGAAAG Apc 1.04 1ins 18: 34261061 +G Apc 1.04 1ins 18: 34261059 +T Pten 0.27 22del 19: 32758448 -CAGCGT Pten 0.28 1del 19: 32758456 -A Tu19 <					
Tet2					
Tet2					
Pten 2.72 1del 19: 32758456 -A Pten 2.74 1del 19: 32758457 -T Tu18 Gene MRF Mut Position Indel Broa2 0.27 1del 5: 150529488 -C p53 8.13 12del 11: 69587427 -TGAAAG Apc 1.04 1ins 18: 34261059 +T Apc 7.50 1ins 18: 34261059 +T Pten 0.27 22del 19: 32758448 -CAGCGT Pten 0.28 1del 19: 32758456 -A Pten 0.28 1del 19: 32758456 -A Tu19 Gene MRF Mut Position Indel Trp53 9.97 1ins 11: 69587440 +A Apc 8.83 4del 18: 34261052 -AAGC Apc 9.82 1ins 18: 34261059 +T Tet2 11.78					
Pten 2.74					
Tu18 Gene MRF Mut Position Indel Brca2 0.27 1del 5: 150529488 -C p53 8.13 12del 11: 69587427 -TGAAAG Apc 1.04 1ins 18: 34261061 +G Apc 7.50 1ins 18: 34261059 +T Pten 0.27 22del 19: 32758448 -CAGCGT Pten 0.28 1del 19: 32758457 -T Pten 8.12 1del 19: 32758456 -A Tu19 Tull Tull<					-T
Gene MRF Mut Position Indel Brca2 0.27 1del 5: 150529488 -C p53 8.13 12del 11: 69587427 -TGAAAG Apc 1.04 1ins 18: 34261061 +G Apc 7.50 1ins 18: 34261059 +T Pten 0.27 22del 19: 32758448 -CAGCGT Pten 0.28 1del 19: 32758456 -A Pten 8.12 1del 19: 32758456 -A Tu19 Gene MRF Mut Position Indel Trp53 9.97 1ins 11: 69587440 +A Apc 8.83 4del 18: 34261052 -AAGC Apc 9.82 1ins 11: 69587440 +A Apc 9.82 1ins 11: 69587440 +A Apc 9.82 1ins 11: 69587440 +A Apc 9.82 1ins 18: 34261059					
Brca2 0.27		MRF	Mut	Position	Indel
P53					
Apc 1.04 1ins 18: 34261061 +G Apc 7.50 1ins 18: 34261059 +T Pten 0.27 22del 19: 32758448 -CAGCGT Pten 0.28 1del 19: 32758456 -A Pten 8.12 1del 19: 32758456 -A Tu19 Gene MRF Mut Position Indel Try53 9.97 1ins 11: 69587440 +A Apc 8.83 4del 18: 34261052 -AAGC Apc 9.82 1ins 18: 34261059 +T Tet2 11.20 4del 3: 133485654 -TGGA Tet2 11.78 1del 3: 133485654 -TGGA Pten 0.40 1ins 19: 32758456 +A Pten 9.40 1del 19: 32758456 -A Tu20 Gene MRF Mut Position Indel Cdkn2a(Ex1β)					
Apc 7.50 1ins 18: 34261059 +T Pten 0.27 22del 19: 32758448 -CAGCGT Pten 0.28 1del 19: 32758457 -T Pten 8.12 1del 19: 32758456 -A Tu19 Gene MRF Mut Position Indel Trp53 9.97 1ins 11: 69587440 +A Apc 8.83 4del 18: 34261052 -AAGC Apc 9.82 1ins 18: 34261059 +T Tet2 11.20 4del 3: 133485654 -TGGA Tet2 11.78 1del 3: 133485658 -T Pten 0.40 1ins 19: 32758456 +A Pten 9.40 1del 19: 32758456 -A TU20 Gene MRF Mut Position Indel Cdkn2a(Ex1β) 3.55 1ins 4: 89294436 +T Apc 2.92 <td></td> <td></td> <td></td> <td></td> <td></td>					
Pten 0.27 22del 19: 32758448 -CAGCGT Pten 0.28 1del 19: 32758457 -T Pten 8.12 1del 19: 32758456 -A Tu19 Gene MRF Mut Position Indel Trp53 9.97 1ins 11: 69587440 +A Apc 8.83 4del 18: 34261052 -AAGC Apc 9.82 1ins 18: 34261059 +T Tet2 11.20 4del 3: 133485654 -TGGA Tet2 11.78 1del 3: 133485658 -T Pten 0.40 1ins 19: 32758456 +A Pten 9.40 1del 19: 32758456 -A Tu20 Gene MRF Mut Position Indel Cdkn2a(Ex1β) 3.55 1ins 4: 89294436 +T Apc 2.92 1ins 18: 34261059 +C Apc					-
Pten 0.28 1del 19: 32758457 -T Pten 8.12 1del 19: 32758456 -A Tu19 Gene MRF Mut Position Indel Trp53 9.97 1ins 11: 69587440 +A Apc 8.83 4del 18: 34261052 -AAGC Apc 9.82 1ins 18: 34261059 +T Tet2 11.20 4del 3: 133485654 -TGGA Tet2 11.78 1del 3: 133485658 -T Pten 0.40 1ins 19: 32758456 +A Pten 9.40 1del 19: 32758457 -T Pten 10.84 1del 19: 32758456 -A Tu20 Gene MRF Mut Position Indel Cdkn2a(Ex1β) 3:55 1ins 4: 89294436 +T Apc 2:92 1ins 18: 34261059 +C Apc <					-CAGCGT
Pten 8.12 1del 19: 32758456 -A Tu19 Gene MRF Mut Position Indel Trp53 9.97 1ins 11: 69587440 +A Apc 8.83 4del 18: 34261052 -AAGC Apc 9.82 1ins 18: 34261059 +T Tet2 11.20 4del 3: 133485654 -TGGA Tet2 11.78 1del 3: 133485658 -T Pten 0.40 1ins 19: 32758456 +A Pten 9.40 1del 19: 32758457 -T Pten 10.84 1del 19: 32758456 -A Tu20 Gene MRF Mut Position Indel Cdkn2a(Ex1β) 3.55 1ins 4: 89294436 +T Apc 2.92 1ins 18: 34261059 +C Apc 6.38 2ins 18: 34261059 +C Apc 6.38 2ins 18: 34261059 <td></td> <td></td> <td></td> <td></td> <td></td>					
Gene MRF Mut Position Indel Trp53 9.97 1ins 11: 69587440 +A Apc 8.83 4del 18: 34261052 -AAGC Apc 9.82 1ins 18: 34261059 +T Tet2 11.20 4del 3: 133485654 -TGGA Tet2 11.78 1del 3: 133485658 -T Pten 0.40 1ins 19: 32758456 +A Pten 9.40 1del 19: 32758456 -A Pten 10.84 1del 19: 32758456 -A Tu20 Gene MRF Mut Position Indel Cdkn2a(Ex1β) 3.55 1ins 4: 89294436 +T Arid1a 9.85 1del 4: 133723007 -G Apc 2.92 1ins 18: 34261059 +C Apc 6.38 2ins 18: 34261059 +T Tet2 2.89 2del 3:133485657 -AT <td></td> <td></td> <td></td> <td></td> <td>-A</td>					-A
Gene MRF Mut Position Indel Trp53 9.97 1ins 11: 69587440 +A Apc 8.83 4del 18: 34261052 -AAGC Apc 9.82 1ins 18: 34261059 +T Tet2 11.20 4del 3: 133485654 -TGGA Tet2 11.78 1del 3: 133485658 -T Pten 0.40 1ins 19: 32758456 +A Pten 9.40 1del 19: 32758456 -A Pten 10.84 1del 19: 32758456 -A Tu20 Gene MRF Mut Position Indel Cdkn2a(Ex1β) 3.55 1ins 4: 89294436 +T Arid1a 9.85 1del 4: 133723007 -G Apc 2.92 1ins 18: 34261059 +C Apc 6.38 2ins 18: 34261059 +T Tet2 2.89 2del 3:133485657 -AT <th>Tu19</th> <th></th> <th></th> <th></th> <th></th>	Tu19				
Trp53 9.97 1ins 11: 69587440 +A Apc 8.83 4del 18: 34261052 -AAGC Apc 9.82 1ins 18: 34261059 +T Tet2 11.20 4del 3: 133485654 -TGGA Tet2 11.78 1del 3: 133485658 -T Pten 0.40 1ins 19: 32758456 +A Pten 9.40 1del 19: 32758456 -A Pten 10.84 1del 19: 32758456 -A Tu20 Gene MRF Mut Position Indel Cdkn2a(Ex1β) 3.55 1ins 4: 89294436 +T Arid1a 9.85 1del 4: 133723007 -G Apc 2.92 1ins 18: 34261059 +C Apc 6.38 2ins 18: 34261059 +TT Apc 15.18 1ins 18: 34261059 +T Tet2 2.89 2del 3:133485658 -T	Gene	MRF	Mut	Position	Indel
Apc 8.83 4del 18: 34261052 -AAGC Apc 9.82 1ins 18: 34261059 +T Tet2 11.20 4del 3: 133485654 -TGGA Tet2 11.78 1del 3: 133485658 -T Pten 0.40 1ins 19: 32758456 +A Pten 9.40 1del 19: 32758457 -T Pten 10.84 1del 19: 32758456 -A Tu20 Gene MRF Mut Position Indel Cdkn2a(Ex1β) 3.55 1ins 4: 89294436 +T Arid1a 9.85 1del 4: 133723007 -G Apc 2.92 1ins 18: 34261059 +C Apc 6.38 2ins 18: 34261059 +TT Apc 15.18 1ins 18: 34261059 +T Tet2 2.89 2del 3:133485658 -T Pten 12.06 1ins 19: 32758457 +T					
Apc 9.82 1ins 18: 34261059 +T Tet2 11.20 4del 3: 133485654 -TGGA Tet2 11.78 1del 3: 133485658 -T Pten 0.40 1ins 19: 32758456 +A Pten 9.40 1del 19: 32758457 -T Pten 10.84 1del 19: 32758456 -A Tu20 Gene MRF Mut Position Indel Cdkn2a(Ex1β) 3.55 1ins 4: 89294436 +T Arid1a 9.85 1del 4: 133723007 -G Apc 2.92 1ins 18: 34261059 +C Apc 6.38 2ins 18: 34261059 +TT Apc 15.18 1ins 18: 34261059 +T Tet2 2.89 2del 3:133485657 -AT Tet2 14.21 1del 3:133485658 -T Pten 12.06 1ins		8.83	4del	18: 34261052	-AAGC
Tet2 11.20 4del 3: 133485654 -TGGA Tet2 11.78 1del 3: 133485658 -T Pten 0.40 1ins 19: 32758456 +A Pten 9.40 1del 19: 32758457 -T Pten 10.84 1del 19: 32758456 -A Tu20 Gene MRF Mut Position Indel Cdkn2a(Ex1β) 3.55 1ins 4: 89294436 +T Arid1a 9.85 1del 4: 133723007 -G Apc 2.92 1ins 18: 34261059 +C Apc 6.38 2ins 18: 34261059 +TT Apc 15.18 1ins 18: 34261059 +T Tet2 2.89 2del 3:133485657 -AT Tet2 14.21 1del 3:133485658 -T Pten 12.06 1ins 19: 32758457 +T		9.82	1ins	18: 34261059	+T
Pten 0.40 1ins 19: 32758456 +A Pten 9.40 1del 19: 32758457 -T Pten 10.84 1del 19: 32758456 -A Tu20 Gene MRF Mut Position Indel Cdkn2a(Ex1β) 3.55 1ins 4: 89294436 +T Arid1a 9.85 1del 4: 133723007 -G Apc 2.92 1ins 18: 34261059 +C Apc 6.38 2ins 18: 34261059 +TT Apc 15.18 1ins 18: 34261059 +T Tet2 2.89 2del 3:133485657 -AT Tet2 14.21 1del 3:133485658 -T Pten 12.06 1ins 19: 32758457 +T		11.20	4del	3: 133485654	-TGGA
Pten 9.40 1del 19: 32758457 -T Pten 10.84 1del 19: 32758456 -A Tu20 Gene MRF Mut Position Indel Cdkn2a(Ex1β) 3.55 1ins 4: 89294436 +T Arid1a 9.85 1del 4: 133723007 -G Apc 2.92 1ins 18: 34261059 +C Apc 6.38 2ins 18: 34261059 +TT Apc 15.18 1ins 18: 34261059 +T Tet2 2.89 2del 3:133485657 -AT Tet2 14.21 1del 3:133485658 -T Pten 12.06 1ins 19: 32758457 +T	Tet2	11.78	1del	3: 133485658	-T
Pten 10.84 1del 19: 32758456 -A Tu20 Gene MRF Mut Position Indel Cdkn2a(Ex1β) 3.55 1ins 4: 89294436 +T Arid1a 9.85 1del 4: 133723007 -G Apc 2.92 1ins 18: 34261059 +C Apc 6.38 2ins 18: 34261059 +TT Apc 15.18 1ins 18: 34261059 +T Tet2 2.89 2del 3:133485657 -AT Tet2 14.21 1del 3:133485658 -T Pten 12.06 1ins 19: 32758457 +T	Pten	0.40	1ins	19: 32758456	+A
$ \begin{array}{c ccccccccccccccccccccccccccccccccccc$	Pten	9.40	1del	19: 32758457	-T
	Pten	10.84	1del	19: 32758456	-A
Cdkn2a(Ex1β) 3.55 1ins 4: 89294436 +T Arid1a 9.85 1del 4: 133723007 -G Apc 2.92 1ins 18: 34261059 +C Apc 6.38 2ins 18: 34261059 +TT Apc 15.18 1ins 18: 34261059 +T Tet2 2.89 2del 3:133485657 -AT Tet2 14.21 1del 3:133485658 -T Pten 12.06 1ins 19: 32758457 +T	Tu20				
Arid1a 9.85 1del 4: 133723007 -G Apc 2.92 1ins 18: 34261059 +C Apc 6.38 2ins 18: 34261059 +TT Apc 15.18 1ins 18: 34261059 +T Tet2 2.89 2del 3:133485657 -AT Tet2 14.21 1del 3:133485658 -T Pten 12.06 1ins 19: 32758457 +T	Gene	MRF	Mut	Position	Indel
Apc 2.92 1ins 18: 34261059 +C Apc 6.38 2ins 18: 34261059 +TT Apc 15.18 1ins 18: 34261059 +T Tet2 2.89 2del 3:133485657 -AT Tet2 14.21 1del 3:133485658 -T Pten 12.06 1ins 19: 32758457 +T	Cdkn2a(Ex1β)	3.55	1ins	4: 89294436	+T
Apc 2.92 1ins 18: 34261059 +C Apc 6.38 2ins 18: 34261059 +TT Apc 15.18 1ins 18: 34261059 +T Tet2 2.89 2del 3:133485657 -AT Tet2 14.21 1del 3:133485658 -T Pten 12.06 1ins 19: 32758457 +T	Arid1a	9.85	1del	4: 133723007	-G
Apc 15.18 1ins 18: 34261059 +T Tet2 2.89 2del 3:133485657 -AT Tet2 14.21 1del 3:133485658 -T Pten 12.06 1ins 19: 32758457 +T	Apc				+C
Tet2 2.89 2del 3:133485657 -AT Tet2 14.21 1del 3:133485658 -T Pten 12.06 1ins 19: 32758457 +T	Apc	6.38	2ins	18: 34261059	+TT
Tet2 14.21 1del 3:133485658 -T Pten 12.06 1ins 19: 32758457 +T	Apc	15.18	1ins	18: 34261059	+T
Pten 12.06 1ins 19: 32758457 +T				3:133485657	-AT
	Tet2	14.21	1del	3:133485658	-T
Pten 12.93 1del 19: 32758456 -A	Pten				+T
	Pten	12.93	1del	19: 32758456	-A

Tu21				
Gene	MRF	Mut	Position	Indel
Smad4	3.22	1del	18: 73675801	-A
Arid1a	3.94	1del	4: 133723007	-G
Cdkn2a(Ex2)	4.59	1ins	4: 89276740	+A
Apc	2.75	7del	18: 34261052	-AAGCAAG
Apc	2.96	2del	18: 34261055	-CA
Арс	3.02	1del	18: 34261058	-G
Арс	3.54	1ins	18: 34261059	+T
Арс	3.86	1ins	18: 34261059	+A
Apc	4.05	1ins	18: 34261058	+G
Apc	4.66	13del	18: 34261045	-GTTCAA
Apc	5.06	3del	18: 34261058	-GTT
Apc	8.49	15del	18: 34261056	-AAGTGA
Tet2	10.96	1del	3:133485658	-T
Pten	0.94	35ins	19: 32758590	+AGAGAC
Pten	1.14	1del	19: 32758456	-A
Pten	2.98	2del	19: 32758455	-CA
Pten	4.40	6del	19: 32758457	-TCAAAG
Pten	5.14	152del	19: 32758305	-CCATCA
Pten	11.65	1del	19: 32758457	-T

Supplementary Table 3. Overview of cohorts and tumor prevalence in CCI₄ treated wild type mice and Alb-Cre;Kras^{LSL-G12D/+} upon 18sgRNA CRISPR/Cas9 mutagenesis. In the carbon tetrachloride (CCI₄) treated cohorts, wild type mice received *hSpCas9* only (control cohort) or *hSpCas9* and 18 sgRNAs (experimental cohort) by hydrodynamic tail vein injection (HTVI). Beginning two weeks after HTVI mice were treated nine times with a weekly intraperitoneal injection of 1µL/g body weight 10% CCI₄. Whereas no tumors were observed in the control cohort by magnetic resonance imaging (MRI) screening or at necropsy, 7 of 16 mice in the experimental cohort developed signs of illness between 30 to 60 weeks post HTVI. All of these mice had HCCs at necropsy. 35 tumors were collected and analyzed so far. In the *Alb-Cre;Kras^{LSL-G12D/+}* cohorts, three out of three mice in the experimental cohorts developed signs of illness between 21 and 32 weeks post HTVI. Six tumors were collected and analyzed. None of the control animals developed ICCs or HCCs within this time span.

Cohort	Alive		Dead	
wild type & CCI ₄	number of mice	number of mice	weeks post HTVI	necropsy
hSpCas9 only (control cohort)	4 (> 50 weeks)	4	20-30	no HCC/ ICC
hSpCas9 & 18 sgRNA (experimental cohort)	9 (> 60 weeks)	7	30-60	all 7 mice had HCCs (Tu28-Tu62)
Alb-Cre; Kras ^{LSL-G12D/+}	number of mice	number of mice	weeks post HTVI	necropsy
hSpCas9 only (control cohort)	-	8	20-30	no HCC/ ICC
hSpCas9 & 18 sgRNA (experimental cohort)	-	3	21-32	all 3 mice had ICCs/ HCCs (Tu22-Tu27)

Supplementary Table 4. Indel analysis in primary tumors and metastases derived from one mouse injected with *hSpCas9* and 18 sgRNAs. *CRISPR-SB* vectors expressing *hSpCas9* and 18 sgRNAs (targeting 18 different tumor suppressor genes) were delivered into livers of *Alb-Cre;Kras^{LSL-G12D/+}* mice using hydrodynamic tail vein injection (HTVI). While most liver tumors were detected 20 to 30 weeks post HTVI due to regular MRI screening and were thus small (1-3mm), one animal developed a large early onset ICC 20 weeks post HTVI (before start of MRI screening) with multiple metastases to lymph nodes, peritoneum and lungs (see Figure 4). DNA was isolated from different areas of the primary tumor (n=10) and from numerous metastases (n=9). Cell lines were generated from primary tumor (n=9) and metastases (n=9). CRISPR/Cas9 target sites in all samples (n=37) were amplified and sequenced using amplicon-based next-generation sequencing. Indel analysis revealed three independent primary tumors (Tu22, Tu23, Tu24), with the largest part of the tumor mass being formed by Tu24 (eight out of ten samples). The table below shows indels detected in the Tu22, Tu23 and Tu24 (for Tu24 two representative samples are shown) and corresponding cell lines (for Tu23 and Tu24). Indels with a mutant read frequency (MRF) of 0.2% or higher are shown. This cut-off takes technical sequencing errors into account.

Tu22				
Gene	MRF	Mut	Position	Indel
Apc	6.8%	1ins	18:34261059	+T
Apc	3.9%	3del	18:34261058	-GTT
Apc	3.8%	4del	18:34261052	-AAGC
Arid1b	0.9%	16del	17:5040686	-CGGGCA
Arid1b	24.0%	1del	17:5040687	-G
Cdkn2a(Ex2)	8.2%	1del	4:89276739	-G
Errfi1	0.6%	2del	4:150866429	-GT
Errfi1	5.1%	1ins	4:150866431	+G
Errfi1	6.9%	4del	4:150866427	-GCGT
Errfi1	10.0%	1del	4:150866431	-G
lgsf10	11.9%	1del	3:59336469	-C
Pten	19.4%	1del	19:32758457	-T
Pten	5.9%	1del	19:32758456	-A
Tet2	9.0%	1del	3:133485658	-T
Tet2	8.4%	1ins	3:133485658	+T
Tet2	7.8%	2del	3:133485657	-AT
Tet2	9.2%	2del	3:133485656	-GA
Trp53	8.2 %	1del	11: 69587440	-G
Tu23				
Gene	MRF	Mut	Position	Indel
Arid1b	31.4%	2del	17:5040686	-CG
Arid2	33.4%	1del	15: 9628729	-G
lgsf10	15.9%	1del	3:59336469	-C
lgsf10	17.4%	5del	3:59336465	-AACGC
Pten	15.7%	1ins	19:32758457	+T
Pten	27.8%	1del	19:32758456	-A
Pten	20.1%	1del	19:32758457	-T
Tu23 cell line	е			
Gene	MRF	Mut	Position	Indel
Arid1b	52.4%	2del	17:5040686	-CG
Arid2	99.8%	1del	15: 9628729	-G
lgsf10	51.2%	1del	3:59336469	-C
lgsf10	48.7%	5del	3:59336465	-AACGC
Pten	50.5%	1ins	19:32758457	+T
Pten	30.1%	1del	19:32758456	-A
Pten	19.3%	1del	19:32758457	-T

T., 24.4				
Tu24.1 Gene	MRF	Mut	Position	Indel
Arid1b	39.2%	1del	17:5040686	-C
Arid1b	46.6%	16del	17:5040686	-CGGGCA
Arid2	76.2%	3del	15: 9628729	-GCG
Cdkn2a(Ex1β)	73.1%	37del	4:89294408	-CGCGAA
Errfi1	73.6%	2del	4:150866429	-GT
Irf2	75.3%	1ins	8:46806498	+T
Pten	41.2%	4del	19:32758457	-TCAA
Pten Trp53	43.6% 43.1%	2ins 1del	19:32758457 11:69587440	+TG -G
Tu24.1 cell lir		ruei	11.09367440	-0
Gene	MRF	Mut	Position	Indel
Arid1b	47.2%	1del	17:5040686	-C
Arid1b	52.8%	16del	17:5040686	-CGGGCA
Arid2	99.4%	3del	15: 9628729	-GCG
Cdkn2a(Ex1β)	99.6%	37del	4:89294408	-CGCGAA
Errfi1	99.8%	2del	4:150866429	-GT
Irf2	99.8%	1ins	8:46806498	+T
Pten	50.5%	4del	19:32758457 19:32758457	-TCAA
Pten Trp53	49.2% 50.6%	2ins 1del	11:69587440	+TG -G
Tu24.2	00.070	1401	11.00001	Ö
Gene	MRF	Mut	Position	Indel
Arid1b	37.8%	1del	17:5040686	-C
Arid1b	43.7%	16del	17:5040686	-CGGGCA
Arid2	75.1%	3del	15: 9628729	-GCG
Cdkn2a(Ex1β)	77.4%	37del	4:89294408	-CGCGAA
Errfi1	68.4%	2del	4:150866429	-GT
Irf2 Pten	69.4%	1ins	8:46806498	+T
	37.6%	4del	19:32758457	-TCAA
		'line	10.22758457	
Pten Trn53	46.0%	2ins 1del	19:32758457 11:69587440	+TG -G
Trp53	41.2%	1del	19:32758457 11:69587440	-G
	41.2%			
Trp53 Tu24.2 cell lir	41.2% ne MRF 46.0%	1del	11:69587440	-G Indel -C
Trp53 Tu24.2 cell lir Gene Arid1b Arid1b	41.2% MRF 46.0% 54.0%	Mut 1del 16del	11:69587440 Position 17:5040686 17:5040686	-G Indel -C -CGGGCA
Trp53 Tu24.2 cell lir Gene Arid1b Arid1b Arid2	41.2% MRF 46.0% 54.0% 99.6%	Mut 1del 16del 3del	11:69587440 Position 17:5040686 17:5040686 15: 9628729	-G Indel -C -CGGGCA -GCG
Trp53 Tu24.2 cell lin Gene Arid1b Arid1b Arid2 Cdkn2a(Ex1β)	41.2% MRF 46.0% 54.0% 99.6% 99.7%	Mut 1del 16del 3del 37del	11:69587440 Position 17:5040686 17:5040686 15: 9628729 4:89294408	-G Indel -C -CGGGCA -GCG -CGCGAA
Trp53 Tu24.2 cell lir Gene Arid1b Arid1b Arid2 Cdkn2a(Ex1β) Errfi1	41.2% MRF 46.0% 54.0% 99.6% 99.7%	Mut 1del 16del 3del 37del 2del	11:69587440 Position 17:5040686 17:5040686 15: 9628729 4:89294408 4:150866429	-G Indel -C -CGGGCA -GCG -CGCGAA -GT
Trp53 Tu24.2 cell lir Gene Arid1b Arid1b Arid2 Cdkn2a(Ex1β) Errfi1 Irf2	41.2% MRF 46.0% 54.0% 99.6% 99.7% 99.7% 99.8%	Mut 1del 16del 3del 37del 2del 1ins	Position 17:5040686 17:5040686 15: 9628729 4:89294408 4:150866429 8:46806498	-G Indel -C -CGGGCA -GCG -CGCGAA -GT +T
Trp53 Tu24.2 cell lir Gene Arid1b Arid1b Arid2 Cdkn2a(Ex1β) Errfi1	41.2% MRF 46.0% 54.0% 99.6% 99.7%	Mut 1del 16del 3del 37del 2del	11:69587440 Position 17:5040686 17:5040686 15: 9628729 4:89294408 4:150866429	-G Indel -C -CGGGCA -GCG -CGCGAA -GT
Trp53 Tu24.2 cell lir Gene Arid1b Arid1b Arid2 Cdkn2a(Ex1β) Errfi1 Irf2 Pten	41.2% 10 MRF 46.0% 54.0% 99.6% 99.7% 99.7% 99.8% 48.7%	Mut 1del 16del 3del 37del 2del 1ins 4del	Position 17:5040686 17:5040686 15: 9628729 4:89294408 4:150866429 8:46806498 19:32758457	-G Indel -C -CGGGCA -GCG -CGCGAA -GT +T -TCAA
Trp53 Tu24.2 cell lir Gene Arid1b Arid2 Cdkn2a(Ex1β) Errfi1 Irf2 Pten Pten	41.2% MRF 46.0% 54.0% 99.6% 99.7% 99.7% 99.8% 48.7% 51.1%	Mut 1del 16del 3del 37del 2del 1ins 4del 2ins	Position 17:5040686 17:5040686 15: 9628729 4:89294408 4:150866429 8:46806498 19:32758457 19:32758457	-G Indel -C -CGGGCA -GCG -CGCGAA -GT +T -TCAA +TG
Trp53 Tu24.2 cell lin Gene Arid1b Arid2 Cdkn2a(Ex1β) Errfi1 Irf2 Pten Pten Trp53	41.2% MRF 46.0% 54.0% 99.6% 99.7% 99.7% 99.8% 48.7% 51.1%	Mut 1del 16del 3del 37del 2del 1ins 4del 2ins	Position 17:5040686 17:5040686 15: 9628729 4:89294408 4:150866429 8:46806498 19:32758457 19:32758457	-G Indel -C -CGGGCA -GCG -CGCGAA -GT +T -TCAA +TG
Trp53 Tu24.2 cell lir Gene Arid1b Arid2 Cdkn2a(Ex1β) Errfi1 Irf2 Pten Pten Trp53 Met24.1 Gene Arid1b	41.2% MRF 46.0% 54.0% 99.6% 99.7% 99.7% 99.8% 48.7% 51.1% 53.3% MRF 35.8%	Mut 1del 1del 16del 3del 37del 2del 1ins 4del 2ins 1del Mut 1del	11:69587440 Position 17:5040686 17:5040686 15: 9628729 4:89294408 4:150866429 8:46806498 19:32758457 11:69587440 Position 17:5040686	-G Indel -C -CGGGCA -GCG -CGCGAA -GT +T -TCAA +TG -G Indel -C
Trp53 Tu24.2 cell lir Gene Arid1b Arid2 Cdkn2a(Ex1β) Errfi1 Irf2 Pten Pten Trp53 Met24.1 Gene Arid1b Arid1b	41.2% MRF 46.0% 54.0% 99.6% 99.7% 99.7% 99.8% 48.7% 51.1% 53.3% MRF 35.8% 43.8%	Mut 1del 16del 3del 37del 2del 1ins 4del 2ins 1del Mut 1del 16del	11:69587440 Position 17:5040686 17:5040686 15: 9628729 4:89294408 4:150866429 8:46806498 19:32758457 11:69587440 Position 17:5040686 17:5040686	-G Indel -C -CGGGCA -GCG -CGCGAA -GT +T -TCAA +TG -G Indel -C -CGGGCA
Trp53 Tu24.2 cell lin Gene Arid1b Arid2 Cdkn2a(Ex1β) Errfi1 Irf2 Pten Pten Trp53 Met24.1 Gene Arid1b Arid1b Arid2	41.2% IC MRF 46.0% 54.0% 99.6% 99.7% 99.7% 99.8% 48.7% 51.1% 53.3% MRF 35.8% 43.8% 68.5%	Mut 1del 1del 16del 3del 37del 2del 1ins 4del 2ins 1del Mut 1del 16del 3del	Position 17:5040686 17:5040686 15: 9628729 4:89294408 4:150866429 8:46806498 19:32758457 11:69587440 Position 17:5040686 17:5040686 15: 9628729	-G Indel -C -CGGGCA -GCG -CGCGAA -GT +T -TCAA +TG -G Indel -C -CGGGCA
Trp53 Tu24.2 cell lir Gene Arid1b Arid1b Arid2 Cdkn2a(Ex1β) Errfi1 Irf2 Pten Pten Trp53 Met24.1 Gene Arid1b Arid1b Arid2 Cdkn2a(Ex1β)	41.2% ICHAPTER 146.0% 54.0% 99.6% 99.7% 99.7% 99.8% 48.7% 51.1% 53.3% MRF 35.8% 43.8% 68.5% 72.3%	Mut	Position 17:5040686 17:5040686 15: 9628729 4:89294408 4:150866429 8:46806498 19:32758457 11:69587440 Position 17:5040686 17:5040686 15: 9628729 4:89294408	Indel -C -CGGGCA -GCG -CGCGAA -GT +T -TCAA +TG -G Indel -C -CGGGCA -GCG -CGCGAA
Trp53 Tu24.2 cell lin Gene Arid1b Arid1b Arid2 Cdkn2a(Ex1β) Errfi1 Irf2 Pten Pten Trp53 Met24.1 Gene Arid1b Arid2 Cdkn2a(Ex1β) Errfi1 Gene Arid1b Arid2 Cdkn2a(Ex1β) Errfi1	41.2% IC MRF 46.0% 54.0% 99.6% 99.7% 99.7% 99.8% 48.7% 51.1% 53.3% MRF 35.8% 43.8% 68.5% 72.3% 64.3%	Mut	11:69587440 Position 17:5040686 17:5040686 15: 9628729 4:89294408 4:150866429 8:46806498 19:32758457 11:69587440 Position 17:5040686 17:5040686 15: 9628729 4:89294408 4:150866429	Indel -C -CGGGCA -GCG -CGCGAA -GT +T -TCAA +TG -G Indel -C -CGGGCA -GCG -CGCGAA
Trp53 Tu24.2 cell lir Gene Arid1b Arid2 Cdkn2a(Ex1β) Errfi1 Irf2 Pten Pten Trp53 Met24.1 Gene Arid1b Arid2 Cdkn2a(Ex1β) Errfi1 Irf2	41.2% IC MRF 46.0% 54.0% 99.6% 99.7% 99.8% 48.7% 51.1% 53.3% MRF 35.8% 43.8% 68.5% 72.3% 64.3% 64.0%	Mut	Position 17:5040686 17:5040686 15: 9628729 4:89294408 4:150866429 8:46806498 19:32758457 11:69587440 Position 17:5040686 17:5040686 17:5040686 15: 9628729 4:89294408 4:150866429 8:46806498	Indel -C -CGGGCA -GCG -CGCGAA -GT +T -TCAA +TG -G Indel -C -CGGGCA -GCG -CGCGAA
Trp53 Tu24.2 cell lin Gene Arid1b Arid1b Arid2 Cdkn2a(Ex1β) Errfi1 Irf2 Pten Pten Trp53 Met24.1 Gene Arid1b Arid2 Cdkn2a(Ex1β) Errfi1 Gene Arid1b Arid2 Cdkn2a(Ex1β) Errfi1	41.2% IC MRF 46.0% 54.0% 99.6% 99.7% 99.7% 99.8% 48.7% 51.1% 53.3% MRF 35.8% 43.8% 68.5% 72.3% 64.3%	Mut	11:69587440 Position 17:5040686 17:5040686 15: 9628729 4:89294408 4:150866429 8:46806498 19:32758457 11:69587440 Position 17:5040686 17:5040686 15: 9628729 4:89294408 4:150866429	Indel -C -CGGGCA -GCG -CGCGAA -GT +T -TCAA +TG -G Indel -C -CGGGCA -GCG -CGCGAA
Trp53 Tu24.2 cell lin Gene Arid1b Arid2 Cdkn2a(Ex1β) Errfi1 Irf2 Pten Pten Trp53 Met24.1 Gene Arid1b Arid2 Cdkn2a(Ex1β) Errfi1 Irf2 Pten Trp53	41.2% MRF 46.0% 54.0% 99.6% 99.7% 99.7% 51.1% 53.3% MRF 35.8% 43.8% 68.5% 72.3% 64.0% 39.2% 43.4% 37.6%	Mut	Position 17:5040686 17:5040686 15: 9628729 4:89294408 4:150866429 8:46806498 19:32758457 11:69587440 Position 17:5040686 17:5040686 17:5040686 15: 9628729 4:89294408 4:150866429 8:46806498 19:32758457	Indel -C -CGGGCA -GCG -CGCGAA -GT +T -TCAA +TG -G Indel -C -CGGGCA -GCG -CGCGAA -GT +T -TCAA
Trp53 Tu24.2 cell lin Gene Arid1b Arid2 Cdkn2a(Ex1β) Errfi1 Irf2 Pten Pten Trp53 Met24.1 Gene Arid1b Arid1b Arid2 Cdkn2a(Ex1β) Errfi1 Irf2 Pten Pten Pten Arid1b Arid1b Arid1b Arid2 Cdkn2a(Ex1β) Errfi1 Irf2 Pten Pten	41.2% MRF 46.0% 54.0% 99.6% 99.7% 99.7% 51.1% 53.3% MRF 35.8% 43.8% 68.5% 72.3% 64.0% 39.2% 43.4% 37.6%	Mut	Position 17:5040686 17:5040686 15: 9628729 4:89294408 4:150866429 8:46806498 19:32758457 11:69587440 Position 17:5040686 17:5040686 17:5040686 15: 9628729 4:89294408 4:150866429 8:46806498 19:32758457 19:32758457	Indel -C -CGGGCA -GCG -CGCGAA -GT +T -TCAA +TG -G Indel -C -CGGGCA -GCG -CGCGAA -GT +T -TCAA +TG -TCAA -TCAA -TCAA -TCAA -TCAA -TCAA -TCAA -TCAA
Trp53 Tu24.2 cell lin Gene Arid1b Arid2 Cdkn2a(Ex1β) Errfi1 Irf2 Pten Pten Trp53 Met24.1 Gene Arid1b Arid2 Cdkn2a(Ex1β) Errfi1 Irf2 Pten Trp53 Met24.1 Gene Arid1b Arid2 Cdkn2a(Ex1β) Errfi1 Irf2 Pten Pten Trp53 Met24.1 cell I Gene	41.2% MRF 46.0% 54.0% 99.6% 99.7% 99.7% 99.8% 48.7% 51.1% 53.3% MRF 35.8% 43.8% 68.5% 72.3% 64.0% 39.2% 43.4% 37.6% ine MRF	Mut	Position 17:5040686 17:5040686 15: 9628729 4:89294408 4:150866429 8:46806498 19:32758457 11:69587440 Position 17:5040686 15: 9628729 4:89294408 4:150866429 8:46806498 19:32758457 11:69587440 Position 17:5040686	Indel -C -CGGGCA -GCG -CGCGAA -GT +T -TCAA +TG -G Indel -C -CGGGCA -GCG -CGCGAA -GT +T -TCAA +TG -G Indel -C -CGGGCA -GCG -CGCGAA -GT -TCAA +TG -G Indel
Trp53 Tu24.2 cell lin Gene Arid1b Arid2 Cdkn2a(Ex1β) Errfi1 Irf2 Pten Pten Trp53 Met24.1 Gene Arid1b Arid2 Cdkn2a(Ex1β) Errfi1 Irf2 Pten Trp53 Met24.1 Gene Arid1b Arid2 Cdkn2a(Ex1β) Errfi1 Irf2 Pten Pten Trp53 Met24.1 cell I Gene Arid1b	41.2% MRF 46.0% 54.0% 99.6% 99.7% 99.7% 99.8% 48.7% 51.1% 53.3% MRF 35.8% 43.8% 68.5% 72.3% 64.0% 39.2% 43.4% 37.6% ine MRF 44.9%	Mut	Position 17:5040686 17:5040686 15: 9628729 4:89294408 4:150866429 8:46806498 19:32758457 11:69587440 Position 17:5040686 15: 9628729 4:89294408 4:150866429 8:46806498 19:32758457 11:69587440 Position 17:5040686 17:5040686 17:5040686	Indel -C -CGGGCA -GCG -CGCGAA -GT +T -TCAA +TG -G Indel -C -CGGGCA -GCG -CGCGAA -GT +T -TCAA -GCG -CGCGAA -GCG -CGCGAA -GT -T -TCAA -TCA
Trp53 Tu24.2 cell lin Gene Arid1b Arid2 Cdkn2a(Ex1β) Errfi1 Irf2 Pten Pten Trp53 Met24.1 Gene Arid1b Arid2 Cdkn2a(Ex1β) Errfi1 Irf2 Pten Trp53 Met24.1 Gene Arid1b Arid2 Cdkn2a(Ex1β) Errfi1 Irf2 Pten Pten Trp53 Met24.1 cell I Gene Arid1b Arid1b Arid1b	41.2% MRF 46.0% 54.0% 99.6% 99.7% 99.7% 99.8% 48.7% 51.1% 53.3% MRF 35.8% 43.8% 68.5% 72.3% 64.0% 39.2% 43.4% 37.6% ine MRF 44.9% 54.9%	Mut	Position 17:5040686 17:5040686 15: 9628729 4:89294408 4:150866429 8:46806498 19:32758457 11:69587440 Position 17:5040686 15: 9628729 4:89294408 4:150866429 8:46806498 19:32758457 11:69587440 Position 17:5040686 15: 9628729 4:89294408 4:150866429 8:46806498 19:32758457 11:69587440 Position 17:5040686 17:5040686	Indel -C -CGGGCA -GCG -CGCGAA -GT +T -TCAA +TG -G Indel -C -CGGGCA -GCG -CGCGAA -GT -T -TCAA -GCG -CGCGAA -GT -T -TCAA -GCG -CGCGAA -GT -T -TCAA -TC
Trp53 Tu24.2 cell lin Gene Arid1b Arid2 Cdkn2a(Ex1β) Errfi1 Irf2 Pten Pten Trp53 Met24.1 Gene Arid1b Arid2 Cdkn2a(Ex1β) Errfi1 Irf2 Pten Pren Trp53 Met24.1 Gene Arid1b Arid2 Cdkn2a(Ex1β) Errfi1 Irf2 Pten Pten Trp53 Met24.1 cell I Gene Arid1b Arid2b Arid1b Arid2	41.2% MRF 46.0% 54.0% 99.6% 99.7% 99.7% 99.8% 48.7% 51.1% 53.3% MRF 35.8% 43.8% 68.5% 72.3% 64.0% 39.2% 43.4% 37.6% ine MRF 44.9% 54.9% 99.2%	Mut	Position 17:5040686 17:5040686 15: 9628729 4:89294408 4:150866429 8:46806498 19:32758457 11:69587440 Position 17:5040686 15: 9628729 4:89294408 4:150866429 8:46806498 19:32758457 11:69587440 Position 17:5040686 15: 9628729 4:89294408 4:150866429 8:46806498 19:32758457 11:69587440 Position 17:5040686 17:5040686 17:5040686 17:5040686 15: 9628729	-G Indel -C -CGGGCA -GCG -CGCGAA -GT +T -TCAA +TG -G Indel -C -CGGGCA -GCG -CGCGAA -GT +T -TCAA -GCG -CGCGAA -GCG -CGCGAA -GCG -CGCGAA -GCG -CGCGAA
Trp53 Tu24.2 cell lin Gene Arid1b Arid2 Cdkn2a(Ex1β) Errfi1 Irf2 Pten Pten Trp53 Met24.1 Gene Arid1b Arid2 Cdkn2a(Ex1β) Errfi1 Irf2 Pten Pren Trp53 Met24.1 Gene Arid1b Arid2 Cdkn2a(Ex1β) Errfi1 Irf2 Pten Pten Trp53 Met24.1 cell I Gene Arid1b Arid2 Cdkn2a(Ex1β)	41.2% MRF 46.0% 54.0% 99.6% 99.7% 99.7% 99.8% 48.7% 51.1% 53.3% MRF 35.8% 43.8% 68.5% 72.3% 64.0% 39.2% 43.4% 37.6% ine MRF 44.9% 54.9% 99.2% 99.4%	Mut	Position 17:5040686 17:5040686 15: 9628729 4:89294408 4:150866429 8:46806498 19:32758457 11:69587440 Position 17:5040686 17:5040686 17:5040686 15: 9628729 4:89294408 4:150866429 8:46806498 19:32758457 11:69587440 Position 17:5040686 15: 9628729 4:89294408 Position 17:5040686 15: 9628729 4:89294408	-G Indel -C -CGGGCA -GCG -CGCGAA -GT +T -TCAA +TG -G Indel -C -CGGGCA -GCG -CGCGAA -GT +T -TCAA -GCG -CGCGAA -GCG -CGCGAA -GCG -CGCGAA
Trp53 Tu24.2 cell lir Gene Arid1b Arid2 Cdkn2a(Ex1β) Errfi1 Irf2 Pten Pten Trp53 Met24.1 Gene Arid1b Arid2 Cdkn2a(Ex1β) Errfi1 Irf2 Pten Pten Trp53 Met24.1 Gene Arid1b Arid2 Cdkn2a(Ex1β) Errfi1 Irf2 Pten Pten Trp53 Met24.1 cell I Gene Arid1b Arid2 Cdkn2a(Ex1β) Errfi1 Errfi1 Irf2 Pten Pten Trp53 Met24.1 cell I Gene Arid1b Arid2 Cdkn2a(Ex1β) Errfi1	41.2% MRF 46.0% 54.0% 99.6% 99.7% 99.7% 99.8% 48.7% 51.1% 53.3% MRF 35.8% 43.8% 68.5% 72.3% 64.0% 39.2% 43.4% 37.6% ine MRF 44.9% 54.9% 99.2% 99.4% 99.0%	Mut	Position 17:5040686 17:5040686 15: 9628729 4:89294408 4:150866429 8:46806498 19:32758457 11:69587440 Position 17:5040686 15: 9628729 4:89294408 4:150866429 8:46806498 19:32758457 11:69587440 Position 17:5040686 15: 9628729 4:89294408 4:150866429 8:46806498 19:32758457 11:69587440 Position 17:5040686 15: 9628729 4:89294408 4:150866429	-G Indel -C -CGGGCA -GCG -CGCGAA -GT +T -TCAA +TG -G Indel -C -CGGGCA -GCG -CGCGAA -GT +T -TCAA -GCG -CGCGAA -GCG -CGCGAA -GCG -CGCGAA -GCG -CGCGAA
Trp53 Tu24.2 cell lin Gene Arid1b Arid2 Cdkn2a(Ex1β) Errfi1 Irf2 Pten Pten Trp53 Met24.1 Gene Arid1b Arid2 Cdkn2a(Ex1β) Errfi1 Irf2 Pten Pren Trp53 Met24.1 Gene Arid1b Arid2 Cdkn2a(Ex1β) Errfi1 Irf2 Pten Pten Trp53 Met24.1 cell I Gene Arid1b Arid1b Arid2 Cdkn2a(Ex1β)	41.2% MRF 46.0% 54.0% 99.6% 99.7% 99.7% 99.8% 48.7% 51.1% 53.3% MRF 35.8% 43.8% 64.3% 64.3% 64.3% 64.3% 64.9% 99.2% 99.4% 99.2% 99.2%	Mut	Position 17:5040686 17:5040686 15: 9628729 4:89294408 4:150866429 8:46806498 19:32758457 11:69587440 Position 17:5040686 17:5040686 17:5040686 15: 9628729 4:89294408 4:150866429 8:46806498 19:32758457 11:69587440 Position 17:5040686 15: 9628729 4:89294408 Position 17:5040686 15: 9628729 4:89294408	-G Indel -C -CGGGCA -GCG -CGCGAA -GT +T -TCAA +TG -G Indel -C -CGGGCA -GCG -CGCGAA -GT +T -TCAA -GT -T -TCAA -GT -T -TCAA -GT -C -CGCGAA -GT -C -CGGGAA -GT -C -CGGGAA -GT
Trp53 Tu24.2 cell lir Gene Arid1b Arid2 Cdkn2a(Ex1β) Errfi1 Irf2 Pten Pten Trp53 Met24.1 Gene Arid1b Arid2 Cdkn2a(Ex1β) Errfi1 Irf2 Pten Pten Arid1b Arid2 Cdkn2a(Ex1β) Errfi1 Irf2 Pten Pten Trp53 Met24.1 cell I Gene Arid1b Arid2 Cdkn2a(Ex1β) Errfi1 Irf2 Pten Pten Trp53 Met24.1 cell I Gene Arid1b Arid2 Cdkn2a(Ex1β) Errfi1	41.2% MRF 46.0% 54.0% 99.6% 99.7% 99.7% 99.8% 48.7% 51.1% 53.3% MRF 35.8% 43.8% 68.5% 72.3% 64.0% 39.2% 43.4% 37.6% ine MRF 44.9% 54.9% 99.2% 99.4% 99.0%	Mut	Position 17:5040686 17:5040686 15: 9628729 4:89294408 4:150866429 8:46806498 19:32758457 11:69587440 Position 17:5040686 15: 9628729 4:89294408 4:150866429 8:46806498 19:32758457 11:69587440 Position 17:5040686 15: 9628729 4:89294408 4:150866429 8:46806498 19:32758457 11:69587440	-G Indel -C -CGGGCA -GCG -CGCGAA -GT +T -TCAA +TG -G Indel -C -CGGGCA -GCG -CGCGAA -GT +T -TCAA +TG -G -CGCGAA -GT +T -TCAA +TG -G -CGCGAA -GT +T -CCGGGCA

Met24.2				
Gene	MRF	Mut	Position	Indel
Arid1b	34.5%	1del	17:5040686	-C
Arid1b	43.1%	16del	17:5040686	-CGGGCA
Arid2	75.8%	3del	15: 9628729	-GCG
Cdkn2a(Ex1β)	80.0%	37del	4:89294408	-CGCGAA
Errfi1	66.1%	2del	4:150866429	-GT
Irf2	59.3%	1ins	8:46806498	+T
Pten	39.1%	4del	19:32758457	-TCAA
Pten	42.7%	2ins	19:32758457	+TG
Trp53	41.8%	1del	11:69587440	-G
Met24.2 cell	line			
Gene	MRF	Mut	Position	Indel
Arid1b	45.7%	1del	17:5040686	-C
Arid1b	54.1%	16del	17:5040686	-CGGGCA
Arid2	99.4%	3del	15: 9628729	-GCG
Cdkn2a(Ex1β)	99.9%	37del	4:89294408	-CGCGAA
Errfi1	98.7%	2del	4:150866429	-GT
Irf2	99.3%	1ins	8:46806498	+T
Pten	45.6%	4del	19:32758457	-TCAA
Pten	54.3%	2ins	19:32758457	+TG
Trp53	51.6%	1del	11:69587440	-G

Supplementary Table 5. Mono- versus biallelic mutations at CRISPR/Cas9 target sites. Analysis of the allelic status of CRISPR/Cas9 target sites in cell lines derived from Tu23 and Tu24. Target sites were regarded as being altered 'homozygously' if no wild type (wt) reads for the respective amplicon emerged from amplicon-based next generation sequencing. In this case, both alleles harbored indels and/or large deletions (fusions). The same indel or large deletion at both alleles indicates either independent identical CRISPR/Cas9-induced mutations on each allele or loss of heterozygosity. Target sites were considered as being altered 'heterozygously' if 50% of reads for the respective amplicon harbored an indel or large deletion and 50% of reads were wt.

Target site	NGS and fusion PCR results	Heterozygous	Homozygous
Tu23			
Arid1b	50% indel - 50% wt	1	
Arid2	100% indel - no wt		1
Igsf10	50% indel - 50% indel		1
Pten	28% indel - 20% indel - 16% indel		1
Arid1a	fusion - wt	1	
Cdkn2b	fusion - no wt		1
Errfi1	fusion - fusion		1
Tu24			
Trp53	50% indel - 50% wt	1	
Irf2	100% indel - no wt		1
Errfi1	100% indel - no wt		1
Pten	50% indel - 50% indel		1
Arid1b	50% indel - 50% indel		1
Cdkn2a-Ex1β	fusion - indel		1
Cdkn2a-Ex2	fusion - no wt		1
	sum	3	11
	percent	21%	79%

Supplementary Table 6. Sequences of the 18 sgRNAs used to target tumor suppressor genes in the mouse liver by hydrodynamic tail vein injection (HTVI).

Gene	Transcript (Ensembl transcript ID)	CCDS	sgRNA sequence (PAM)	Exon
Apc	Apc-001 (ENSMUST00000079362)	CCDS29125	TCAGTTGTTAAAGCAAGTTG (AGG)	2
Arid1a	Arid1a-201 (ENSMUST00000105897)	CCDS38908	TTAGTCCCACCATACGGCTG (AGG)	2
Brca1	Brca1-001 (ENSMUST00000017290)	CCDS25474	AAATCTTAGAGTGTCCGATC (TGG)	2
Brca2	Brca2-201 (ENSMUST00000044620)	CCDS39411	TAGGACCGATAAGCCTCAAT (TGG)	3
Cdkn2a (ex1β)	Cdkn2a-201 (ENSMUST00000107131)	CCDS18350	TGGTGAAGTTCGTGCGATCC (CGG)	1
Cdkn2a (ex2)	Cdkn2a-001 (ENSMUST00000060501) Cdkn2a-201 (ENSMUST00000107131)	CCDS38812 CCDS18350	GTGCGATATTTGCGTTCCGC (TGG)	2
Pten	Pten-001 (ENSMUST00000013807)	CCDS29753	GCTAACGATCTCTTTGATGA (TGG)	1
Smad4	Smad4-001 (ENSMUST00000025393)	CCDS29337	GACAACCCGCTCATAGTGATA (TGG)	2
Tet2	Tet2-201 (ENSMUST00000098603)	CCDS51071	GAAAGTGCCAACAGATATCC (AGG)	3
Trp53	Trp53-202 (ENSMUST00000171247)	CCDS48826	GACACTCGGAGGGCTTCACT (TGG)	4
Arid1b	Arid1b-201 (ENSMUST00000115797)	CCDS49929	CTGTGCACCTGGGGGACCGT (AGG)	2
Arid2	Arid2-001 (ENSMUST00000096250)	CCDS37185	AGGCGCCTCCGGACGAGCGG (AGG)	1
Arid5b	Arid5b-201 (ENSMUST00000020106)	CCDS35929	GCTATGCAAATCGGATCCTT (TGG)	2
Atm	Atm-001 (ENSMUST00000118282)	CCDS40636	GGCTGTCAACTTCCGAAAAC (GGG)	7
Cdkn2b	Cdkn2b-201 (ENSMUST00000097981)	CCDS18351	GGCGCCTCCCGAAGCGGTTC (AGG)	1
Errfl1	Errfi1-001 (ENSMUST00000030811)	CCDS18974	AAGCTCGGGACAGCGTGAAG (AGG)	4
lgsf10	Igsf10-201 (ENSMUST00000039419)	CCDS50915	TGAGTCCGTAAAACGCCTCG (GGG)	4
Irf2	Irf2-201 (ENSMUST00000034041)	CCDS22295	GTGCCGAGCCGCATGCATCC (AGG)	3

Supplementary Table 7. Primary antibodies used for immunohistochemistry.

Antibody	Company/Source	Host	Pretreatment	Dilution
A6	Engelhardt et al Differentiation; research in biological diversity, 1990	rat	Proteinase; 37°C; 10min	1:100
AFP	R&D (AF5369)	goat	Citrate; 100°C; 30min	1:100
Collagen-4	Cedarlane (CL50451AP)	rabbit	Proteinase; 37°C; 10min	1:50
Cytokeratin 19	Hybridoma bank (TROMAIIIc)	rat	EDTA; 100°C; 20min	1:500
Ki67	Neo Markers (Clone SP6)	rabbit	EDTA; 95°C; 30min	1:200

Supplementary Table 8. Primer sequences for target site amplicons. Primers used for amplifying CRISPR/Cas9 target sites (length of PCR products is between 400bp and 600bp) and oligonucleotides used for amplicon-based next-generation sequencing.

Guide	Forward primer	Reverse primer		
Apc	GCGAATAAGCACCACTCCTC	AAGAATGAACCAACACCAAGG		
Arid1a	GTTCTGATTCCTGTGCTCGC	TCCATCACCTACCTGCTGTG		
Brca1	AGCGTGAGAACTCCTCCAAA	CTGCCATGAGGAAGAACACA		
Brca2	TCACGAGTTTCTCCGTGTCA	GCTCTGGCTGTCTCGAACTT		
Cdkn2a (ex1β)	TCTCACCTCGCTTGTCACAG	AAGTACTCCATCTCCCGGGA		
Cdkn2a (ex2)	TCAACTACGGTGCAGATTCG	CGGGTGGGTAAAATGGGAAC		
Pten	TGCGAGGATTATCCGTCTTC	CATCCGTCTACTCCCACGTT		
Smad4	TGCAGTGTCACAGATGCTCA	CTCAGGAACTGGAGGAAGCA		
Tet2	CAGATGCTTAGGCCAATCAAG	AGAAGCAACACACATGAAGATG		
Trp53	ACATAGCAAGTTGGAGGCCA	CCACTCACCGTGCACATAAC		
Arid1b	AGTTCTGGGGTACTTGGAATCA	GGTACTGCAAGCCTCCCA		
Arid2	ATGACTGAGCCCCGCCA	GAGCAGACTTTTCCGAGCAG		
Arid5b	TGGCTTGCACGGACCTTATA	ATCAGCAGTTGGACGGTCTT		
Atm	TCCTTTTCAACTGTTCCTGTTACA	GACAATGGAAAGGCGAGTCA		
Cdkn2b	CCGAAGCTACTGGGTCTCC	CACTTGCCCAGCTTGTACG		
Errfl1	GTGTTCCCCTACTCTGGCTC	TCTTCAGAGATGGGCAGTGG		
lgsf10	CTGTCCACCTGAGTCCACTT	TGTCAGCCGGTTTCCTTCTA		
Irf2	TGTCTGACAGTCGACTTCCC ACTGGGAACTTCTGGGATGG			
Oligonucleotides for library preparation				
PE adapter top strand	ACACTCTTTCCCTACACGACGCTCTTCCGATCT			
PE adapter bottom strand	GATCGGAAGAGCGGTTCAGCAGGAATGCCGAG			
PE 1.0	AATGATACGGCGACCACCGAGATCTACACTCTTTCCCTACACGACGCTCTTCCGATCT			
iPCRtag	CAAGCAGAAGACGGCATACGAGATXXXXXXXXCGGTCTCGGCATTCCTGCTGAACCGCTCTTCCGATCT			

Supplementary Table 9. qPCR primers for hSpCas9 quantification by real time quantitative PCR.

Target	Forward primer	Reverse primer
hSpCas9	GCCTATTCTGTGCTGGTGGT	ATCCCCAGCAGCTCTTTCAC
Apob	CACGTGGGCTCCAGCATT	TCACCAGTCATTTCTGCCTTTG

Supplementary Table 10. qPCR primers for sgRNA distribution analysis. Primers used for sgRNA distribution analysis (real time quantitative PCR). *CRISPR-SB-fwd* and *CRISPR-SB-rev* amplify a 763bp product containing the cloned 20bp sgRNA sequence. Nested real time quantitative PCR was performed to analyze distribution of specific sgRNAs using *CRISPR-SB-quant-fwd* and the specific reverse oligonucleotides of each sgRNA.

Primer	Sequence
CRISPR-SB-fwd	GAGGGCCTATTTCCCATGAT
CRISPR-SB-rev	CGACTCGGTGCCACTTTT
CRISPR-SB-quant-fwd	ACTATCATATGCTTACCGTAAC
Apc_rev	AAACCAACTTGCTTTAACAACTGAC
Arid1a_rev	AAACCAGCCGTATGGTGGGACTAAC
Brca1_rev	AAACGATCGGACACTCTAAGATTTC
Brca2_rev	AAACATTGAGGCTTATCGGTCCTAC
Cdkn2a_(ex1β)_rev	AAACGGATCGCACGAACTTCACCAC
Cdkn2a_(ex2)_rev	AAACGCGGAACGCAAATATCGCAC
Pten_rev	AAACTCATCAAAGAGATCGTTAGC
Smad4_rev	AAACTATCACTATGAGCGGGTTGTC
Tet2_rev	AAACGGATATCTGTTGGCACTTTC
Trp53_rev	AAACAGTGAAGCCCTCCGAGTGTC

Supplementary Table 11. qPCR primers used for quantification of $Cdkn2a\ exon-1\beta/exon-2$ fusion products by real time quantitative PCR.

Target	Forward primer	Reverse primer
Cdkn2a-ex1β-quant	CAAGAGAGGTTTTCTTGGTGA	
Cdkn2a-ex2-quant	ACAACATGTTCACGAAAGCCA	GGGACATCAAGACATCGTGC

Supplementary Table 12. Primers used for CRISPR-SB integrations analysis.

Target	Forward primer	Reverse primer
CRISPR-SB-int	GAGGGCCTATTTCCCATGAT	CGACTCGGTGCCACTTTT

Supplementary Table 13. Information about off-target sites. Location, sequence and number of mismatches (in regard to the on-target) for each potential off-target site analyzed by amplicon-based next-generation sequencing.

Name	Chr	Strand	Location (mm9)	Sequence	Mismatches	Gene
Арс			, ,	·		
OT_Apc_1	9	-1	26741476	TCAGTTATTAAAGCAAATTGGGG	2	None
OT_Apc_2	14	1	78004236	GCAGTTGAGAAAGCAAGTTGGAG	3	None
OT_Apc_3	3	-1	114079728	TCAGATTATAAAGCAAGTTGTGG	3	None
OT_Apc_4	5	1	76213674	TTAGCTGTTAAAGCAAGTTACAG	3	None
OT_Apc_5	10	1	93842567	TCAGATGGGAAAGCAAGTTGCAG	3	None
OT Apc 6	13	1	107647475	TAAGTTGCTATAGCAACTTGAAG	4	NM 029665
OT Apc 7	7	1	13570187	TCAGTTCCTACAGCAAGTTCCAG	4	NM 001168561
OT_Apc_8	10	-1	51914804	AGAGTTCTTAAAGCAAGGTGGAG	4	NM_011282
Arid1a						
OT_Arid1a_1	17	1	27589623	CCAGGCCCACCATATGGCTGAGG	4	None
OT Arid1a 2	5	-1	123157730	TGAGCCCCACTTTACGGCTGCGG	4	NM 011026
OT Arid1a 3	8	1	92089504	TGGGACCCACCATACCGCTGTGG	4	None
OT Arid1a 4	16	-1	13033016	TTAAACCCACCATACGCCTAAAG	4	None
OT Arid1a 5	8	-1	128820603	ATAGTCCATCCATAGGGCTGAAG	4	None
OT Arid1a 6	15	1	79748335	TGTGTCCCACCACAAGGCTGGAG	4	NM 144811
OT Arid1a 7	1	1	166141978	ATAGACCCACCCTTCGGCTGGAG	4	NM 007976
Brca1	•	•				_
OT Brca1 1	18	1	11328992	AAATCTTGGAGTGTCCGGTCAAG	2	None
OT Brca1 2	10	-1	124791436	AAATTTTAGTGTGTCCCATCAAG	3	None
OT Brca1 3	11	1	111352929	AATTCTTAGAATGTCCCATCCAG	3	None
OT Brca1 4	5	-1	34545145	ACATCTGTGAGTGTCCCATCCAG	4	None
OT Brca1 5	3	-1	7612605	AAGTCTGGGAGTTTCCGATCCAG	4	None
OT Brca1 6	17	1	35264433	GAACCTTGGAGTGTCCGCTCAAG	4	NM 033477
OT Brca1 7	12	1	112094143	ACATCTTACAGTGTCAGATGGGG	4	NM 001199785
OT Brca1 8	1	1	60543179	AAATCTTAAATTGTCTTATCTGG	4	NM_001045513
Brca2						
OT Brca2 1	16	16	7627877	TATGACCAATGAGCCTCAATAAG	3	None
OT Brca2 2	5	5	37739749	GATGACCCATAAGCCTCAAAGAG	4	NM 145920
OT Brca2 3	7	7	90824129	TGGAACAGCTAAGCCTCAATCAG	4	None
OT Brca2 4	6	6	101189127	TTAGACCTATAAACCTCAATGAG	4	None
OT Brca2 5	X	X	10413660	GAGAACTGATTAGCCTCAATAGG	4	None
OT Brca2 6	12	12	37203260	AAGGACAGATAAACCTCATTAGG	4	NM 178629
OT Brca2 7	5	5	124269242	TAGGAACGCTACGGCTCAATAGG	4	NM 001042421
Cdkn2a-ex1β			1 12 12 0 2 12		•	
OT Cdkn2a-ex1β 1	8	1	45813437	TGATTAAGTTCGTGAGATCCTGG	3	None
OT Cdkn2a-ex1β 2	2	-1	30064240	CAGTGAAGTGCCTGCGATCCCAG	4	None
OT Cdkn2a-ex1ß 3	1	1	39634432	TGGGGAAGTTTGTGCGCTCCGGG	3	None
OT Cdkn2a-ex1β 4	6	-1	87783496	AGGTGTGGTGCGATCCCAG	4	None
OT Cdkn2a-ex1β 5	16	1	39487138	AAGTGAAGTTTGTGCGTTCCCAG	4	None
OT Cdkn2a-ex1β 6	13	-1	50513278	TGCTGCAGTTCGTGCGGGCCAAG	4	NM 175401
OT Cdkn2a-ex1β 7	11	-1	120670835	TGTGGAAGTTCGTCGGGGCCAAG	4	NM 007988
OT Cdkn2a-ex1β 8	X	1	56172330	TGGTGAAGTTTCTGAGCTCCAAG	4	NM 023774
Cdkn2a-ex2		· ·	30112000	. co. crato i i ci dide i cond	· ·	1411_020774
OT Cdkn2a-ex2 1	4	1	148248166	GTGGGAGATCTGCGTTCCGTAAG	4	None
OT Cdkn2a-ex2 2	7	1	134068454	GTGCGTTCTTTGCGTTGCGTGGG	4	None
OT Cdkn2a-ex2_2	4	1	45268111	GTGCCATATTCCAGTTCCGCAAG	4	None
OT Cdkn2a-ex2_3	2	1	180660612	GTGGGACATTTGGGTTCCTCTGG	4	None
OT Cdkn2a-ex2_4 OT Cdkn2a-ex2_5	8	-1	74680985	GTTCAATATTTGTGTTCTGCCAG	4	None
OT Cdkn2a-ex2_5	11	-1	95536456	GTGTGATATTGACGTTCTGCAAG	4	NM 008831
OT_Cdkn2a-ex2_6 OT Cdkn2a-ex2_8	3	-1	53278662	GTGCGATAGTTGCGTTCTGCAAG	4	NM 173382
OI_CUKIIZa-exz_0	J	-1	J321000Z	U TUCUATAUTTUCATUCUUCCUU	+	141VI_1/330Z

Pten						
OT_Pten_1	1	-1	98296790	CCTATCGATTTCTTTGATGATGG	3	None
OT_Pten_2	10	1	11506620	AATACCGGTCTCTTTGATGATGG	4	None
OT_Pten_3	6	1	110090641	TGTCACGATGTCTTTGATGAAGG	4	None
OT_Pten_4	1	-1	148546230	GCTTACGATGTATTTGATGATGG	3	None
OT_Pten_5	12	-1	8417202	AGTAGCTATCTCTTTGATGAGAG	4	None
OT_Pten_6	2	1	37283155	TGTAACAATGTCTTTGATGAAAG	4	NM_146253
OT_Pten_7	3	1	138114184	GCTGACACTGTCTTTGATGATAG	4	NM_007410
OT Pten 8	10	-1	62480288	GGAAACGATGGCTTTGATGACAG	4	NM_001079824
Smad4						
OT_Smad4_1	18	1	39860049	AATAGCAGCTCATAGTGATAGAG	4	None
OT_Smad4_2	6	-1	127173197	ATAACCCGCTTATAGTGATGTGG	3	None
OT_Smad4_3	8	-1	88373851	ACAGCCCTTACATAGTGATAGGG	4	None
OT_Smad4_4	13	1	31227591	ACAAACATCTCCTAGTGATATGG	4	None
OT_Smad4_5	1	1	170162378	GAAACCAGCTCAAAGTGATAGAG	4	None
OT_Smad4_6	10	1	20868341	ACTATCTGCTCAAAGTGATACGG	4	NM_001198914
Tet2						
OT_Tet2_1	9	1	45417670	TAGTGTGACAACAGATATCCTGG	4	None
OT_Tet2_2	2	1	30832627	GATTATGACAACAGATATCCTGG	4	None
OT_Tet2_3	1	1	89767330	GGAATTGCCAACAGATCTCCTGG	3	None
OT_Tet2_4	17	1	30344787	GCCAGTGCCAACAGATTTCCCAG	3	None
OT_Tet2_5	13	-1	51963540	GAAAGACCCTACAGATATCCCAG	3	None
OT_Tet2_6	7	-1	115756426	GACAGTGCCAACAGATATAGTGG	3	NM_001011871
OT_Tet2_7	10	1	5219200	GAACGTGCTTACAGATATCAAAG	4	NM_001079686
OT_Tet2_8	4	1	132622017	GACACTGCCTACAGGTATCCAGG	4	NM_146155
Trp53						
OT_Trp53_1	17	-1	54559163	AACACTTGGAGGGCTTCACTTGG	2	None
OT_Trp53_2	5	-1	107143107	ATCACTTGGAGGGCTTCACTCAG	3	None
OT_Trp53_3	10	-1	109084970	GGCTGTCAGAGGGCTTCACTCAG	4	None
OT_Trp53_4	9	-1	49608135	GTCTGTCAGAGGGCTTCACTGAG	4	None
OT_Trp53_5	5	-1	117474920	CACACTGGGAAGGCTTCACTTAG	3	None
OT_Trp53_6	2	-1	35586131	GGCAGTCAGAGGTCTTCACTCAG	4	NM_001114125
OT_Trp53_7	2	-1	62339193	GACAGTCTGAAGGCTTCACATGG	4	NM_007986
OT_Trp53_8	2	-1	158087116	AACACTCGGAGGCCATCACTGGG	3	NM_177850

Supplementary Table 14. Primer sequences for off-target site amplicons. Primers used for amplifying CRISPR/Cas9 off-target sites (length of PCR products is between 400bp and 450bp).

Nama	Forward primar	Boyoroo primor
Name	Forward primer	Reverse primer
Apc OT Apc 1	CTGAGTGTGGTGCTATACTCAAG	ACTAGGATTAGGACCTAGGAAACA
OT Apc_1	AGATCTGCAGTTCACCCCAA	GGGAGTCCAGGAAGCAGAAT
OT_Apc_2	AGTTACTGGTGGCTGTAAGACA	AGAGTGGCAGTTCAAGGTAGT
OT Apc 4	ATCCAACGCTGATTCCTTGC	GGGAGGTGATTGAGGGGAC
OT_Apc_5	CCTGGTTTTACGTTGCTGCT	CTATTTGCCTGCACCTCCAG
OT Apc 6	CAATGCAAAAGGTGTTCTGACA	TCACCACCCTTGCTGTAACT
OT Apc 7	CACTTGCTTCAGTCTGAGCC	CCTGCAGTCAACCTTGGTTC
OT Apc 8	CGAACCTGTCAGTTGCAAGT	TGCGATGTTCTGGGCTATCT
Arid1a		
OT Arid1a 1	TCCAGATGCCAACCCCTATC	GCCACAGACCCTATTCCTCA
OT_Arid1a_2	TGAGAGGTCACGAGTTGG	CTATTGCCCCAGACCCAGAG
OT_Arid1a_3	TGTCTACGATCACAGTGCAGT	ACACAGGCTGTAACTCTGAAGA
OT_Arid1a_4	CAGAGGAAGTTGGGTGAGGA	TCATGCTCATCAGGGCTTCT
OT_Arid1a_5	GCCAACAGGTGAGTCTTCTAAC	CAGGCCCATGTTGTCTGAAG
OT_Arid1a_6	CGGCAAGTTCTGTTTGTGCT	GTCTGGGTCTCATCTCCTGG
OT_Arid1a_7	TCCTCGAAGTAGACATATCCACA	TGCAAAGGTTCTTCTGGAGC
Brca1		
OT_Brca1_1	GACTTCGTGGACAGAATGGC	TCCAGCCCTGTTTGATTCCT
OT_Brca1_2	GAGAACTGCAGAGCCCATTG	ACCGACATTTTCCCCTCCTT
OT_Brca1_3	TCCAAAGGCTGCTAGTGGAA	CCTCGACCCCTCCCAATTTT
OT_Brca1_4	CCCAACACAGCCCACTACA	ACCTGCAGAGTAAAGGGCTC
OT_Brca1_5	TGGATTCCAGCCTCTGTCAA	TGTCCCTAGCCAGTACCTCT
OT_Brca1_6	TAGCAGGACCTCAAAGTGG	ATAGCAGCCCATGAAGCCAG
OT_Brca1_7	GCACTGTAAGCTCAACCCAG	CCTCTGCCACATGAGTACCA
OT_Brca1_8	ACATGACTGGAGTTAGAAAAGGA	TGTGCTTGCTATTCCTATGATGA
Brca2		
OT_Brca2_1	CACAGTAGGTTGGGTCTTCC	GACAGGGTTGGAGAGTGCC
OT_Brca2_2	GCGCTGTTATTTCCTCCGTT	AGCAAGGCCAGTGATCTCAT
OT_Brca2_3	TGAGCAAGTCACTTTGGAAAACA	AAGTGGGAACTTCAGGAGGG
OT_Brca2_4	CACTGAGTGTCATGCTTGGC	ACTAGTGAGCCCTGCCTTTC
OT_Brca2_5	GACACAGGAAGAGGAGACA	ATCAAGCCACCAGAATCCCT
OT_Brca2_6	TGCATTTCCTTTGACACCAGT	ATCAGAGATCTCCGTGGCTG
OT_Brca2_7 Cdkn2a-ex1β	AGAAGGAATTTGGGATTTTGGCA	TGGAGAGTGAGCTAGCCAAG
OT Cdkn2a-ex1β 1	GCTTCCCTGAAACCTGCATC	CATCAAGGACTAGGAGCAATGA
OT Cdkn2a-ex1β 2	GTTGCCCTCATCTCAGACCT	TTCCAAGTGCAGCAAAGGTC
OT Cdkn2a-ex1β 3	GCGACTCACTCCAGGCTG	ACAAAAGGCATCTGGACAACT
OT Cdkn2a-ex1β 4	GGGAGAGGGTCTAGAAGGA	TCCACAGATCATTGGCGAGA
OT_Cdkn2a-ex1β_5	GGCATCTTTTCATTTGTCAGCC	ACACAGACACAGATCCAAT
OT Cdkn2a-ex1β 6	ACTTCAGTGATCGCTAGGCC	CACACAGTGGGGCATAGAGA
OT Cdkn2a-ex1β 7	TGAGGACATGCACACAGACT	AATGCTTGGCTGGGTGATTG
OT Cdkn2a-ex1β 8	CTGCAGAGAGTTCCCAGGAA	CTCTTCATTGCTGATCCGCC
Cdkn2a-ex2		
OT_Cdkn2a-ex2_1	TGGGCTTGTTTTAAAGGGGC	CAATGTCTGCTGCTCACCTG
OT_Cdkn2a-ex2_2	GTCTGTTTGGATGCCCTTGG	AGGCTACTCTTGCTGTCTCC
OT_Cdkn2a-ex2_3	AAACTGAACTTGCTCGGCTC	TTGAGCATGAGAGGGAAGCA
OT_Cdkn2a-ex2_4	TACCACTTCCTTCCCTGCAG	ATTGACTGTCCTACCCTGGG
OT_Cdkn2a-ex2_5	TTACCTAACTCCTGGGGCAG	CAGGAAGCTAGACTGTGCCT
OT_Cdkn2a-ex2_6	CCATCCTGTCAGTGGTTCCT	GCTACCTACCCACCACTACTC
OT_Cdkn2a-ex2_7	ACTGGGGCATCTTCAGTCTC	AGTGAAAAGCCCCAATGATAAGT
Pten	1	
OT_Pten_1	CAAGAGAAAGACAAGGCATGGT	AGAAGGGAGGAAGGAA
OT_Pten_2	GGAGCAGCTTGGAGTCTGAT	CATTGCCAGCACAGTTCTCA
OT_Pten_3	GGAACATTAAGAGTGAAACAGCT	AAATAGGTGGCAGAACGGGT
OT_Pten_4	CATGCAACACAGAGGACACA	TCCTTCTTCTGACCAAATGTGA
OT_Pten_5	AACAATGCTCAGAGGGTCCC	GATGGAATGTTGGGCCTCAA
OT_Pten_6	AAGGGTGGACTACAAAAGAGC	ACAGAAAGGTTTGTCTTGGCC
OT_Pten_7	GCTGTGGTATTTCAACTGGCT	TGACCTTCACGTTGCCAATG
OT_Pten_8	CCATAGCCATGTCCTCCCAT	GCTGCAAACATTAATGAAGAAGC

Smad4		
OT_Smad4_1	CATCATCTCCAAGGCCCTCA	GCCATTCCAGGGATCAAACC
OT_Smad4_2	CAGATATGGTGGTGCATGCC	TTGGAAAGCAGAGCAACAGG
OT_Smad4_3	GGGGTTCCTGGGAGTCTTTT	TACTGTGGCCTTGAGAAGCA
OT_Smad4_4	TAAGCAGCACTCACCAC	GCTCAGTCACCTAAGCTTGT
OT_Smad4_5	AAAGTGGGACTCATAGGGCC	TCCCGTCTCAGGTCACAAAA
OT_Smad4_6	TAATGCCTGCTGTCCCTTCA	TGAGATCATCTGACGGGCAA
Tet2		
OT_Tet2_1	AATTCAAGTGCAGAGCCAGG	GCCAGTCTGCAAATGAAATCT
OT_Tet2_2	CAACACCTGCCTCCAAC	CTGAGTTCACTGTGCAAGCA
OT_Tet2_3	TCTAGGGAATGTGGCCTGAG	CCCTGCAGATCCCCTAAATGA
OT_Tet2_4	CCGCACCCATTTTCTGATAGG	CTTTCCGGTCCAGTTTCACC
OT_Tet2_5	GCTGTCCTGGAACTCACTCT	ACTGAGCCTAAGATTGTCCCA
OT_Tet2_6	TAATGCATCCTCCTTCACCCT	GGGGTTCAACATGGGGATCA
OT_Tet2_7	ACATGACCCAAGATTTCCCAA	GGCCTGAGAAGCGAAATGAG
OT_Tet2_8	CTATGAAGGCAAGGTGGGC	CATCCCCAGACTTACCCAGG
Trp53		
OT_Tp53_1	CCTAGCATTCAGGCCCTCAT	TGAGGGAGAGAGTACAGT
OT_Tp53_2	GGATTGTCCCTTGTACCACTTC	AACAAATGTGCGGGCAACTT
OT_Tp53_3	GCATGCACTGAACAGAAATTGG	TCAGAGGAGATTTGCTTGGGA
OT_Tp53_4	CCCTGGCTCTTCTGTGTGTA	GAACCCGCAGCATGTGATAG
OT_Tp53_5	CATGATGCCTGTTCACGAGG	CTGGTAAAAGGTGCTGGCTT
OT_Tp53_6	CATGCTGTTTGGGTGGAAGG	AGAAAAGAGGGCTGGTTCC
OT_Tp53_7	CTACCCGGCAATGAACAGGT	CCAAGTGGCCAAGAAGCAAA
OT_Tp53_8	GGCTTGCCGTCTTTGTTGAT	AAGTGGACAGTTCTCCCAGC